Network Formation with Local Complements and Global Substitutes: The Case of R&D Networks.

Konig, M.D.; Hsieh, Chih-Sheng; Liu, Xiaodong

2018

Network Formation with Local Complements and Global Substitutes: The Case of R&D Networks[☆]

Chih-Sheng Hsieh[a], Michael D. König[b,c,d], Xiaodong Liu[e]

[a] *Department of Economics, Chinese University of Hong Kong, CUHK Shatin, Hong Kong, China.*
[b] *Centre for Economic Policy Research (CEPR), London, United Kingdom.*
[c] *ETH Zurich, Swiss Economic Institute (KOF), Zurich, Switzerland.*
[d] *Department of Spatial Economics, VU Amsterdam, De Boelelaan 1105, 1081 HV Amsterdam, The Netherlands.*
[e] *Department of Economics, University of Colorado Boulder, Boulder, Colorado 80309–0256, United States.*

Abstract

We introduce a stochastic network formation model where agents choose both actions and links. Neighbors in the network benefit from each other's action levels through local complementarities and there exists a global interaction effect reflecting a strategic substitutability in actions. We provide a complete equilibrium characterization in the form of a Gibbs measure, and show that the model is consistent with empirically observed networks. We then use our equilibrium characterization to show that the model can be conveniently estimated even for large networks. The policy relevance is demonstrated with examples of firm exit, mergers and subsidies in R&D collaboration networks.

Key words: network formation, peer effects, technology spillovers, key player, mergers and acquisitions, subsidies
JEL: C11, C63, C73, D83, L22

[☆] We would like to thank Anton Badev, Filomena Garcia, David Hemous, Matt Jackson, Paolo Pin, Terence Johnson, Alexey Kushnir, Lung-Fei Lee, Elena Manresa, Andrea Montanari, Nick Netzer, Onur Özgür, Agnieszka Rusinowska, María Sáez-Martí, Armin Schmutzler, Martin Summer, Adam Szeidl, Fernando Vega-Redondo, Joachim Voth, Timothy Van Zandt, Yves Zenou, Fabrizio Zilibotti, and seminar participants at the Workshop on Networks: Dynamics, Information, Centrality, and Games at Centre d'Economie de la Sorbonne in Paris, the Second Annual NSF Conference on Network Science in Economics at Stanford University, the Econometric Society World Congress in Montreal, the congress of the European Economic Association in Mannheim, the 25^{th} Stony Brook International Conference on Game Theory, the Public Economic Theory Conference in Lisbon, the Universities of Zurich, Bonn, Geneva, Cologne, Bern, Constance, Bocconi, Amsterdam, the National Taiwan University, the Austrian National Bank and Stanford University for the helpful comments and advice. We further thank Christian Helmers for data sharing and Sebastian Ottinger for the excellent research assistance. A previous version of this paper has been circulated under the title "Dynamic R&D Networks" as Working Paper No. 109 in the Department of Economics working paper series of the University of Zurich. Michael König acknowledges financial support from Swiss National Science Foundation through research grants PBEZP1–131169 and 100018_140266, and thanks SIEPR and the Department of Economics at Stanford University for their hospitality during 2010–2012.

Email addresses: cshsieh@cuhk.edu.hk (Chih-Sheng Hsieh), michael.koenig@econ.uzh.ch (Michael D. König), xiaodong.liu@colorado.edu (Xiaodong Liu)

1. Introduction

The many aspects that are governed by networks make it critical to understand how networks impact behavior (and vice versa), which network structures are likely to emerge, and how they affect welfare in the society [Jackson, 2008; Jackson et al., 2017]. A crucial aspect of such environments is the coevolution of networks and behaviors. An example is the coevolution of R&D collaboration networks and firms' R&D investment choices. Technology spillovers across collaborations in R&D alliance networks affect the firms' R&D investment portfolios. Conversely, the R&D investment portfolios determine which R&D collaborations are being formed. In this paper we introduce a tractable framework to account for the joint evolution of networks and behaviors, which can be applied to real world network data and used for policy analysis.

Overview of the results and contributions Our paper makes three interrelated contributions: (i) a theoretical, (ii) an econometric, and (iii) a policy contribution. Our framework has a broad range of applications in various fields [Jackson et al., 2015]. To give a concrete example, in the following we will illustrate our contributions with the example of firms forming R&D collaborations to benefit from technology spillovers while, at the same time, being competitors in the product market [D'Aspremont and Jacquemin, 1988].

(i) We provide an analytic characterization of both, equilibrium networks and endogenous effort choices, by making the network in the model introduced by Ballester et al. [2006] endogenous. We show that equilibrium networks are "nested split graphs" [König et al., 2014a],[1] providing an explanation for why nestedness has been observed in empirical R&D networks [Tomasello et al., 2016]. Nested graphs further have a core-periphery structure [cf. Hojman and Szeidl, 2008], which has also been documented in empirical studies on R&D networks [Kitsak et al., 2010; Rosenkopf and Schilling, 2007]. In particular, Kitsak et al. [2010] find that firms in the core have a higher market value, consistent with the predictions of our model. Moreover, we show that the firms' output levels and degrees follow a Pareto distribution, consistent with the data [König et al., 2018; Powell et al., 2005]. We then investigate the efficient network structure that maximizes social welfare, and find that equilibrium networks tend to be under-connected compared to the social optimum.[2]

(ii) We provide an estimation framework that can handle the endogeneity of both, the network structure and (either continuous or discrete) action choices. This generalizes previous works such as Mele [2017], where only the formation of the network has been considered. Importantly, the analytic equilibrium characterization allows us to design an estimation algorithm that can handle large network datasets. We illustrate how our estimation framework can be applied to the data by using a unique dataset on R&D collaborations matched to firm's balance sheets and patents. Using R&D tax credits as exogenous instruments and our structural model, we are able to separately identify the technology spillover and the product market rivalry effects from the exogenous variations in the firms' productivities that affect both, their R&D investment

[1] A network is a nested split graph if the neighborhood of every node is contained in the neighborhoods of the nodes with higher degrees [Mahadev and Peled, 1995]. See supplementary Appendix B for further network definitions and characterizations.

[2] In Section 4.3 we analyze the effectiveness of a subsidy on firms' R&D collaboration costs, that provides firms with additional incentives to form collaborations and thus increases the network connectivity.

levels as well as their propensities to form R&D collaborations. As predicted by the theory, our estimates show that the technology spillover effect has a positive and significant impact on output and investment while the competition effect has a negative and significant impact, with the first dominating the latter.

(iii) We provide a counterfactual policy analysis with an endogenous network structure that we illustrate with three real world examples. First, we use our estimated model to investigate the impact of exogenous shocks on the network. More precisely, we perform a dynamic "key player" analysis [Zenou, 2015], and identify the firm whose exit would have the largest impact on welfare (endogenizing Ballester et al. [2006]).[3,4] Focusing on the chemicals and pharmaceutical sectors, our results indicate that the exit of *Pfizer Inc.*, one of the world's largest pharmaceutical companies, would lead to a reduction in welfare of 0.47%. We then provide a ranking of the firms in our sample according to their impact on welfare upon exit. The ranking shows that the most important firms are not necessarily the ones with the highest market share, but that in order to evaluate the importance of a firm, we need to take into account the positions of these firms in a network of R&D collaborations, and how this network dynamically responds to shocks.

Second, our framework allows us to study mergers and acquisitions, and their impact on welfare [Farrell and Shapiro, 1990]. Traditional market concentration indices are not adequate to correctly account for the network effect of a merger on welfare [Encaoua and Hollander, 2002]. This is because the effect of a merger on industry profits, consumer surplus and welfare depends not only on the market structure, but also on the architecture of the R&D collaboration network between firms through which R&D spillovers are channelled. In such networked markets, benefits from concentration of R&D activities can arise through economies of scale and faster diffusion of technologies in more centralized networks [Daughety, 1990]. Our framework allows us to determine which mergers lead to welfare losses due to market concentration, or to welfare gains through efficient R&D concentration.[5] Our results show that a merger between *Xoma* and *DOV Pharmaceutical Inc.*, two American biotech companies, would result in a welfare loss of 0.075%. In contrast, a welfare gain of 0.86% from a merger would be obtained between *Novartis* and *Pfizer Inc.*. Our results indicate that the R&D spillover effect is larger when two well connected, R&D intensive firms merge, while welfare losses from increased market concentration dominate when less connected and more market dominant firms are involved in the merger.

Third, we identify which R&D collaborations should be subsidized. Our study indicates that subsidizing an R&D collaboration between *Exelixis*, an American genomics-based drug discovery company, and *Colgate-Palmolive Co.*, a worldwide consumer and pharmaceutical products company, would increase welfare by 0.94%. Typically, collaborations between firms with only

[3]We note that our model is formulated in a fairly flexible way, and because we consider the general payoff structure introduced in Ballester et al. [2006], one could use our framework also to investigate key players in criminal networks, or other related contexts [see also Zenou, 2015].

[4]The exit of a firm could be due to either financial reasons, such as the recession experienced by the American automobile manufacturing industry during the global financial downturn, or legal reasons, such as the recent emission-fraud scandal of Volkswagen. In the latter case, policy makers want to know the overall cost they impose on the economy by inflicting high fines that might threaten the continued existence of a firm.

[5]This is highly relevant in practice, as for example in 2014 more than half of the merger proposals that were investigated by the U.S. Department of Justice involved R&D-efficiency claims [Marshall and Parra, 2015].

a few if any collaborations yield the largest welfare gains. As subsidies have been increasingly used by governmental organizations to stimulate collaborative R&D activities,[6] our framework could assist governmental funding agencies that typically do not take into account the aggregate spillovers generated within a dynamic R&D network structure.

Related literature There is a growing literature on the stochastic evolution of networks going back to Jackson and Watts [2002], with more recent examples including Hojman and Szeidl [2006], Feri [2007] and Dawid and Hellmann [2014], using tools from evolutionary game theory [Blume, 1993; Kandori et al., 1993; Sandholm, 2010] to analyze the formation of social and economic networks. In this literature agents form links over time based on myopic improvements that the resulting network offers them relative to the current network. While there is a small probability that agents make mistakes, the stochastically stable states are identified when this probability vanishes. Our paper uses similar techniques to analyze the stationary states in a stochastic network formation model, but different from the aforementioned works, we investigate the coevolution of links and actions, and develop an estimable framework from our theory that can be applied to real world networks.

There also exist related studies on the formation of R&D networks in the economics literature. Similar to our framework, Goyal and Moraga-Gonzalez [2001], Dawid and Hellmann [2014], and Westbrock [2010] study the formation of R&D networks in which firms can form collaborations to reduce their production costs. In particular, Dawid and Hellmann [2014] study a perturbed best response dynamic process as we do here, and analyze the stochastically stable states. However, different from the current model, they ignore the R&D investment decision, and the technology spillovers from a collaboration in these models is independent of the identity and the characteristics of the firms involved.[7]

Similarly, Ehrhardt et al. [2008] analyze the formation of a network in which agents play a coordination game with their neighbors, while König et al. [2014a], Marsili et al. [2004], and Fosco et al. [2010] study the coevolution of networks and behavior. As in the present paper, these authors show that the interplay between action choice and link creation may feed on each other to generate sharp transitions from sparse to dense networks. The underlying payoff structure, however, is different from ours. Further, while these authors assume that links decay at random, here link removal depends on whether the agents find this profitable.

Our analysis also bears similarities with a number of other recent contributions in the literature which analyze a similar payoff structure. In the papers by Ballester et al. [2006] and König et al. [2018] the authors derive equilibrium outcomes in a linear quadratic game where agents' efforts are local complements in an exogenously given network. Different from these works we make the network as well as effort choices endogenous.[8] Cabrales et al. [2011] allow the network to be

[6] For example, total subsidies for cooperative R&D provided by EUREKA, a Europe-wide network for industrial R&D, accumulated to more than €37 billion in 2015.

[7] Goyal and Moraga-Gonzalez [2001] present a more general setup which relaxes this assumption but their analysis is restricted to regular graphs and networks comprising of four firms. In this paper we take into account general equilibrium structures with an arbitrary number of firms and make no ex ante restriction on the potential collaboration pattern between them.

[8] It is straightforward to see that the results obtained in this paper can be generalized to the payoff structure introduced in Ballester et al. [2006]. See in particular the general payoff structure considered in Equation (1). We provide a complete equilibrium characterization for the model introduced in Ballester et al. [2006], but allow both agents' actions and links to be endogenously determined.

formed endogenously, but assume that link strengths are proportional to effort levels, while we make the linking decision depending on marginal payoffs. Hiller [2013] studies the joint formation of links and actions using a similar payoff structure as we do here, however, abstracting from any global substitutability effects, and shows that equilibrium networks are nested split graphs [see also König et al., 2014a]. Similarly, Belhaj et al. [2016] analyze the design of optimal networks with the same payoff function but without global substitutabilities, and show that when the planner chooses links, but not the level of output (second best), the optimal network is a nested split graph. We find that when the planner chooses both actions and links (first best), both equilibrium and efficient structures are nested spit graphs, even when allowing for global substitutes and incorporating heterogeneous firms, and we provide a more precise equilibrium characterization beyond the general class of nested split graphs. In particular, we identify conditions under which both the output and the degree distributions follow a power law, consistent with the empirical data [Gabaix, 2016; Powell et al., 2005].

Our approach is a further generalization of the endogenous network formation mechanisms proposed in Snijders [2001], Chandrasekhar and Jackson [2012], and Mele [2017]. As in these papers, we use a potential function to characterize the stationary states [Monderer and Shapley, 1996], but here both, the action choices as well as the linking decisions are fully endogenized. Moreover, different from these papers we provide a microfoundation (from a Cournot competition model with externalities) for the potential function. Further, in a recent paper by Badev [2013] a potential function is used to analyze the formation of networks in which agents not only form links but also make a binary choice of adopting a certain behavior depending on the choices of their neighbors. Different from Badev [2013], we consider a continuum of choices, and provide a microfoundation derived from the payoff function introduced in Ballester et al. [2006]. Moreover, different from the previous authors we provide an explicit equilibrium characterization, use an alternative estimation method (which can also be applied to large networks and addresses the "local trap" problem of non-concave likelihood functions),[9] apply our model to a different context, and study a range of novel counterfactual policy scenarios. Relatedly, in a recent paper, Hsieh and Lee [2013] apply a potential function to an empirical model of joint network formation and action choices. However, their potential function is based on a transferable utility function so that linking decisions are based on maximizing aggregate payoffs, while here we consider decentralized link formation between payoff maximizing agents.

Organization of the paper The paper is organized as follows. The theoretical model is outlined in Section 2. In particular, Section 2.1 introduces the linear-quadratic payoff function considered in this paper. Section 2.2 defines the stochastic network formation and output adjustment process and provides a complete characterization of the stationary state. In Section 2.3 the welfare maximizing networks are derived. Section 2.4 discusses several extensions of the model that allow for firm heterogeneity. Next, Section 3 provides information about the data that we use and explains the estimation methods and results. Section 4 then uses the estimated model to analyze several counterfactual policy experiments. Finally, Section 5 concludes. All proofs are relegated to Appendix A.

[9]Note also that classical Maximum Likelihood Estimation (MLE) methods such as the one considered in Badev [2013] are greatly influenced by the choice of initial parameter values, and if these are not close enough to the true values, the method may converge to a sub-optimal solution [Airoldi et al., 2009].

Additional relevant material can be found in the supplementary appendices. In particular, supplementary Appendix B provides basic definitions and characterizations of networks. Supplementary Appendix C provides a motivation for the linear quadratic payoff function from a model of R&D collaborating firms that are competing on the product market à la Cournot. Supplementary Appendix D explains the distinction between continuous and discrete quantity choices. Supplementary Appendix E explains in detail the extensions mentioned in the main text. Supplementary Appendix F provides a detailed description of the data used for our empirical analysis in Section 3, while supplementary Appendix G provides additional details of the estimation algorithms. Supplementary Appendix H provides a simulation study to examine the performance and consistency of our various estimation algorithms, as well as the impact of missing observations on estimation.

2. Theoretical Framework

2.1. Payoffs

Each firm (agent) $i \in \mathcal{N} = \{1, \ldots, n\}$ in the network $G \in \mathcal{G}^n$ with an output level $q_i \in \mathcal{Q}$ and obtains a linear-quadratic profit (payoff) $\pi_i : \mathcal{Q}^n \times \mathcal{G}^n \to \mathbb{R}$ given by[10]

$$\pi_i(\mathbf{q}, G) = \eta_i q_i - \nu q_i^2 - b q_i \sum_{j \neq i}^{n} q_j + \rho \sum_{j=1}^{n} a_{ij} q_i q_j - \zeta d_i, \tag{1}$$

where $\mathcal{Q}$ is the (bounded) output choice set of a firm, $\mathcal{G}^n$ denotes the set of all graphs with $n \geq 2$ nodes, $a_{ij} = 1$ if firms i and j set up a collaboration (0 otherwise) and $a_{ii} = 0$.[11] Equation (1) is concave in own output, q_i, with parameters $\eta_i \geq 0$ and $\nu \geq 0$. Moreover, $b > 0$ is a global substitutability parameter, $\rho \geq 0$ is a local complementarity parameter, $\zeta \geq 0$ is a fixed linking cost and d_i is the number of collaborations of firm i. A derivation of the profit function in Equation (1) in the context of R&D collaborating firms competing à la Cournot can be found in supplementary Appendix C.

The profit function introduced in Equation (1) admits a (cardinal) potential function [Monderer and Shapley, 1996].

Proposition 1. *The profit function of Equation (1) admits a potential game where firms choose both output and links with a potential function* $\Phi \colon \mathcal{Q}^n \times \mathcal{G}^n \to \mathbb{R}$ *given by*

$$\Phi(\mathbf{q}, G) = \sum_{i=1}^{n} (\eta_i q_i - \nu q_i^2) - \frac{b}{2} \sum_{i=1}^{n} \sum_{j \neq i}^{n} q_i q_j + \frac{\rho}{2} \sum_{i=1}^{n} \sum_{j=1}^{n} a_{ij} q_i q_j - \zeta m, \tag{2}$$

for any $\mathbf{q} \in \mathcal{Q}^n$ *and* $G \in \mathcal{G}^n$ *where* m *denotes the number of links in* G.

The potential function has the property that the marginal profit of a firm from adding or removing a link is exactly equivalent to the difference in the potential function from adding or removing a link. Similarly, the marginal profit of a firm from changing its output level is

[10] See also Ballester et al. [2006] and Jackson et al. [2015] for a more general discussion of the payoff function introduced in Equation (1).

[11] See supplementary Appendix B for further network definitions and characterizations.

exactly equivalent to the change of the potential function.[12] The potential function thus allows to aggregate the incentives of the firms to either change their links or adjust their production levels in a single global function. The existence of a potential function will be crucial for the equilibrium characterization of the network formation process that will be introduced in the following section.

2.2. Network Dynamics and Equilibrium Characterization

In the following we introduce a dynamic model where firms choose both output and links, based on the profit function of Equation (1). In this model the network is formed endogenously from the decisions of firms with whom to collaborate,[13] and share knowledge about a cost reducing technology. The opportunities for change arrive as a Poisson process [Blume, 1993; Sandholm, 2010], similar to Calvo models of pricing [Calvo, 1983]. We follow the *best response* dynamics analyzed in Cournot [1838]:[14] Firms maximize profits by taking the output levels and collaborations of the other firms as given. To capture the fact that R&D projects and collaborations are fraught with ambiguity and uncertainty [Czarnitzki et al., 2015; Kelly et al., 2002], we will introduce noise in this decision process. The precise definition of the dynamics of output adjustment and network evolution is given in the following.

Definition 1 (Cournot Best Response Dynamics). *The evolution of the population of firms and the collaborations between them is characterized by a sequence of states* $(\boldsymbol{\omega}_t)_{t\in\mathbb{R}_+}$, $\boldsymbol{\omega}_t \in \Omega = \mathcal{Q}^n \times \mathcal{G}^n$, *where each state* $\boldsymbol{\omega}_t = (\mathbf{q}_t, G_t)$ *consists of a vector of firms' output levels,* $\mathbf{q}_t \in \mathcal{Q}^n$, *and a network of collaborations,* $G_t \in \mathcal{G}^n$. *We assume that* $\mathcal{Q}$ *is a bounded output choice set of a firm. In a short time interval* $[t, t+\Delta t)$, $t \in \mathbb{R}_+$, *one of the following events happens:*

Output adjustment *At rate* $\chi \geq 0$ *a firm* $i \in \mathcal{N}$ *is receives an output adjustment opportunity. The profit of firm* i *from choosing an output level* $q \in \mathcal{Q}$ *is then given by* $\pi_i(q, \mathbf{q}_{-it}, G) + \varepsilon_{it}$. *When* ε_{it} *is identically and independently type-I extreme value distributed with parameter* ϑ,[15] *then the probability that an adjustment to an output level* q *conditional on the output levels of all other firms,* $\mathbf{q}_{-it}$, *and the network,* G_t, *at time* t *is profitable for firm* i *is given by*[16]

$$\mathbb{P}\left(\boldsymbol{\omega}_{t+\Delta t} = (q, \mathbf{q}_{-it}, G_t) | \boldsymbol{\omega}_t = (\mathbf{q}_t, G_t)\right) = \chi \frac{e^{\vartheta \pi_i(q, \mathbf{q}_{-it}, G_t)}}{\int_{\mathcal{Q}} e^{\vartheta \pi_i(q', \mathbf{q}_{-it}, G_t)} dq'} \Delta t + o(\Delta t). \tag{3}$$

Link formation *With rate* $\tau \geq 0$ *a pair of firms* i, j *which is not already connected receives an opportunity to form a link. The formation of a link depends on the marginal profits the firms receive from the link plus an additive pairwise i.i.d. error term* $\varepsilon_{ij,t}$. *The probability that link* (i, j) *is created is then given by* $\mathbb{P}\left(\boldsymbol{\omega}_{t+\Delta t} = (\mathbf{q}_t, G_t \oplus (i,j)) | \boldsymbol{\omega}_t = (\mathbf{q}_t, G_t)\right) =$

[12] More formally, the potential Φ has the property that for any $\mathbf{q} \in \mathcal{Q}^n$ and $G, G' \in \mathcal{G}^n$ with $G' = G \oplus (i,j)$ or $G' = G \ominus (i,j)$ we have that $\Phi(\mathbf{q}, G') - \Phi(\mathbf{q}, G) = \pi_i(\mathbf{q}, G') - \pi_i(\mathbf{q}, G)$, where $G \oplus (i,j)$ ($G \ominus (i,j)$) denotes the network obtained from G by adding (removing) the link (i,j). Moreover, for $q_i, q_i' \in \mathcal{Q}$, $\mathbf{q}_{-i} \in \mathcal{Q}^{n-1}$ and $G \in \mathcal{G}^n$ we have that $\Phi(q_i', \mathbf{q}_{-i}, G) - \Phi(q_i, \mathbf{q}_{-i}, G) = \pi_i(q_i', \mathbf{q}_{-i}, G) - \pi_i(q_i, \mathbf{q}_{-i}, G)$.

[13] Note that the formation of a collaboration requires the *mutual agreement* of both firms involved in a collaboration, while for the termination of a collaboration it is sufficient that one of the firms finds this profitable [Jackson and Watts, 2002].

[14] Cournot [1838] analyzed a dynamic process in which firms myopically best respond in the current period to the existing output levels of all rivals [cf. Daughety, 2005]. For similar network formation models see Jackson and Watts [2002]; Watts [2001]. The assumption of myopic agents is also common in incomplete information dynamic decision-making as considered in Gabaix [2014].

[15] For a type-I extreme value distributed random variable ε we have that $\mathbb{P}(\varepsilon \leq c) = e^{-e^{c/\zeta - \gamma}}$, where $\gamma \approx 0.58$ is Euler's constant. The mean is $\mathbb{E}(\varepsilon) = 0$ and the variance is given by $\mathrm{Var}(\varepsilon) = \frac{\pi^2 \zeta^2}{6}$.

[16] The multinomial choice probability can be derived from a random utility model where firms maximize profits subject to a random error term [Anderson et al., 2004; McFadden, 1976]. See supplementary Appendix D for more details.

$\tau\,\mathbb{P}\left(\{\pi_i(\mathbf{q}_t, G_t \oplus (i,j)) - \pi_i(\mathbf{q}_t, G_t) + \varepsilon_{ij,t} > 0\} \cap \{\pi_j(\mathbf{q}_t, G_t \oplus (i,j)) - \pi_j(\mathbf{q}_t, G_t) + \varepsilon_{ij,t} > 0\}\right)\Delta t + o(\Delta t)$. *Using the fact that* $\pi_i(\mathbf{q}_t, G_t \oplus (i,j)) - \pi_i(\mathbf{q}_t, G_t) = \pi_j(\mathbf{q}_t, G_t \oplus (i,j)) - \pi_j(\mathbf{q}_t, G_t) = \Phi(\mathbf{q}_t, G_t \oplus (i,j)) - \Phi(\mathbf{q}_t, G_t)$, *and assuming that the error term* $\varepsilon_{ij,t}$ *is independently logistically distributed,*[17] *we obtain*

$$\mathbb{P}\left(\boldsymbol{\omega}_{t+\Delta t} = (\mathbf{q}_t, G_t \oplus (i,j)) | \boldsymbol{\omega}_t = (\mathbf{q}_t, G_t)\right) = \tau \frac{e^{\vartheta \Phi(\mathbf{q}_t, G_t \oplus (i,j))}}{e^{\vartheta \Phi(\mathbf{q}_t, G_t \oplus (i,j))} + e^{\vartheta \Phi(\mathbf{q}_t, G_t)}} \Delta t + o(\Delta t). \quad (4)$$

Link removal *With rate* $\xi \geq 0$ *a pair of connected firms* i, j *receives an opportunity to terminate their collaboration. The link is removed if at least one firm finds this profitable. The marginal profits from removing the link* (i,j) *are perturbed by an additive pairwise i.i.d. error term* $\varepsilon_{ij,t}$. *The probability that the link* (i,j) *is removed is then given by* $\mathbb{P}\left(\boldsymbol{\omega}_{t+\Delta t} = (\mathbf{q}_t, G_t \ominus (i,j)) | \boldsymbol{\omega}_t = (\mathbf{q}_t, G_t)\right) = \xi\,\mathbb{P}(\{\pi_i(\mathbf{q}_t, G_t \ominus (i,j)) - \pi_i(\mathbf{q}_t, G_t) + \varepsilon_{ij,t} > 0\} \cup \{\pi_j(\mathbf{q}_t, G_t \ominus (i,j)) - \pi_j(\mathbf{q}_t, G_t) + \varepsilon_{ij,t} > 0\})\Delta t + o(\Delta t)$. *Using the fact that* $\pi_i(\mathbf{q}_t, G_t \ominus (i,j)) - \pi_i(\mathbf{q}_t, G_t) = \pi_j(\mathbf{q}_t, G_t \ominus (i,j)) - \pi_j(\mathbf{q}_t, G_t) = \Phi(\mathbf{q}_t, G_t \ominus (i,j)) - \Phi(\mathbf{q}_t, G_t)$, *and assuming that the error term is independently logistically distributed, we obtain*

$$\mathbb{P}\left(\boldsymbol{\omega}_{t+\Delta t} = (\mathbf{q}_t, G_t \ominus (i,j)) | \boldsymbol{\omega}_t = (\mathbf{q}_t, G_t)\right) = \xi \frac{e^{\vartheta \Phi(\mathbf{q}_t, G_t \ominus (i,j))}}{e^{\vartheta \Phi(\mathbf{q}_t, G_t \ominus (i,j))} + e^{\vartheta \Phi(\mathbf{q}_t, G_t)}} \Delta t + o(\Delta t). \quad (5)$$

We assume that the set $\mathcal{Q}$ is a discretization of the bounded interval $[0, \overline{q}]$, with $\overline{q} < \infty$. The fact that $\mathcal{Q}$ is a countable set allows us to use standard results for discrete state space, continuous time Markov chains [Norris, 1998]. For an increasingly fine discretization, we can then use Equation (3) as a continuous analogue of the standard multinomial logit probabilistic choice framework [see also Anderson et al., 2004, 2001; Ben-Akiva and Watanatada, 1981; McFadden, 1976], where the probability of choosing an output level is proportional to an exponential function of the firm's profit. The standard derivation of the logit model is based on the assumption that profits are subject to noise from a type-I extreme value distribution [Anderson et al., 1992].[18] The parameter ϑ is inversely related to the level of noise, so that in the limit of $\vartheta \to \infty$ the noise vanishes and firms choose the output level that maximizes their profit, while in the limit of $\vartheta \to 0$ the noise dominates and output adjustments in Equation (3) become random. The same holds for the link formation and removal decisions in Equations (4) and (5), respectively.[19]

Note that we can numerically implement the stochastic process introduced in Definition 1 using the "next reaction method" for simulating a continuous time Markov chain [Gibson and Bruck, 2000]. We will use this method throughout the paper to illustrate our theoretical predictions for various network statistics (see Figures 1 and 3). However, this method becomes computationally infeasible for large networks, where we have to rely on our theoretical equilibrium characterization and alternative simulation methods.

We next introduce some definitions and notations that allow us to characterize the stochastic

[17] Let z be i.i.d. logistically distributed with mean 0 and scale parameter ϑ, i.e. $F_z(x) = \frac{e^{\vartheta x}}{1+e^{\vartheta x}}$. Consider the random variable $\varepsilon = g(z) = -z$. Since g is monotonic decreasing, and z is a continuous random variable, the distribution of ε is given by $F_\varepsilon(y) = 1 - F_z(g^{-1}(y)) = \frac{e^{\vartheta y}}{1+e^{\vartheta y}}$.

[18] See supplementary Appendix D for a derivation of the multinomial logit model with a continuous choice set from a mulitnomial model with a discrete choice set [see also McFadden, 1976]. This illustrates that our framework can also be applied to cases where agents choose from an arbitrary discrete set of alternatives.

[19] While in Definition 1 pairs of firms are selected in a global way to form collaborations, it is possible to consider a local approach where new links are more likely to be formed among firms which already have a common neighbor [Jackson and Rogers, 2007]. This can be captured by a linking cost that is decreasing in the number of common neighbors of the firms. We explicitly consider such a formulation in the empirical model in Section 3.2.

process in Definition 1. Let $\mathcal{F}$ denote the smallest σ-algebra generated by $\sigma(\boldsymbol{\omega}_t : t \in \mathbb{R}_+)$. The filtration is the non-decreasing family of sub-σ-algebras $\{\mathcal{F}_t\}_{t\in\mathbb{R}_+}$ on the measure space $(\Omega, \mathcal{F})$, $\Omega = \mathcal{Q}^n \times \mathcal{G}^n$, with the property that $\mathcal{F}_0 \subseteq \mathcal{F}_1 \subseteq \cdots \subseteq \mathcal{F}_t \subseteq \cdots \subseteq \mathcal{F}$. The probability space is given by the triple $(\Omega, \mathcal{F}, \mathbb{P})$, where $\mathbb{P}\colon \mathcal{F} \to [0,1]$ is the probability measure satisfying $\int_\Omega \mathbb{P}(d\boldsymbol{\omega}) = 1$. As we will see below in Theorem 1 the sequence of states $(\boldsymbol{\omega}_t)_{t\in\mathbb{R}_+}$, $\boldsymbol{\omega}_t \in \Omega$, induces an irreducible and positive recurrent (i.e. ergodic) time homogeneous Markov chain.

The one step transition probability matrix $\mathbf{P}^\vartheta(t) : \Omega^2 \to [0,1]^{|\Omega|^2}$ has elements which determine the probability of a transition from a state $\boldsymbol{\omega} \in \Omega$ to a state $\boldsymbol{\omega}' \in \Omega$ in a small time interval $[t, t+\Delta t)$ of length Δt given by $\mathbb{P}(\boldsymbol{\omega}_{t+\Delta t} = \boldsymbol{\omega}' | \mathcal{F}_t = \sigma(\boldsymbol{\omega}_0, \boldsymbol{\omega}_1, \ldots, \boldsymbol{\omega}_t = \boldsymbol{\omega})) = \mathbb{P}(\boldsymbol{\omega}_{t+\Delta t} = \boldsymbol{\omega}' | \boldsymbol{\omega}_t = \boldsymbol{\omega}) = q^\vartheta(\boldsymbol{\omega}, \boldsymbol{\omega}')\Delta t + o(\Delta t)$ if $\omega' \neq \omega$ and $\mathbb{P}(\boldsymbol{\omega}_{t+\Delta t} = \boldsymbol{\omega} | \mathcal{F}_t = \sigma(\boldsymbol{\omega}_0, \boldsymbol{\omega}_1, \ldots, \boldsymbol{\omega}_t = \boldsymbol{\omega})) = \mathbb{P}(\boldsymbol{\omega}_{t+\Delta t} = \boldsymbol{\omega} | \boldsymbol{\omega}_t = \boldsymbol{\omega}) = 1 + q^\vartheta(\boldsymbol{\omega}, \boldsymbol{\omega})\Delta t + o(\Delta t)$, where $q^\vartheta(\boldsymbol{\omega}, \boldsymbol{\omega}')$ is the transition rate from state $\boldsymbol{\omega}$ to state $\boldsymbol{\omega}'$ and $\lim_{\Delta t \to 0} \frac{o(\Delta t)}{\Delta t} = 0$ (see Theorem 2.8.2 in Norris [1998]). From the stochastic process of Definition 1 we see that the transition rate matrix (or infinitesimal generator) $\mathbf{Q}^\vartheta = (q^\vartheta(\boldsymbol{\omega}, \boldsymbol{\omega}'))_{\boldsymbol{\omega}, \boldsymbol{\omega}' \in \Omega}$ of the Markov chain has the elements

$$q^\vartheta(\boldsymbol{\omega}, \boldsymbol{\omega}') = \begin{cases} \chi \frac{e^{\vartheta \pi_i(q', \mathbf{q}_{-i}, G)}}{\int_{\mathcal{Q}} e^{\vartheta \pi_i(q'', \mathbf{q}_{-i}, G)} dq''} & \text{if } \boldsymbol{\omega}' = (q', \mathbf{q}_{-i}, G) \text{ and } \boldsymbol{\omega} = (\mathbf{q}, G), \\ \tau \frac{e^{\vartheta \Phi(\mathbf{q}, G \oplus (i,j))}}{e^{\vartheta \Phi(\mathbf{q}, G \oplus (i,j))} + e^{\vartheta \Phi(\mathbf{q}, G)}} & \text{if } \boldsymbol{\omega}' = (\mathbf{q}, G \oplus (i,j)) \text{ and } \boldsymbol{\omega} = (\mathbf{q}, G), \\ \xi \frac{e^{\vartheta \Phi(\mathbf{q}, G \ominus (i,j))}}{e^{\vartheta \Phi(\mathbf{q}, G \ominus (i,j))} + e^{\vartheta \Phi(\mathbf{q}, G)}} & \text{if } \boldsymbol{\omega}' = (\mathbf{q}, G \ominus (i,j)) \text{ and } \boldsymbol{\omega} = (\mathbf{q}, G), \\ -\sum_{\boldsymbol{\omega}' \neq \boldsymbol{\omega}} q^\vartheta(\boldsymbol{\omega}, \boldsymbol{\omega}') & \text{if } \boldsymbol{\omega}' = \boldsymbol{\omega}, \\ 0 & \text{otherwise}, \end{cases} \tag{6}$$

with $\sum_{\boldsymbol{\omega}' \in \Omega} q^\vartheta(\boldsymbol{\omega}, \boldsymbol{\omega}') = 0$.[20] As the Markov chain is time homogeneous, the transition rates are independent of time. The stationary distribution $\mu^\vartheta : \Omega \to [0,1]$ is then the solution to $\mu^\vartheta \mathbf{P}^\vartheta = \mu^\vartheta$, or equivalently $\mu^\vartheta \mathbf{Q}^\vartheta = \mathbf{0}$ [Norris, 1998].

With the potential function Φ of Proposition 1 we can compute the stationary distribution of the Cournot best response dynamics in the form of a Gibbs measure [Grimmett, 2010].

Theorem 1. *The stochastic process $(\boldsymbol{\omega}_t)_{t\in\mathbb{R}_+}$ with states $\boldsymbol{\omega}_t \in \Omega = \mathcal{Q}^n \times \mathcal{G}^n$ is an ergodic Markov chain with a unique stationary distribution $\mu^\vartheta\colon \Omega \to [0,1]$ such that $\lim_{t\to\infty} \mathbb{P}(\boldsymbol{\omega}_t = (\mathbf{q}, G) | \boldsymbol{\omega}_0 = (\mathbf{q}_0, G_0)) = \mu^\vartheta(\mathbf{q}, G)$. The distribution μ^ϑ is given by*

$$\mu^\vartheta(\mathbf{q}, G) = \frac{e^{\vartheta(\Phi(\mathbf{q}, G) - m \ln\left(\frac{\xi}{\tau}\right))}}{\sum_{G' \in \mathcal{G}^n} \int_{\mathcal{Q}^n} e^{\vartheta(\Phi(\mathbf{q}', G') - m' \ln\left(\frac{\xi}{\tau}\right))} d\mathbf{q}'}, \tag{7}$$

for any $\mathbf{q} \in \mathcal{Q}^n$ and $G \in \mathcal{G}^n$.

From Theorem 1 we know that the Markov chain is ergodic, so that the Ergodic Theorem applies [Norris, 1998], which states that

$$\lim_{t\to\infty} \frac{1}{t} \int_0^t \mathbb{1}_{\{\omega_s \in \mathcal{A}\}} ds = \mu^\vartheta(\mathcal{A}), \quad \mathbb{P}\text{-a.s.}, \tag{8}$$

for any measurable set $\mathcal{A} \in \Omega$, and long-run averages of sample paths converge to the invariant

[20] The transition rate matrix satisfies the Chapman-Kolmogorov forward equation $\frac{d}{dt}\mathbf{P}^\vartheta(t) = \mathbf{P}^\vartheta(t)\mathbf{Q}^\vartheta$ so that $\mathbf{P}^\vartheta(t) = \mathbf{I}_{|\Omega|} + \mathbf{Q}^\vartheta \Delta t + o(\Delta t)$ [Norris, 1998]. Conversely, we have that $\mathbf{Q}^\vartheta = \lim_{\Delta t \to 0} \frac{\mathbf{P}^\vartheta(t+\Delta t) - \mathbf{I}_{|\Omega|}}{\Delta t}$.

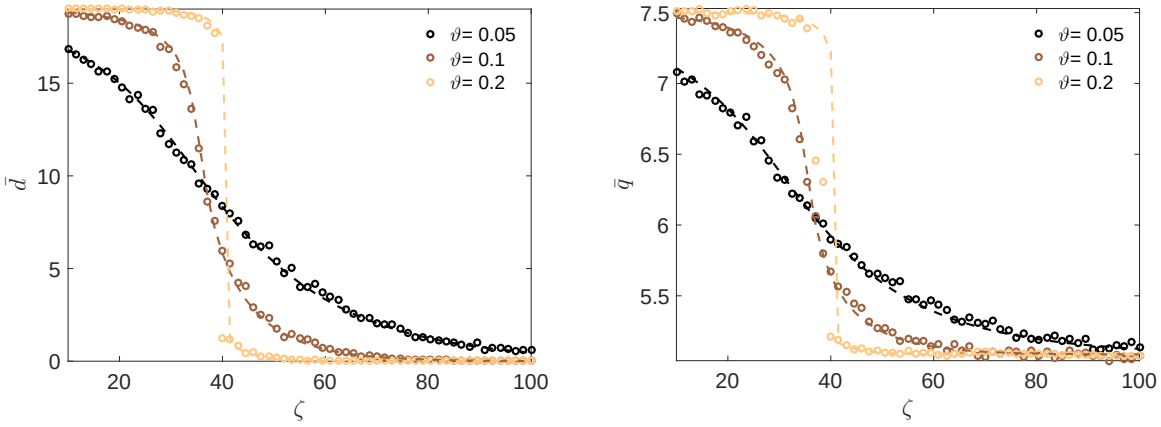

Figure 1: The average degree $\bar{d}$ (left panel) and the average output $\bar{q}$ (right panel) as a function of the linking cost ζ for varying values of $\vartheta \in \{0.05, 0.1, 0.2\}$ with $n = 20$ firms and $\tau = \xi = \chi = 1$, $\eta = 300$, $\rho = 1$, $b = 1$ and $\nu = 20$. Dashed lines indicate the theoretical predictions of Equations (10) and Equation (12) in Proposition 2, respectively.

distribution. Moreover, for any measurable function $f : (\Omega, \mathcal{F}) \to (\mathbb{R}, \mathcal{B})$ in $L^1(\mathbb{P})$ we have that

$$\lim_{t\to\infty} \frac{1}{t} \int_0^t f(\omega_s)\, ds = \mathbb{E}_{\mu^\vartheta}(f), \quad \mathbb{P}\text{-a.s.},$$

where $\mathbb{E}_{\mu^\vartheta}(f)$ is the expected value of f under the invariant probability measure μ^ϑ. Note that the stationary distribution μ^ϑ in Equation (7) does not depend on the output adjustment rate χ. It also does not depend on the link adjustment rates τ and ξ, when the rates for link creation and removal are the same. In the following we will make the simplifying assumption that $\tau = \xi$.

In the limit of vanishing noise, i.e., $\vartheta \to \infty$, we call the states in the support of μ^ϑ the *stochastically stable* states [Jackson and Watts, 2002; Kandori et al., 1993]. A state $(\mathbf{q}, G) \in \Omega$ is stochastically stable if $\lim_{\vartheta\to\infty} \mu^\vartheta(\mathbf{q}, G) > 0$. In the following we will denote $\mu^*(\mathbf{q}, G) \equiv \lim_{\vartheta\to\infty} \mu^\vartheta(\mathbf{q}, G)$. The set of stochastically stable states is denoted by $\Omega^* \subseteq \Omega$. From the Gibbs distribution in Equation (7) it follows that $(\mathbf{q}, G) \in \Omega^*$ if and only if $\Phi(\mathbf{q}, G) \geq \Phi(\mathbf{q}', G')\ \forall \mathbf{q}' \in \mathcal{Q}^n$ and $\forall G' \in \mathcal{G}^n$.

As the potential function Φ in Equation (2) is continuous on the compact set Ω it has a global maximum, stochastically stable states always exist and $\Omega^* \neq \emptyset$. An explicit characterization of the stationary distribution μ^ϑ in Equation (7) requires the computation of the *partition function*

$$\mathscr{Z}_\vartheta = \sum_{G\in\mathcal{G}^n} \int_{\mathcal{Q}^n} e^{\vartheta\Phi(\mathbf{q},G)} d\mathbf{q}, \tag{9}$$

so that we can write $\mu^\vartheta(\mathbf{q}, G) = \frac{1}{\mathscr{Z}_\vartheta} e^{\vartheta\Phi(\mathbf{q},G)}$ for any $\mathbf{q} \in \mathcal{Q}^n$ and $G \in \mathcal{G}^n$. We also introduce the *Hamiltonian*, defined by $\mathscr{H}_\vartheta(\mathbf{q}) \equiv \frac{1}{\vartheta} \ln\left(\sum_{G\in\mathcal{G}^n} e^{\vartheta\Phi(\mathbf{q},G)}\right)$, which allows us to write the partition function more compactly as $\mathscr{Z}_\vartheta = \int_{\mathcal{Q}^n} e^{\vartheta\mathscr{H}_\vartheta(\mathbf{q})} d\mathbf{q}$.

In the following we provide an explicit characterization of the Gibbs distribution in Theorem 1 and derive the stochastically stable states. We first consider the special case of ex ante homogeneous firms with identical marginal costs.

Proposition 2. *Consider homogeneous firms such that $\eta_i = \eta$ in the profit function of Equation (1) for all $i = 1, \ldots, n$, and let the evolution of the firms' output levels and collaborations be governed by the stochastic process in Definition 1. Denote $\eta^* \equiv \eta/(n-1)$ and $\nu^* \equiv \nu/(n-1)$. Moreover, let the empirical average output be denoted by $\bar{q} \equiv \frac{1}{n}\sum_{i=1}^n q_i$ and the average degree be $\bar{d} \equiv \frac{1}{n}\sum_{i=1}^n d_i$. Further, let the empirical degree distribution be given by $\bar{P}^\vartheta(k) \equiv \frac{1}{n}\sum_{i=1}^n \mathbb{1}_{\{d_i=k\}}$, and be denoted by $P^\vartheta(k) \equiv \mathbb{E}_{\mu^\vartheta}\left(\bar{P}^\vartheta(k)\right)$.*

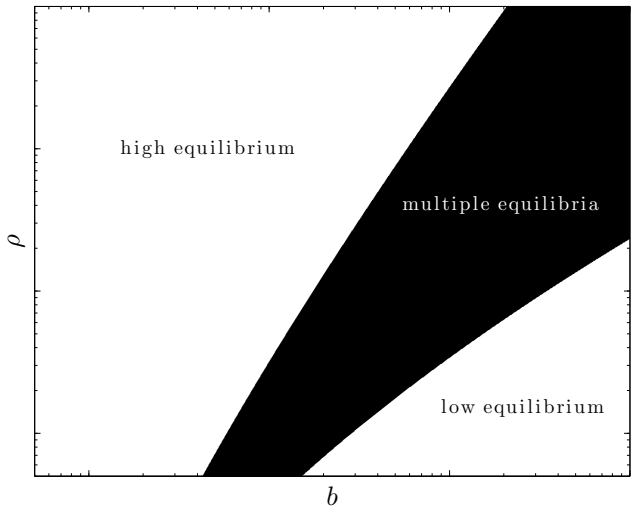

Figure 2: A phase diagram illustrating the regions with a unique and with multiple equilibria according to Equation (10) in Proposition 2 for varying values of $b \in \{0, \ldots, 0.01\}$ and $\rho \in \{0, \ldots, 0.01\}$ with $n = 100$, $\nu = 0.5$, $\eta = 100$ $\vartheta = 1$ and $\zeta = 50$.

(i) Let $q^* \in \mathcal{Q}$ be the root of

$$(b + 2\nu^*)q - \eta^* = \frac{\rho}{2}\left(1 + \tanh\left(\frac{\vartheta}{2}\left(\rho q^2 - \zeta\right)\right)\right) q, \tag{10}$$

which has at least one solution if $b+2\nu^* > \rho$. Then, $\bar{q} \xrightarrow{a.s.} q^*$. Moreover, for large n, the firms' output levels become independent Gaussian distributed random variables, $q_i \xrightarrow{d} \mathcal{N}(q^*, \sigma^2)$, with mean q^* and variance $\sigma^2 = n/\left(2\vartheta\nu^* + \vartheta^2(bq^* - \eta^* + 2\nu^* q^*)(q^*(b + 2\nu^* - \rho) - \eta^*)\right)$. The degree d_i of firm i follows a mixed Poisson distribution with mixing parameter $\int_{\mathcal{Q}} p^\vartheta(q, q')\mu^\vartheta(dq')$, where $p^\vartheta(q, q') = e^{\vartheta(\rho q q' - \zeta)}/(1 + e^{\vartheta(\rho q q' - \zeta)})$, and for any $1 < m \leq n$ the degrees $d_1, \ldots, d_m$ are asymptotically independent. In particular,

$$P^\vartheta(k) = \mathbb{E}_{\mu^\vartheta}\left(\frac{e^{-\bar{d}(q_1)}\bar{d}(q_1)^k}{k!}\right)(1 + o(1)), \tag{11}$$

where the expected degree for large ϑ is given by

$$\mathbb{E}_{\mu^\vartheta}\left(\bar{d}\right) = \frac{n-1}{2}\left(1 + \tanh\left(\frac{\vartheta}{2}\left(\rho(q^*)^2 - \zeta\right)\right)\right) + \frac{1}{2\vartheta}\mathscr{R}_\vartheta, \tag{12}$$

q^* is given by Equation (10) and the expression of the remainder term $\mathscr{R}_\vartheta$ can be found in the proof of the proposition.

(ii) For $\vartheta \to \infty$, in the stochastically stable state, the probability measure μ^* is concentrated on

$$q^* = \begin{cases} \frac{\eta^*}{b+2\nu^*-\rho}, & \text{if } \zeta < \frac{\rho(\eta^*)^2}{(b+2\nu^*)^2}, \\ \left\{\frac{\eta^*}{b+2\nu^*-\rho}, \frac{\eta^*}{b+2\nu^*}\right\}, & \text{if } \frac{\rho(\eta^*)^2}{(b+2\nu^*)^2} < \zeta < \frac{\rho(\eta^*)^2}{(b+2\nu^*-\rho)^2}, \\ \frac{\eta^*}{b+2\nu^*}, & \text{if } \frac{\rho(\eta^*)^2}{(b+2\nu^*-\rho)^2} < \zeta, \end{cases} \tag{13}$$

and we refer to the two possible output levels in Equation (13) as the high equilibrium *and the* low equilibrium*, respectively. The expected average degree in the high equilibrium is $\mathbb{E}_{\mu^*}\left(\bar{d}\right) = \lim_{\vartheta\to\infty}\mathbb{E}_{\mu^\vartheta}\left(\bar{d}\right) = n - 1$, which corresponds to a complete graph, K_n, and $\mathbb{E}_{\mu^*}\left(\bar{d}\right) = \lim_{\vartheta\to\infty}\mathbb{E}_{\mu^\vartheta}\left(\bar{d}\right) = 0$ in the low equilibrium, which corresponds to an empty graph, $\overline{K}_n$.*

Figure 1 shows the average output $\bar{q}$ of Equation (10) and the average degree $\bar{d}$ of Equation (12) in part (i) Proposition 2 as a function of the linking cost ζ. With increasing cost, both the

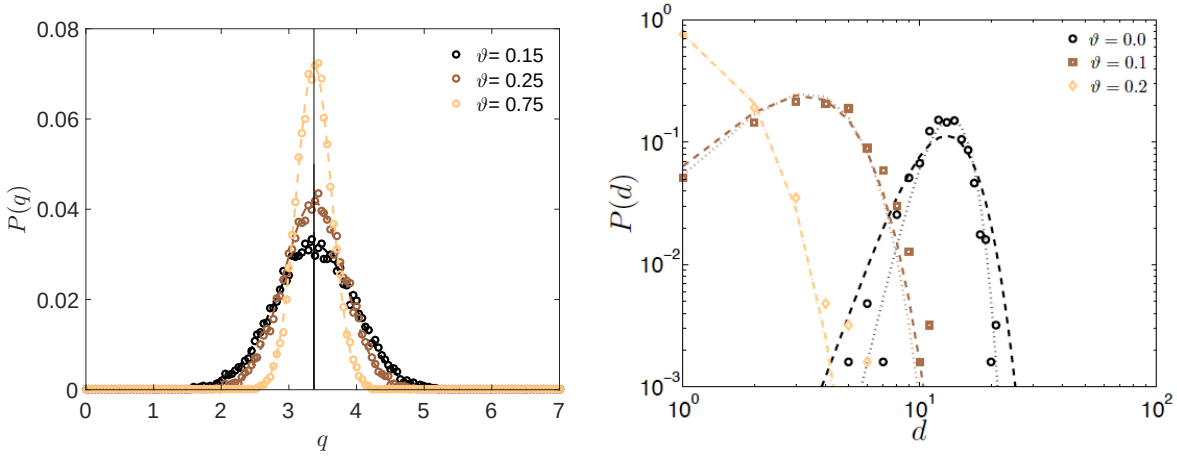

Figure 3: (Left panel) The stationary output distribution $P(q)$ for $n = 50$, $\eta = 150$, $b = 0.5$, $\nu = 10$, $\rho = 1$, $\vartheta \in \{0.1, 0.25, 0.75\}$ and $\zeta = 60$. Dashed lines indicate the normal distribution $\mathcal{N}(q^*, \sigma^2)$ of part(i) of Proposition 2). (Right panel) The stationary degree distribution $P(k)$ for the same parameter values. The dashed lines indicate the solution in Equation (11) of Proposition 2.

network connectivity and the output produced are decreasing. The transition from an economy with high output and collaboration intensity to an economy with low output and collaboration intensity is becoming sharper as ϑ increases, consistent with the limit of part (ii) in Proposition 2. An illustration of μ^ϑ of the output distribution $\mathcal{N}(q^*, \sigma^2)$ in part (i) of Proposition 2 together with the results of numerical simulations can be seen in the left panel in Figure 3. The figure shows that the analytic prediction reproduces the simulation results fairly well even for small values of ϑ. A phase diagram illustrating the regions with a unique and with multiple equilibria according to Equation (10) can be seen in Figure 2. Note that the stationary output levels in Equation (10) are increasing in ρ and η, and decreasing in ζ and b (see also Figure 1 in Appendix A). The latter implies that both higher collaboration cost (weaker spillovers) and more intense competition (larger market size/lower production costs) decrease overall production.

We next consider the more general case of firms with heterogeneous marginal production costs.

Proposition 3. *Let the firms' profits be given by Equation (1), and let the evolution of the firms' output levels and collaborations be governed by the stochastic process in Definition 1.*

(i) For any $\mathbf{q} \in \mathcal{Q}^n$ *and* $G \in \mathcal{G}^n$ *the stationary distribution of Equation (7) can be written as* $\mu^\vartheta(\mathbf{q}, G) = \mu^\vartheta(G|\mathbf{q})\mu^\vartheta(\mathbf{q})$*, where, for large* ϑ*, the marginal distribution* $\mu^\vartheta(\mathbf{q})$ *of the firms' output levels is asymptotically Gaussian and given by*

$$\mu^\vartheta(\mathbf{q}) = \left(\frac{2\pi}{\vartheta}\right)^{-\frac{n}{2}} |-\Delta\mathscr{H}_\vartheta(\mathbf{q}^*)|^{\frac{1}{2}} \exp\left\{-\frac{1}{2}\vartheta(\mathbf{q}-\mathbf{q}^*)^\top(-\Delta\mathscr{H}_\vartheta(\mathbf{q}^*))(\mathbf{q}-\mathbf{q}^*)\right\} + o\left(\|\mathbf{q}-\mathbf{q}^*\|^2\right), \tag{14}$$

with mean $\mathbf{q}^* \in \mathcal{Q}^n$ *solving* $q_i^* = \eta_i + \sum_{j\neq i}^n \left(\frac{\rho}{2}\left(1+\tanh\left(\frac{\vartheta}{2}\left(\rho q_i^* q_j^* - \zeta\right)\right)\right) - b\right) q_j^*$*, and variance-covariance matrix given by the inverse of* $-\Delta\mathscr{H}_\vartheta(\mathbf{q}^*)$*,*[21] *while the conditional distribution* $\mu^\vartheta(G|\mathbf{q})$ *is given by*

$$\mu^\vartheta(G|\mathbf{q}) = \prod_{i=1}^n \prod_{j=i+1}^n \frac{e^{\vartheta a_{ij}(\rho q_i q_j - \zeta)}}{1 + e^{\vartheta(\rho q_i q_j - \zeta)}}, \tag{15}$$

for any $\mathbf{q} \in \mathcal{Q}^n$ *and* $G \in \mathcal{G}^n$*, which corresponds to an inhomogeneous random graph with*

[21] The variance-covariance matrix can be computed in closed form: $(\Delta\mathscr{H}_\vartheta(\mathbf{q}))_{ii} = \frac{\vartheta\rho^2}{4}\sum_{j\neq i}^n q_j^2\left(1-\tanh\left(\frac{\vartheta}{2}\left(\rho q_i q_j - \zeta\right)\right)^2\right) - 1$, and $(\Delta\mathscr{H}_\vartheta(\mathbf{q}))_{ij} = \frac{\rho}{2}\left(1+\tanh\left(\frac{\vartheta}{2}\left(\rho q_i q_j - \zeta\right)\right)\right)$ $\left(1 + \frac{\vartheta\rho}{2} q_i q_j \left(1-\tanh\left(\frac{\vartheta}{2}\left(\rho q_i q_j - \zeta\right)\right)\right)\right) - b$, for $j \neq i$.

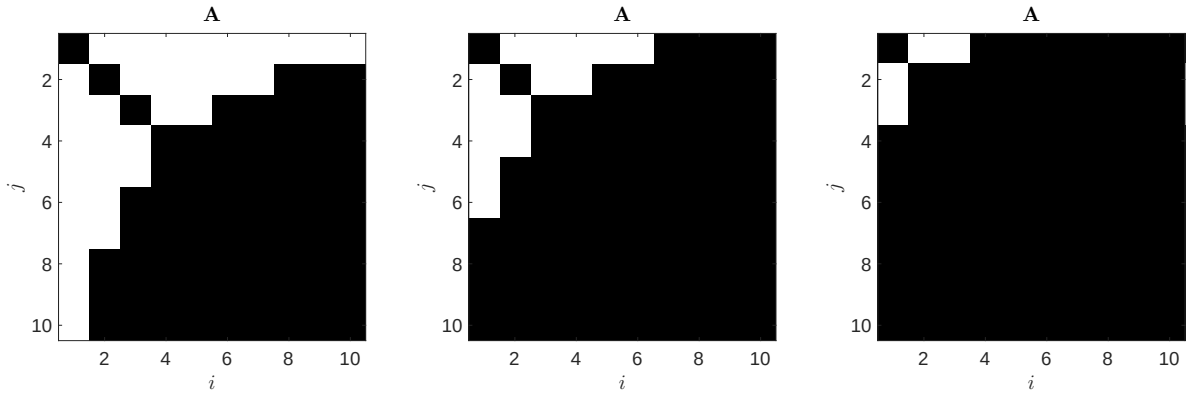

Figure 4: The (stepwise) adjacency matrix $\mathbf{A} = (a_{ij})_{1\leq i,j\leq n}$, characteristic of a nested split graph, with elements given by $a_{ij} = \mathbb{1}_{\left\{q_i q_j > \frac{\zeta}{\rho}\right\}}$, where the vector $\mathbf{q}$ is the solution to Equation (17) in Proposition 3. The panels from the left to the right correspond to increasing linking costs $\zeta \in \{0.0075, 0.01, 0.02\}$. The parameters used are $n = 10$, $\nu = 0.5$, $b = 0.06$, $\rho = 0.02$ and $\boldsymbol{\eta} = (1.00, 0.71, 0.58, 0.50, 0.45, 0.41, 0.38, 0.35, 0.33, 0.32)^\top$.

linking probability

$$p^\vartheta(q_i, q_j) = \frac{e^{\vartheta(\rho q_i q_j - \zeta)}}{1 + e^{\vartheta(\rho q_i q_j - \zeta)}}. \tag{16}$$

(ii) In the limit of $\vartheta \to \infty$, the stochastically stable network $G \in \mathcal{G}^n$ in the support of μ^* is a nested split graph in which a link between the pair of firms i and j is present if and only if $\rho q_i q_j > \zeta$, and the output profile, $\mathbf{q} \in \mathcal{Q}^n$, is the fixed point to the following system of equations

$$q_i = \frac{\eta_i}{2\nu} + \frac{1}{2\nu} \sum_{j \neq i}^{n} q_j \left(\rho \mathbb{1}_{\{\rho q_i q_j > \zeta\}} - b \right), \quad \mu^*\text{-a.s.}. \tag{17}$$

Moreover, if firms i and j are such that $\eta_i > \eta_j$ then i has a higher output than j, $q_i > q_j$ and a larger number of collaborations, $d_i > d_j$, μ^*-a.s..

(iii) Assume that $(\eta_i)_{i=1}^n$ are identically and independently Pareto distributed with density function $f(\eta) = (\gamma - 1)\eta^{-\gamma}$ for $\eta \geq 1$. Denote $\mathbf{M} \equiv \mathbf{I}_n + b\mathbf{B} - \rho\mathbf{A}$, where $\mathbf{B}$ is an $n \times n$-dim. matrix of ones with zero diagonal and $\mathbf{A}$ has elements $a_{ij} = \mathbb{1}_{\{\rho q_i q_j > \zeta\}}$. Then the stochastically stable output distribution is given by $\mu^*(\mathbf{q}) = (\gamma - 1)^n |\det(\mathbf{M})| \prod_{i=1}^n (\mathbf{M}\mathbf{q})_i^{-\gamma}$. In particular, for $\mathbf{q} = c\mathbf{u}$, with $c > 0$, and $\mathbf{u}$ being an n-dim. vector of ones, we have that $\mu^*(c\mathbf{u}) \sim \prod_{i=1}^n O\left(c^{-\gamma}\right)$ as $c \to \infty$, i.e., the output levels are asymptotically independently Pareto distributed.

Note that the marginal probability derived in Equation (14) will be important for our estimation algorithm introduced in Section 3.3.1. Moreover, Figure 4 shows the adjacency matrix $\mathbf{A} = (a_{ij})_{1\leq i,j\leq n}$ whose elements are given by $a_{ij} = \mathbb{1}_{\left\{q_i q_j > \frac{\zeta}{\rho}\right\}}$ and the vector $\mathbf{q}$ is the solution to Equation (17) in part (ii) of Proposition 3. We observe that firms with higher η_i also have higher output levels, q_i, in the stationary state. Moreover, the corresponding adjacency matrix is stepwise, characterizing a nested split graph,[22] and becomes increasingly sparse with increasing linking cost ζ. The fact that empirical R&D networks are characterized by nestedness has been documented in Tomasello et al. [2016]. Further, note that nested split graphs are paramount examples of core-periphery networks [Hojman and Szeidl, 2008]. The core-periphery structure of R&D alliance networks has also been documented empirically in Kitsak et al. [2010] and Rosenkopf and Schilling [2007]. Our model thus provides a theoretical explanation for why real-world R&D networks exhibit such a core-periphery structure. Moreover, Kitsak et al. [2010]

[22] A nested split graph is characterized by the fact that the neighborhood of every node is contained in the neighborhoods of the nodes with higher degrees [König et al., 2014a; Mahadev and Peled, 1995]. See supplementary Appendix B for the definition of nested split graphs.

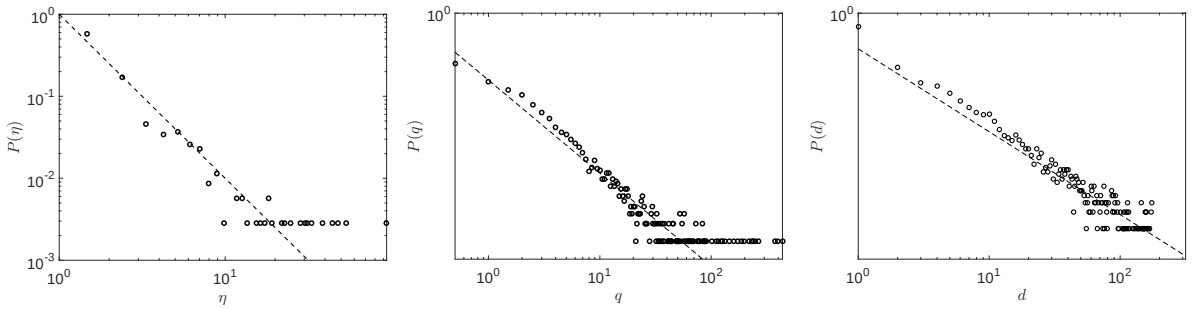

Figure 5: The distribution $P(\eta)$ of η following a Pareto distribution with exponent 2 (left panel), the resulting stationary output distribution $P(q)$ (middle panel) and the degree distribution $P(d)$ (right panel) from a numerical simulation of the stochastic process of Definition 1. Dashed lines indicate a power-law fit. Observe that $P(\eta)$ and $P(q)$ exhibit a power law tail with the same exponent, consistent with part (iii) of Proposition 3. The parameters used are $n = 350$, $\nu = 0.95$, $b = 0.75$, $\rho = 2$ and $\zeta = 75$.

find that firms in the core have a higher market value, consistent with the predictions of our model. More productive firms have lower marginal costs of production, and thus higher output, R&D expenditures, and can form more links, which makes them more central in the network.

When the firms' marginal costs are not exogenously given, but when the $(\eta_i)_{i=1}^n$ follow a power law distribution (which would correspond to Pareto distributed productivity levels that have been documented for example in König et al. [2016]), then part (iii) of Proposition 3 shows that the stationary output distribution is also a power law. The resulting degree distribution will then also be a power law.[23] An example based on a numerical simulation of the stochastic process of Definition 1 can be seen in Figure 5. Our model can thus provide an explanation for the joint occurrence of heavy tailed distributions not only in the firms' sizes [Gabaix, 2016], but also in their degrees [Powell et al., 2005].

2.3. Efficiency

Social welfare, W, is given by the sum of consumer surplus, U, and firms' profits, Π. Consumer surplus is given by $U(\mathbf{q}) = \frac{1}{2}\sum_{i=1}^n q_i^2 + \frac{b}{2}\sum_{i=1}^n \sum_{j\neq i}^n q_i q_j$ (see supplementary Appendix C, Footnote 13). In the special case of non-substitutable goods, when $b \to 0$, we obtain $U(\mathbf{q}) = \frac{1}{2}\sum_{i=1}^n q_i^2$, while in the case of perfectly substitutable goods, when $b \to 1$, we get $U(\mathbf{q}) = \frac{1}{2}\left(\sum_{i=1}^n q_i\right)^2$. Producer surplus is given by aggregate profits $\Pi(\mathbf{q}, G) = \sum_{i=1}^n \pi_i(\mathbf{q}, G)$. As a result, assuming

[23] Note that in the limit of $\vartheta \to \infty$ the linking probability between two firms with output levels q and q', respectively, is given by Equation (16):

$$\lim_{\vartheta\to\infty} p^\vartheta(q, q') = \lim_{\vartheta\to\infty} \frac{e^{\vartheta(\rho q q' - \zeta)}}{1 + e^{\vartheta(\rho q q' - \zeta)}} = \mathbb{1}_{\{\rho q q' > \zeta\}} = \mathbb{1}_{\left\{\log q + \log q' > \log\left(\frac{\zeta}{\rho}\right)\right\}}. \tag{18}$$

When the output levels are power law distributed, with density $f(x) = \frac{\gamma}{c}\left(\frac{c}{x}\right)^{\gamma+1}$ for $x > c$, where $c > 0$ is a lower-cut-off and $\gamma > 0$ is a positive parameter, then the log-ouptut levels, $\ln q$, follow an exponential distribution with density $f(y) = \gamma c^\gamma e^{-\gamma y}$.The linking probability in Equation (18) then induces an inhomogenous random graph identical to the one analyzed in Boguná and Pastor-Satorras [2003] (see also Appendix B). In particular, the authors show that this random graph is characterized by a power law degree distribution, a negative clustering degree correlation and a decaying average nearest neighbor degree distribution indicating a dissortative network. In Section 2.4.1 and Appendix E.1 we discuss how such network characteristics can also be obtained when firms are heterogeneous in terms of their marginal collaboration costs.

homogeneous firms, total welfare is equal to

$$W(\mathbf{q},G) = U(\mathbf{q}) + \Pi(\mathbf{q},G) = \frac{1}{2}\sum_{i=1}^{n} q_i^2 + \frac{b}{2}\sum_{i=1}^{n}\sum_{j\neq i}^{n} q_i q_j + \sum_{i=1}^{n}\pi_i(\mathbf{q},G)$$
$$= \frac{1}{2}\sum_{i=1}^{n} q_i^2 + \frac{b}{2}\sum_{i=1}^{n}\sum_{j\neq i}^{n} q_i q_j + \sum_{i=1}^{n}\left(\eta q_i - \nu q_i^2 - b\sum_{j\neq i}^{n} q_i q_j + \rho\sum_{j=1}^{n} a_{ij} q_i q_j\right) - 2\zeta m, \quad (19)$$

where m denotes the number of links in G. The efficient state is then defined by the network $G^* \in \mathcal{G}^n$ and output profile $\mathbf{q}^* \in \mathcal{Q}^n$ that maximize welfare $W(\mathbf{q},G)$ in Equation (19), that is, $W(\mathbf{q}^*,G^*) \geq W(\mathbf{q},G)$ for all $G \in \mathcal{G}^n$ and $\mathbf{q} \in \mathcal{Q}^n$.[24] The following proposition shows that the decentralized equilibrium is efficient only when the linking costs are sufficiently high. Otherwise, equilibrium networks are under-connected, and production is too low compared to what would be socially optimal.

Proposition 4. *Let the firms' profits be given by Equation (1), define welfare as in Equation (19), and let the evolution of the firms' output levels and collaborations be governed by the stochastic process in Definition 1. Further, denote $\eta^* \equiv \eta/(n-1)$ and $\nu^* \equiv \nu/(n-1)$.*

(i) In the case of homogeneous firms such that $\eta_i = \eta$ for all $i = 1,\ldots,n$, the efficient network $G^* \in \mathcal{G}^n$ and output profile $\mathbf{q}^* \in \mathcal{Q}^n$ are given by $q^*\mathbf{u}$, with $\mathbf{u}$ denoting an n-dimensional vector of ones, and

$$(q^*,G^*) = \begin{cases} \left(\frac{\eta^*}{b+2(\nu^*-\rho)-\frac{1}{n-1}}, K_n\right), & \text{if } \zeta \leq \zeta^*, \\ \left(\frac{\eta^*}{b+2\nu^*-\frac{1}{n-1}}, \overline{K}_n\right), & \text{if } \zeta^* < \zeta, \end{cases} \quad (20)$$

where K_n denotes the complete graph, $\overline{K}_n$ denotes the empty graph and

$$\zeta^* = \frac{\rho\,(\eta^*)^2}{\left(b+2\nu^*-\frac{1}{n-1}\right)\left(b+2(\nu^*-\rho)-\frac{1}{n-1}\right)}. \quad (21)$$

Moreover, in the limit of $\vartheta \to \infty$ the stochastically stable equilibrium network is efficient if $\zeta > \zeta^*$, μ^*-a.s..

(ii) In the case of heterogeneous firms, the efficient network $G^* \in \mathcal{G}^n$ is a nested split graph, where the output profile $\mathbf{q}^* \in \mathcal{Q}^n$ is the solution to the following system of equations

$$q_i = \frac{\eta_i}{2\nu-1} + \frac{1}{2\nu-1}\sum_{j\neq i}^{n} q_j\left(\rho\mathbb{1}_{\{\rho q_i q_j > \zeta\}} - b\right). \quad (22)$$

Further, when Equation (22) admits an interior solution, then the stochastically stable equilibrium output (and R&D expenditures) and the collaboration intensity are too low compared to the social optimum (μ^*-a.s.).

The left panel of Figure 6 shows welfare as a function of the linking cost ζ for varying values of ϑ, while the right panel shows the ratio of welfare relative to welfare in the efficient graph in

[24] Observe that this is different from the efficiency analysis in Ballester et al. [2006], where the planner chooses links, but not the effort levels, and there are not linking costs. It is also different from the efficiency analysis in Hiller [2013] and Belhaj et al. [2016], where global substitutability effects are not taken into account.

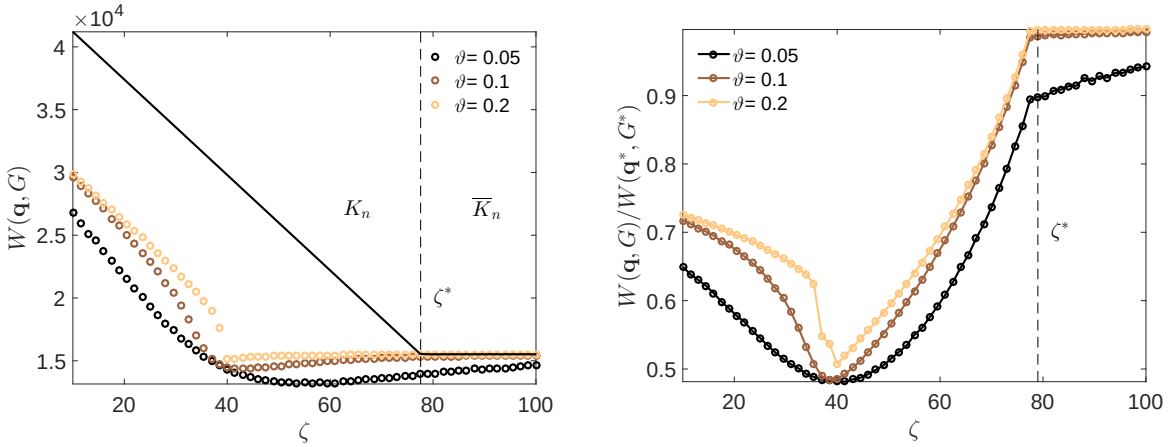

Figure 6: (Left panel) Welfare $W(\mathbf{q}, G)$ as a function of the linking cost ζ for varying values of $\vartheta \in \{0.05, 0.1, 0.2\}$ with $n = 20$ firms and $\tau = \xi = \chi = 1$, $\eta = 300$, $\rho = 1$, $b = 1$ and $\nu = 20$. The solid line indicates welfare in the efficient graph of Proposition 4 (which is either complete or empty). (Right panel) The ratio of welfare relative to welfare in the efficient graph.

the case of homogeneous firms considered in part (i) of Proposition 4. It illustrates the region of inefficiency of the equilibrium network for linking costs $\zeta < \zeta^*$, where equilibrium networks typically tend to be under-connected.[25] As similar observation can also be made for heterogeneous firms considered in part (ii) of Proposition 4. In Section 4.3 we analyze the welfare improving impact of a subsidy on firms' R&D collaboration costs, that motivates firms to form collaborations and thus increases the network connectivity.

2.4. Extensions

The model presented so far can be extended in a number of different directions that account for firm heterogeneity, which are summarized below and described in greater detail in supplementary Appendix E.

2.4.1. Heterogeneous Collaboration Costs

We can extend the model by assuming that firms with higher productivity incur lower collaboration costs (see also supplementary Appendix E.1). One can show that a similar equilibrium characterization using a Gibbs measure as in Theorem 1 is possible. Moreover, in the special case that the productivity is power law distributed, one can show that the degree distribution also follows a power law distribution (see Proposition 5),[26] consistent with previous empirical studies of R&D networks [see e.g., Powell et al., 2005], together with other empirically relevant correlations (see Propositions 6 and 7).[27]

[25] In contrast, when the linking costs are very high, then the R&D externalities are not high enough to compensate for the costs of maintaining the network, and so the social planner prefers not to form any links. In this high cost region also the individual firms do not want to form links, so that the social planners solution and the decentralized equilibrium coincide.

[26] In particular, assume that the productivity s are distributed as a power law $s^{-\gamma}$ with exponent γ. Then one can show that the asymptotic degree distribution is also power law distributed, $P(k) \sim k^{-\frac{\gamma}{\gamma-1}}$, with exponent $\frac{\gamma}{\gamma-1}$.

[27] We note that also other statistics such as the clustering degree distribution can be computed. See supplementary Appendix E.2 for further details. In particular, under the assumptions of a power law productivity distribution, we can generate two-vertex and three-vertex degree correlations, such as a decreasing average nearest neighbor connectivity, $k_{\rm nn}(d)$, indicating a dissortative network, as well as a decreasing clustering degree distribution, $C(d)$, with the degree d.

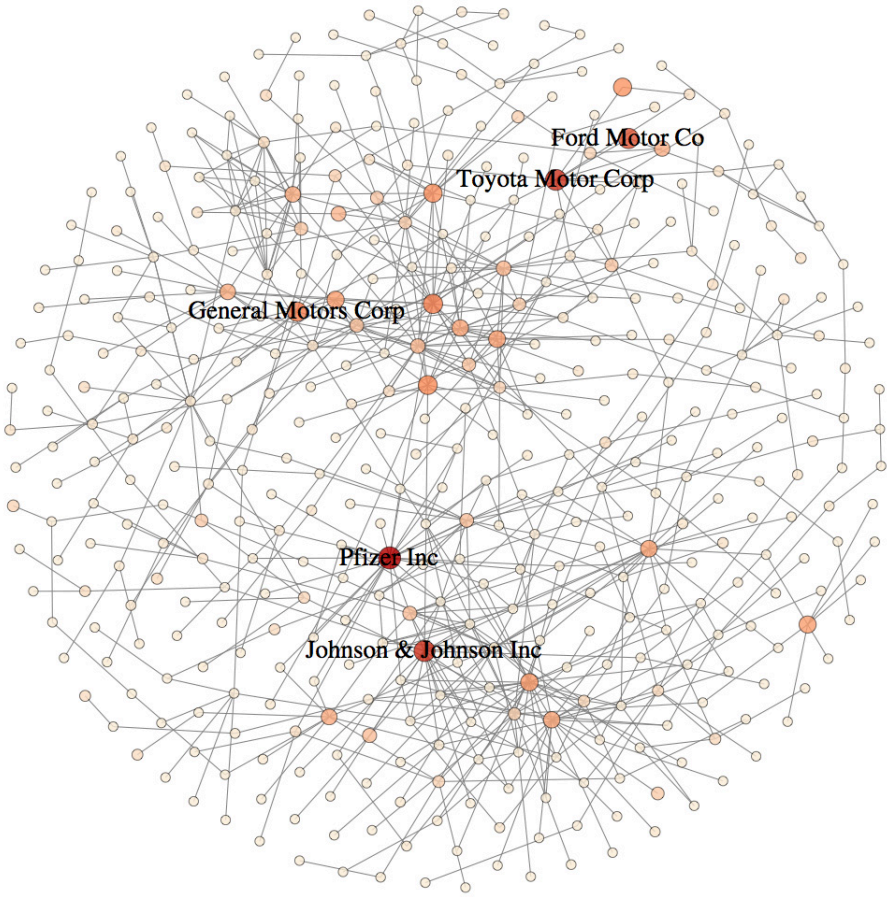

Figure 7: The largest connected component in the observed network of R&D collaborations in the year 2006 for the firms without missing observations on R&D expenditures and industry classifications. The shade and size of a node indicates its R&D expenditures, with the 5 largest firms mentioned in the graph. The number of firms is 1014 and the number of firms in the largest connected component is 431. The figure indicates two clusters representing the car producing and the pharmaceuticals sectors, with most of the collaborations within a sector and a few collaborations across sectors.

2.4.2. Heterogeneous Technology Spillovers

We can further extend the model by assuming that there are heterogeneous spillovers between collaborating firms depending on their technology portfolios [Griffith et al., 2003] (see also supplementary Appendix E.2). For example, assume that firms can only benefit from collaborations if they have at least one technology in common. Then one can show that our model is a generalization of a "random intersection graph" [Deijfen and Kets, 2009] (see supplementary Appendix B) for which positive degree correlations can be obtained (i.e., "assortativity", see Proposition 8).

The above extensions show that our model is capable of generating networks with properties that can be observed in real world networks, such as power law degree distributions and various degree correlations, once we introduce firm heterogeneity. This counteracts general criticism of (simple variants of) exponential random graphs, which often have difficulties in generating networks with empirically relevant characteristics [Chandrasekhar and Jackson, 2012].

3. Empirical Study

3.1. Data

To get a comprehensive picture of R&D alliances we use data of interfirm R&D collaborations stemming from two sources which have been widely used in the literature [Schilling, 2009]. The first is the Cooperative Agreements and Technology Indicators (CATI) database [Hagedoorn,

2002]. The database only records agreements for which a combined innovative activity or an exchange of technology is at least part of the agreement. Moreover, only agreements that have at least two industrial partners are included in the database, thus agreements involving only universities or government labs, or one company with a university or lab, are disregarded. The second is the Thomson Securities Data Company (SDC) alliance database. SDC collects data from the U. S. Securities and Exchange Commission (SEC) filings (and their international counterparts), trade publications, wires, and news sources. We include only alliances from SDC which are classified explicitly as R&D collaborations.[28] Supplementary Appendix F provides more information about the databases used for this study.

We then merged the CATI database with the Thomson SDC alliance database. For the matching of firms across datasets we adopted and extended the name matching algorithm developed as part of the NBER patent data project [Trajtenberg et al., 2009].[29] The systematic collection of inter-firm alliances in CATI started in 1987 and ended in 2006. As the CATI database only includes collaborations up to the year 2006, we take this year as the base year for our empirical analysis. We then construct the R&D alliance network by assuming that an alliance lasts for 5 years [similar to e.g., Rosenkopf and Padula, 2008]. The corresponding entry in the adjacency matrix between two firms is coded as one if an alliance between them exists during this period, and zero otherwise. An illustration of the observed R&D network can be seen in Figure 7. The figure indicates two clusters representing the car manufacturing and the pharmaceuticals sectors, respectively, with most of the collaborations within a sector and a few collaborations across sectors. The non-overlap of these sectors and the R&D collaborations (within and across sectors) will allow us to separately identify the technology spillover effect and the product market competition effect.

The combined CATI-SDC database provides only the names of the firms in an alliance. To obtain also information about their balance sheets and income statements we matched the firms' names in the CATI-SDC database with the firms' names in Standard & Poor's Compustat U.S. and Global Fundamentals databases, as well as Bureau van Dijk's Orbis database [see e.g., Bloom et al., 2013]. For the purpose of matching firms across databases, we employ the above mentioned name matching algorithm. We could match roughly 25% of the firms in the alliance data for which balance sheet information was available.[30] From our match between the firms' names in the alliance database and the firms' names in the Compustat and Orbis databases, we obtained a firm's R&D expenditures, sales, primary industry code and location.

We use a firm's log-R&D expenditure to measure its R&D effort.[31] Moreover, the firms' productivities are measured by their log-R&D capital stocks (lagged by one year). As in Hall et al. [2000], Bloom et al. [2013] and König et al. [2018] the R&D capital stock is computed using a perpetual inventory method based on the firms' R&D expenditures with a 15% depreciation rate. We further identify the patent portfolios of the firms in our dataset using the EPO Worldwide

[28] For a comparison and summary of different alliance databases, including CATI and SDC, see Schilling [2009].

[29] See `https://sites.google.com/site/patentdataproject`. We would like to thank Enghin Atalay and Ali Hortacsu for sharing their name matching algorithm with us.

[30] Note that for many small private firms no balance sheet information is available, and hence these firms could not be matched by our algorithm. We therefore typically exclude smaller private firms from our analysis, but this is inevitable if one is going to use market value data. Nevertheless, R&D is mostly concentrated in publicly listed firms, which cover most of the R&D activities in the economy, and these firms are typically included in our sample [see e.g., Bloom et al., 2013].

[31] As illustrated in supplementary Appendix C, R&D effort is proportional to output in our model.

Table 1: Descriptive statistics.

		Log R&D Expenditures			Productivity			Log # of Patents		
Sample	# of firms	mean	min	max	mean	min	max	mean	min	max
Full	1014	9.7092	3.2109	15.2467	11.2292	5.0706	17.0613	4.9587	0.0000	11.8726
SIC-28	347	9.6574	3.2109	15.2467	11.1018	5.0706	16.8160	4.7960	0.0000	11.8014
U.S. manuf.	165	10.6796	4.5972	15.2467	12.4617	6.7889	17.0613	6.4891	0.0000	11.6349

Note: R&D expenditure is measured by thousand U.S. dollars in 2006. A Firm's productivity is measured by its log-R&D capital stock (lagged by one year). To compute the R&D capital stocks we use a perpetual inventory method based on the firms' R&D expenditures with a 15% depreciation rate (following Hall et al. [2000] and Bloom et al. [2013]). The logarithm of the number of patents in 2006 is used as a control variable in the linking cost function [Hanaki et al., 2010]. We impute zero when the number of patents is zero.

Patent Statistical Database (PATSTAT) [Jaffe and Trajtenberg, 2002] (see also supplementary Appendix F.4). We only consider granted patents (or successful patents), as opposed to patents applied for, as they are the main drivers of revenue derived from R&D [Copeland and Fixler, 2012]. We obtained matches for roughly 30% of the firms in the data. The technology classes were identified using the main international patent classification (IPC) numbers at the 4-digit level. We drop firm observations with missing values on either R&D expenditure or patents which results in a sample of 1,014 firms (with 428 R&D collaborations) for our analysis.[32] Descriptive statistics of the sample are shown in Table 1.

The size of the sample is somewhat too large for implementing some of the estimation methods that we will introduce below due to computational complexity (in particular the exchange and adaptive exchange algorithms in Sections 3.3.2 and 3.3.3, respectively).[33] Therefore, we further consider a subsample of the data where we can apply all of our estimation strategies. The subsample we consider in the following is restricted to firms in the SIC-28 sector, "chemicals and allied products," which consists of 347 firms and 139 within sector R&D collaborations. Compared to other 2-digit SIC sectors, the SIC-28 sector has the largest number of within sectoral R&D collaborations, and the smallest percentage of R&D collaborations to other 2-digit SIC sectors. The SIC-28 sector contains eight 3-digit SIC sub-sectors, ranging from "industrial inorganic chemicals" (SIC-281) to "miscellaneous chemical products" (SIC-289). The summary statistics of firms in SIC-28 are provided in Table 1 and the number of R&D collaborations across major 2-digit SIC sectors (with more than twenty firms) and within the SIC-28 sectors are shown in Figure 8. Among the eight 3-digit SIC sub-sectors within SIC-28, the drugs development sector (SIC-283) is the largest one. It consists of 256 firms and 119 within sector R&D collaborations.

3.2. Firm Heterogeneity

To account for the firm level heterogeneity that we observe in the data, we extend the profit function of Equation (1) in Section 2 to accommodate heterogeneous marginal costs of production, substitution effects, and heterogeneous technology spillovers (see also Section 2.4), so that the

[32] To understand the impact of missing observations due to incomplete matching between databases, we conducted a Monte Carlo simulation study in supplementary Appendix H.

[33] See Section 3.3 and supplementary Appendix H for a more detailed discussion of the various estimation procedures that we introduce in this paper. Further, note that the restriction to small sample sizes does not apply to the likelihood partition approach introduced in Section 3.3.1, for which we can use the full sample to estimate the parameters of the model. We find, however, that the estimation results are similar, irrespective of whether we use only a subsample of the data or the full sample. Compared to several existing studies [e.g., Badev, 2013; Hsieh and Lee, 2013; Mele, 2017], which analyze networks with a few hundred nodes, the size of one single network that we handle in this paper is significantly larger.

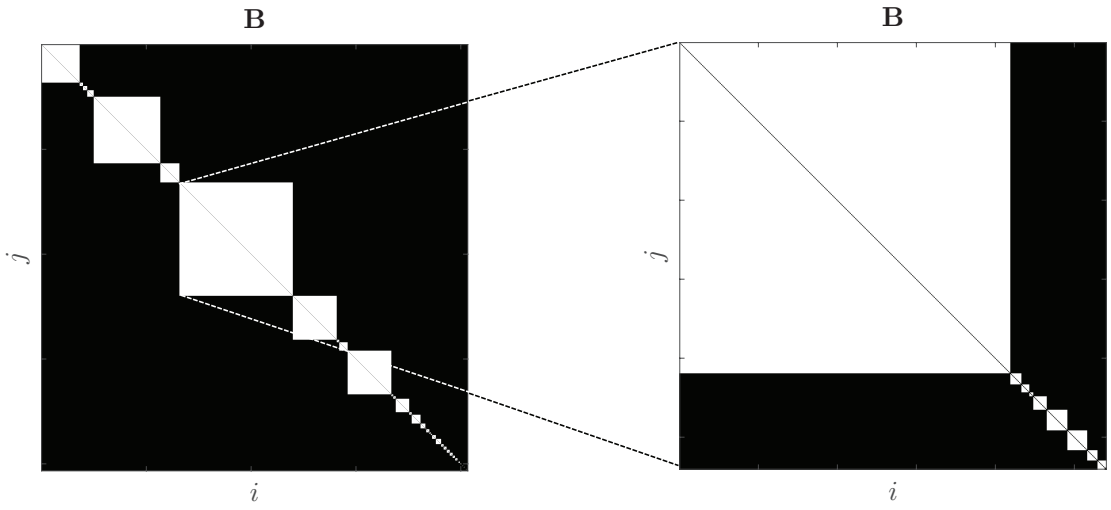

	37	73	35	38	36	28
37	22	6	3	7	4	2
73	6	4	17	7	17	8
35	3	17	11	4	26	2
38	7	7	4	5	13	26
36	4	17	26	13	29	3
28	2	8	2	26	3	139

	281	282	283	284	285	286	287	289
281	1	2	13	0	0	0	0	0
282	2	1	1	0	0	0	0	0
283	13	1	119	0	2	0	0	0
284	0	0	0	0	0	0	0	0
285	0	0	2	0	0	0	0	0
286	0	0	0	0	0	0	0	0
287	0	0	0	0	0	0	0	0
289	0	0	0	0	0	0	0	0

Figure 8: (Top left panel) The empirical competition matrix **B** across all 2-digit SIC sectors. The largest sector is the SIC-28 sector with 347 firms, which comprises 34.22% of all firms in the sample. (Top right panel) The empirical competition matrix **B** across all 3-digit SIC sectors within the SIC-28 sector. The largest sector is the SIC-283 "drugs" sector with 256 firms, which comprises 73.78% of all firms in the SIC-28 sector. (Bottom left panel) The number of R&D collaborations across all 2-digit SIC sectors. The sector SIC-28 has 139 within sector R&D collaborations. (Bottom right panel) The number of R&D collaborations within the sector SIC-28. The sector SIC-283 has 119 within sector R&D collaborations.

profit of firm i can be written as follows:

$$\pi_i(\mathbf{q}, G) = \eta_i q_i - \frac{1}{2} q_i^2 - b \sum_{j \neq i}^{n} b_{ij} q_j q_i + \rho \sum_{j=1}^{n} f_{ij} a_{ij} q_j q_i - \zeta_i(G). \tag{23}$$

As compared to Equation (1), in Equation (23) we have normalized ν to 1/2. The term η_i represents an individual fixed effect for each firm and we capture it by $\mathbf{X}_i \boldsymbol{\delta}$, where $\mathbf{X}_i$ includes firm i's productivity and a sector dummy (at the two-digit SIC level). To allow for additional heterogeneity among firms, the substitution effect is considered at the three-digit SIC level. Each firm faces a substitution effect from all other firms within the same sector, i.e., we set $b_{ij} = 1$, if both firms i and j are in the same sector, and zero otherwise. In Equation (23) we have further introduced the symmetric weights $(f_{ij})_{1 \leq i,j \leq n}$, with $f_{ij} = f_{ji}$, to capture heterogeneous technology spillovers across firms, based on the technological proximities of firms i and j measured either by Jaffe's or the Mahalanobis patent similarity indices [Bloom et al., 2013; Jaffe, 1989] criteria (see the supplementary Appendices E.2 and F.4 for further details).

The total cost of R&D collaborations for firm i is captured by the term $\zeta_i(G) = \sum_{j=1}^{n} a_{ij}(\psi_{ij} + \varphi_{ij})$, with the pairwise symmetric functions $\psi_{ij} = \boldsymbol{\gamma}^\top \mathbf{c}_{ij}$ and $\varphi_{ij} = \varkappa t_{ij}$. In our study the r-dimensional vector of dyadic-specific variables, $\mathbf{c}_{ij}$, represents measures of similarity between firms i and j regarding sector, location, technology, research quality, etc., that might have an effect on the collaboration costs (see e.g., Lychagin et al. [2016] and supplementary Appendix E.1 for a simple example). The term $t_{ij} = \sum_{k \neq i,j}^{n} a_{ik} a_{jk}$ counts the number of common collaborators shared by firms i and j ("cyclic triangles" effect). It allows for R&D collaborations to be less

costly between firms that have mutual third-party collaborators [Hanaki et al., 2010].[34]

The potential function $\Phi\colon \mathbb{R}^n_+ \times \mathcal{G}^n \to \mathbb{R}$ corresponding to Equation (23) is given by[12]

$$\Phi(\mathbf{q}, G) = \sum_{i=1}^{n}\left(\eta_i q_i - \frac{1}{2}q_i^2\right) - \frac{b}{2}\sum_{i=1}^{n}\sum_{j\neq i}^{n} b_{ij}q_i q_j + \frac{\rho}{2}\sum_{i=1}^{n}\sum_{j\neq i}^{n} f_{ij}a_{ij}q_i q_j - \frac{1}{2}\sum_{i=1}^{n}\sum_{j\neq i}^{n} a_{ij}\psi_{ij} - \frac{1}{3}\sum_{i=1}^{n}\sum_{j\neq i}^{n} a_{ij}\varphi_{ij}. \tag{24}$$

In the vector-matrix form this is

$$\Phi(\mathbf{q}, G) = \boldsymbol{\eta}^\top \mathbf{q} - \frac{1}{2}\mathbf{q}^\top \mathbf{M}(G)\mathbf{q} - \frac{1}{2}\mathrm{tr}(\mathbf{A}\boldsymbol{\Psi}^\top) - \frac{1}{3}\mathrm{tr}(\mathbf{A}\boldsymbol{\varphi}^\top), \tag{25}$$

where $\boldsymbol{\eta} = (\eta_1, \eta_2, \ldots, \eta_n)^\top$, $\boldsymbol{\Psi} = (\psi_{ij})_{1\leq i,j\leq n}$ and $\boldsymbol{\varphi} = (\varphi_{ij})_{1\leq i,j\leq n}$. In the following, we denote $\mathbf{M}(G) \equiv \mathbf{I}_n + b\mathbf{B} - \rho(\mathbf{A}\circ\mathbf{F})$, where $\mathbf{F}$ is the matrix with elements f_{ij} for $1 \leq i, j \leq n$, and $\circ$ denotes the Hadamard element wise matrix product.[35] The stationary distribution of the Markov process of Definition 1 is then given by the Gibbs measure $\mu^\vartheta(\mathbf{q}, G)$ of Equation (7) in Theorem 1 with the potential function $\Phi(\mathbf{q}, G)$ of Equation (25).

3.3. Exponential Random Graph Models

When both the quantity produced, $\mathbf{q}$, and the network, G, are endogenous, the stationary distribution $\mu^\vartheta(\mathbf{q}, G)$ is determined by Equation (7). The parameters of the model can be summarized by $\boldsymbol{\theta} = (\rho, b, \boldsymbol{\delta}^\top, \boldsymbol{\gamma}^\top, \varkappa) \in \boldsymbol{\Theta}$ with parameter space $\boldsymbol{\Theta}$.[36] This empirical model belongs to the family of exponential random graph models (ERGMs) or p^* models [see Frank and Strauss, 1986]. The closed form expression of the likelihood function given in Equation (7) establishes a straightforward channel to check identification of the parameter vector $\boldsymbol{\theta}$. Following the theory of exponential family distributions, identification of the parameters $\boldsymbol{\theta}$ is guaranteed as long as the regressors in $\Phi(\mathbf{q}, G)$ of Equation (25) are not linearly dependent [Badev, 2013; Mele, 2017; Lehmann and Casella, 2006]. ERGMs are notorious for the difficulty of estimation due to existence of an "intractable normalizing constant" in the probability likelihood function.[37,38] Using classical estimation methods such as a Maximum likelihood (MLE) approach, one needs to simulate a set of auxiliary networks in order to approximate the intractable normalizing constant (MCMC-MLE) [Badev, 2013]. However, the performance of the MCMC-MLE method is greatly influenced by the choice of initial parameter values, $\boldsymbol{\theta}^{(0)}$ [Airoldi et al., 2009]. If $\boldsymbol{\theta}^{(0)}$ is not close enough to the true value, without resorting to a global searching algorithm such as

[34] Hanaki et al. [2010] argue that the existence of mutual collaborators may enhance the effectiveness of penalties and improve the appropriability of the outcomes of joint R&D projects, and that firms can use pre-existing collaborations as conduits of information about the reliability of potential collaboration partners. The authors further find empirical evidence that R&D collaborations are more likely to be undertaken between firms that have mutual third-party collaborators.

[35] Let $\mathbf{A}$ and $\mathbf{B}$ be $m \times n$ matrices. The Hadamard product of $\mathbf{A}$ and $\mathbf{B}$ is defined by $[\mathbf{A}\circ\mathbf{B}]_{ij} = [\mathbf{A}]_{ij}[\mathbf{B}]_{ij}$ for all $1 \leq i \leq m$, $1 \leq j \leq n$, i.e. the Hadamard product is simply an element-wise multiplication.

[36] Similar to the standard logistic regression framework, the parameter ϑ cannot be separately identified, and we therefore omit it from estimation for simplicity.

[37] This corresponds to the denominator of Equation (7) which involves a summation over all networks $G \in \mathcal{G}^n$, that is, a sum with $2^{\binom{n}{2}}$ terms.

[38] Other than the difficulty of estimation, the most basic exponential random graphs are statistically equivalent to an Erdös-Rény random graph in the limit of large n unless the model contains at least one non-trivial negative network externality effect [Bhamidi et al., 2011; Mele, 2017]. We show in section 2.4 how the introduction of various forms of firm heterogeneity leads to correlated networks with structural properties that differ significantly from an Erdös-Rény random graph.

simulated annealing, the method may converge to a sub-optimal solution.

Alternatively, the Bayesian MCMC approach has recently gained more attention on ERGM estimation [see e.g., Hsieh and Lee, 2013; Mele, 2017; Snijders, 2002; Liang, 2010]. The intractable normalizing constant in the likelihood function also makes the standard MCMC algorithm infeasible. The standard MH algorithm to update the parameters from $\boldsymbol{\theta}$ to $\boldsymbol{\theta}'$ depends on the acceptance probability,

$$\alpha(\boldsymbol{\theta}'|\boldsymbol{\theta}) = \min\left\{1, \frac{\pi(\boldsymbol{\theta}')\mu^{\vartheta}(\mathbf{q}, G|\boldsymbol{\theta}')T_1(\boldsymbol{\theta}|\boldsymbol{\theta}')}{\pi(\boldsymbol{\theta})\mu^{\vartheta}(\mathbf{q}, G|\boldsymbol{\theta})T_1(\boldsymbol{\theta}'|\boldsymbol{\theta})}\right\}, \tag{26}$$

where π denotes the prior density and $T_1(\boldsymbol{\theta}'|\boldsymbol{\theta})$ denotes the symmetric proposal density for the independent MH draw, i.e., $T_1(\boldsymbol{\theta}' - \boldsymbol{\theta}) = T_1(\boldsymbol{\theta} - \boldsymbol{\theta}')$. In the above acceptance probability, two normalizing terms in $\mu^{\vartheta}(\mathbf{q}, G|\boldsymbol{\theta}')$ and $\mu^{\vartheta}(\mathbf{q}, G|\boldsymbol{\theta})$ do not cancel each other and therefore, $\alpha(\boldsymbol{\theta}'|\boldsymbol{\theta})$ cannot be calculated.

In the following subsections, we will focus on the MCMC approach and discuss three strategies to bypass the evaluation of the intractable normalizing term. Among these three strategies, when the cyclic triangles effect is absent from the model, i.e., setting $\varkappa = 0$, link independence holds (conditional on output), and we can use a likelihood partition approach (Section 3.3.1), which is generally applicable to large network samples. In a dependent link case, where $\varkappa \neq 0$, we will use an exchange algorithm (Section 3.3.2) and an adaptive exchange algorithm (Section 3.3.3). The adaptive exchange algorithm is an extension of the exchange algorithm in order to avoid the local trap problem. In supplementary Appendix H, we conduct a simulation study to demonstrate the consistency of each method and to compare their computational costs.

3.3.1. Likelihood Partition Approach

In the absence of cyclic triangles effects, i.e., when we set $\varkappa = 0$, conditional link independence holds (given the output levels of any pair of firms). The probability of observing a network $G \in \mathcal{G}^n$, given an output distribution $\mathbf{q} \in \mathcal{Q}^n$, is then determined by the conditional distribution (see Equation (15) and supplementary Appendix E):

$$\mu^{\vartheta}(G|\mathbf{q}) = \frac{\mu^{\vartheta}(\mathbf{q}, G)}{\mu^{\vartheta}(\mathbf{q})} = \prod_{i<j}^{n} \frac{e^{\vartheta a_{ij}(\rho f_{ij} q_i q_j - \boldsymbol{\gamma}^{\top}\mathbf{c}_{ij})}}{1 + e^{\vartheta(\rho f_{ij} q_i q_j - \boldsymbol{\gamma}^{\top}\mathbf{c}_{ij})}}. \tag{27}$$

Such a factorization would not be possible if the linking cost would allow for higher order network effects captured by $\varkappa \neq 0$. The marginal distribution of the firms' output levels $\mathbf{q} \in \mathcal{Q}^n$ for large ϑ is given by Equation (14) and supplementary Appendix E:

$$\mu^{\vartheta}(\mathbf{q}) \approx \left(\frac{2\pi}{\vartheta}\right)^{-\frac{n}{2}} |-\Delta\mathscr{H}_{\vartheta}(\mathbf{q}^*)|^{\frac{1}{2}} \exp\left\{-\frac{1}{2}\vartheta(\mathbf{q} - \mathbf{q}^*)^{\top}(-\Delta\mathscr{H}_{\vartheta}(\mathbf{q}^*))(\mathbf{q} - \mathbf{q}^*)\right\}, \tag{28}$$

where

$$(\Delta\mathscr{H}_{\vartheta}(\mathbf{q}))_{ii} = -1 + \frac{\vartheta\rho^2}{4}\sum_{j\neq i}^{n} f_{ij}^2 q_j^2 \left(1 - \tanh\left(\frac{\vartheta}{2}\left(\rho f_{ij} q_i q_j - \boldsymbol{\gamma}^{\top}\mathbf{c}_{ij}\right)\right)^2\right),$$

and

$$(\Delta\mathscr{H}_\vartheta(\mathbf{q}))_{ij} = -bb_{ij} + \frac{\rho f_{ij}}{2}\left(1+\tanh\left(\frac{\vartheta}{2}\left(\rho f_{ij}q_iq_j - \boldsymbol{\gamma}^\top \mathbf{c}_{ij}\right)\right)\right) \times \left(1+\frac{\vartheta\rho f_{ij}}{2}q_iq_j\left(1-\tanh\left(\frac{\vartheta}{2}\left(\rho f_{ij}q_iq_j - \boldsymbol{\gamma}^\top \mathbf{c}_{ij}\right)\right)\right)\right),$$

for $j \neq i$. Further, $\mathbf{q}^*$ in Equation (28) solves the following system of equations (see Equation (10) and supplementary Appendix E):

$$q_i = \eta_i + \sum_{j\neq i}^{n}\left(\frac{\rho f_{ij}}{2}\left(1+\tanh\left(\frac{\vartheta}{2}\left(\rho f_{ij}q_iq_j - \boldsymbol{\gamma}^\top \mathbf{c}_{ij}\right)\right)\right) - bb_{ij}\right)q_j. \tag{29}$$

Equation (28) shows that in the limit of large ϑ, $\mathbf{q}$ is asymptotically normally distributed with mean $\mathbf{q}^*$ and variance-covariance matrix $-\frac{1}{\vartheta}\Delta\mathscr{H}_\vartheta(\mathbf{q}^*)^{-1}$. It then follows that the likelihood of the network G and the quantity profile $\mathbf{q}$ in the large ϑ limit can be partitioned as follows [Smyth, 1996]

$$\mu^\vartheta(\mathbf{q},G) = \mu^\vartheta(G|\mathbf{q})\cdot\mu^\vartheta(\mathbf{q}) \approx \prod_{i<j}^{n}\frac{e^{\vartheta a_{ij}(\rho f_{ij}q_iq_j - \boldsymbol{\gamma}^\top\mathbf{c}_{ij})}}{1+e^{\vartheta(\rho f_{ij}q_iq_j - \boldsymbol{\gamma}^\top\mathbf{c}_{ij})}} \times \left(\frac{2\pi}{\vartheta}\right)^{-\frac{n}{2}}|-\Delta\mathscr{H}_\vartheta(\mathbf{q}^*)|^{\frac{1}{2}}\exp\left\{-\frac{1}{2}\vartheta(\mathbf{q}-\mathbf{q}^*)^\top(-\Delta\mathscr{H}_\vartheta(\mathbf{q}^*))(\mathbf{q}-\mathbf{q}^*)\right\}, \tag{30}$$

where we have inserted Equation (27) for $\mu^\vartheta(G|\mathbf{q})$ and Equation (28) for $\mu^\vartheta(\mathbf{q})$. Based on the partition of $\mu^\vartheta(\mathbf{q},G)$ in Equation (30), we do not need to evaluate the intractable normalizing constant in the likelihood function of Equation (7), and can estimate the parameters by a standard Bayesian MCMC algorithm. The key step of solving $\mathbf{q}^*$ from Equation (29) can be implemented efficiently by recognizing it as a fixed point system, and using a fast fixed point algorithm. As supplementary Appendix H shows, computation of this likelihood partition (LP) approach is much less costly than the other two methods outlined below. Therefore, we apply the LP approach to estimate the model for both, the full sample including all sectors and the SIC-28 sector subsample.

3.3.2. Exchange Algorithm

When we allow for cyclic triangles effects, i.e., $\varkappa \neq 0$, then we can no longer use the LP estimation algorithm from the previous section. An alternative is the exchange algorithm, which provides a way to bypass evaluation of the intractable normalizing constant in the Metropolis-Hastings (MH) acceptance probability [see e.g., Liang et al., 2011]. The name "exchange" comes from its similarity with the swapping operation of exchange Monte Carlo [Geyer, 1991]. It is different from the conventional MH algorithm by having a proposal density $T_1(\boldsymbol{\theta}'|\boldsymbol{\theta})\mu(\mathbf{q}',G'|\boldsymbol{\theta}')$, which involves simulation of auxiliary data $(\mathbf{q}',G')$ from the distribution $\mu(\mathbf{q}',G'|\boldsymbol{\theta}')$. The acceptance probability of the exchange algorithm can be written as

$$\begin{aligned}\alpha(\boldsymbol{\theta}'|\boldsymbol{\theta},\mathbf{q}',G') &= \min\left\{1, \frac{\pi(\boldsymbol{\theta}')\mu(\mathbf{q},G|\boldsymbol{\theta}')}{\pi(\boldsymbol{\theta})\mu(\mathbf{q},G|\boldsymbol{\theta})}\cdot\frac{T_1(\boldsymbol{\theta}|\boldsymbol{\theta}')\mu(\mathbf{q}',G'|\boldsymbol{\theta})}{T_1(\boldsymbol{\theta}'|\boldsymbol{\theta})\mu(\mathbf{q}',G'|\boldsymbol{\theta}')}\right\} \\ &= \min\left\{1, \frac{\pi(\boldsymbol{\theta}')e^{\Phi(\mathbf{q},G,\boldsymbol{\theta}')}}{\pi(\boldsymbol{\theta})e^{\Phi(\mathbf{q}',G',\boldsymbol{\theta}')}}\cdot\frac{T_1(\boldsymbol{\theta}|\boldsymbol{\theta}')e^{\Phi(\mathbf{q}',G',\boldsymbol{\theta})}}{T_1(\boldsymbol{\theta}'|\boldsymbol{\theta})e^{\Phi(\mathbf{q},G,\boldsymbol{\theta})}}\right\}.\end{aligned} \tag{31}$$

Intractable normalizing terms in Equation (31) are cancelled out and thus the acceptance probability $\alpha(\boldsymbol{\theta}'|\boldsymbol{\theta}, \mathbf{q}', G')$ can be computed.

A problem of the exchange algorithm is that it requires a perfect sampler of G' and $\mathbf{q}'$ from $\mu(\cdot|\boldsymbol{\theta}')$ [Propp and Wilson, 1996], which is computationally intense for most of ERGM applications. To overcome this issue, Liang [2010] proposed the double MH (DMH) algorithm to replace the perfect sampler with a finite MH chain initialized at the observed network. In this paper, we use the DMH algorithm for parameter estimation, and more specific details about its implementation can be found in supplementary Appendix G.1.

To improve the computational speed of the DMH algorithm, we assume that during the dynamic network formation process, whenever a firm changes its R&D collaborations, all firms adjust output levels immediately and thus the new output levels will be the profit-maximizing output given by the best response function $\mathbf{q}^* = \mathbf{M}(G)^{-1}\boldsymbol{\eta}$ plus a stochastic error term.[39] The size of error, according to the approximation derived in supplementary Appendix G.4, should be determined by $\mathbf{M}(G)^{-1}$. This assumption means that we impose two different time scales: a *fast time scale* of output adjustments, and a *slow time scale* of link adjustments [Khalil, 2002].[40] When simulating auxiliary data for the output levels and the network, this assumption saves firm's infinitesimal adjustments on output and turns it into an implicit function of the network. However, we will have to evaluate $\mathbf{M}(G)^{-1}$ whenever a link has been added or removed from the auxiliary network and this may still be computationally costly. To do this in an efficient way, we use a matrix perturbation result that is derived in supplementary Appendix G.5.

3.3.3. Adaptive Exchange Algorithm

Even though the DMH algorithm alleviates the computational burden by replacing the perfect sampling, convergence of the finite MH chain in the DMH algorithm is not theoretically guaranteed. Therefore, the DMH estimates are only approximately correct no matter how long the algorithm has been run. Especially, if the network distribution represented by an ERGM is multi-modal, the finite MH run may be trapped at one of the local maxima of the likelihood function ("local trap problem"). Consequentially, the Markov chain of the DMH algorithm may mix very slowly and require unaffordable computation time for achieving convergence [Bhamidi et al., 2011].[41]

In this paper, we therefore additionally adopt an adaptive exchange (AEX) algorithm, which has recently been developed by Jin et al. [2013] and Liang et al. [2015], to overcome the uncertainty of slow mixing faced by the DMH algorithm. The foundation of the AEX algorithm is an MCMC sampling scheme called stochastic approximation Monte Carlo (SAMC) algorithm [Liang et al.,

[39] Note that $\mathbf{q}^*$ maximizes the potential function of Equation (25) for an exogenously given network G.

[40] Observe that the stationary distribution $\mu(\mathbf{q}, G)$ in Equation (7) does not depend on the parameter χ that governs the speed of the output adjustment. This means that the stationary distribution $\mu(\mathbf{q}, G)$ is independent of how quickly the output levels adjust. As a consequence, we can use it as a degree of freedom in our estimation algorithms, that is, the stationary distribution is not affected whether we make the time scale separation assumption or not.

[41] To overcome the local trap problem and thus speed up convergence during network simulation, Snijders [2002] and Mele [2017] proposed MH samplers which consist of both local and non-local steps. In the local step, only one random edge is updated in an iteration. With a certain probability, the sampler will implement the non-local step where multiple (or even all) edges are updated in an iteration. Although Mele [2017] used a simulation study to demonstrate convergence of the MH sampler with a non-local step, the simulation result is based on a simple model specification with one indirect link effect and may not be extended to a more general case. Therefore, it is still questionable whether the finite MH runs with non-local steps can always achieve convergence for general ERGMs.

2007]. The main feature of SAMC is that it applies importance sampling to prevent the local trap problem. In SAMC, the sample space is partitioned into non-overlapping subregions. Different importance weights are assigned to each subregion so that SAMC draws samples from a kind of "mixture distribution" that avoids being trapped by a local extremum. Additionally, SAMC contains a self-adjusting mechanism to the weights of each subregion so that it can escape from local extrema of the likelihood function very quickly.

In the AEX algorithm, two Markov chains are running in parallel. In the first chain, we draw auxiliary data $(\widetilde{\mathbf{q}}, \widetilde{G})$ from a family of distributions $\mu(\widetilde{\mathbf{q}}, \widetilde{G}|\boldsymbol{\theta}_1), \ldots, \mu(\widetilde{\mathbf{q}}, \widetilde{G}|\boldsymbol{\theta}_m)$ with frequencies determined by the SAMC algorithm, where $(\boldsymbol{\theta}_1, \ldots, \boldsymbol{\theta}_m)$ are pre-specified parameter points. In practice, we set $m = 50$ and $(\boldsymbol{\theta}_1, \ldots, \boldsymbol{\theta}_{50})$ are chosen by the Max-Min procedure from the DMH draws [Liang et al., 2015]. We have also tried $m = 30$ and $m = 100$ and the results are largely similar. In the second chain, we implement the exchange algorithm for updating the target parameters, where auxiliary data, $\mathbf{q}'$ and G', are re-sampled from the first chain by an importance sampling procedure. Convergence of the AEX algorithm, i.e., $\mathbf{q}'$ and G' from the importance sampling procedure of the AEX converge to $\mu(\cdot|\boldsymbol{\theta}')$ and the draws of $\boldsymbol{\theta}$ from the target chain will converge weakly to the posterior $\mu(\boldsymbol{\theta}|\mathbf{q}, G)$, can be shown when the number of iterations of both the auxiliary and target chains go to infinity. Details of implementing the AEX algorithm and the proof of convergence are provided in supplementary Appendices G.2 and G.3.

3.4. Empirical Results

The first column in Table 2 presents our estimation results for the full sample encompassing all sectors in the data, columns 2 to 4 analyze the subsample restricted to the SIC-28 sector, and columns 5 and 6 analyze the U.S. manufacturing sector. Due to the aforementioned computational constraints, we only apply the LP algorithm to estimate the full sample, while applying all three estimation algorithms to the subsample for the SIC-28 sector. In the full sample both, estimates of the technology spillover parameter ρ (0.0230) and the competition parameter b (0.0001) are significant and have the expected signs. The two effects match our theoretical predictions from Section 2, showing that firms face a positive complementary effect from R&D collaborations and a negative product substitution effect from competing firms in the same market. Furthermore, we find that the technology spillover effect ρ is much larger than the product market rivalry effect b [Bloom et al., 2013]. This suggests that the marginal returns from R&D collaborations are positive even between competing firms. We also find that a higher productivity is associated with higher R&D expenditures [see e.g., Cohen et al., 1987]. The estimation results further show significant effects from the control variables in the linking cost function, including the same sector (at 3-digit SIC level) and the same country dummies (respectively, city dummies in the U.S. sample), and the sum of log patent counts from each of the two firms involved in a collaboration. Results on the two dummies reveal that the R&D collaboration cost are lower among two firms in the same sector or in the same location. The sum of the log patent numbers acts as a proxy for the research capacities of collaborating firms [Hanaki et al., 2010] and a higher value indicates lower R&D collaboration costs between them.

In the SIC-28 subsample, the estimates are similar across different estimation methods in columns 2 to 4 in Table 2, using either the LP, DMH or AEX estimation algorithm. This illustrates the robustness of our results. Further, compared to the full sample, in the SIC-28 sector there are additional significant effects from the differences in productivities between collaborating firms in

Table 2: Estimation results for the full sample and various subsamples.

		Full sample	SIC-28 subsample			U.S. manufacturing	
		LP	LP	DMH	AEX	LP	LP
		(1)	(2)	(3)	(4)	(5)	(6)
R&D Spillover	(ρ)	0.0230***	0.0266***	0.0312***	0.0293***	0.0368***	0.0480***
		(0.0013)	(0.0018)	(0.0021)	(0.0031)	(0.0068)	(0.0085)
Substitutability	(b)	0.0001**	0.0001**	0.0002**	0.0001**	0.0004**	0.0004**
		(0.0000)	(0.0000)	(0.0001)	(0.0000)	(0.0002)	(0.0002)
Productivity	(δ_1)	0.8537***	0.8034***	0.7356***	0.7418***	0.9773***	1.2336***
		(0.0160)	(0.0744)	(0.0911)	(0.0364)	(0.0306)	(0.2203)
Sector FE	(δ_2)	Yes	Yes	Yes	Yes	Yes	Yes
R&D Tax Credit IVs		No	No	No	No	No	Yes
Linking Cost							
Constant	(γ_0)	12.6642***	11.8554***	12.6239***	12.7124***	14.5007***	16.1998***
		(0.2338)	(0.3706)	(0.7079)	(0.3420)	(1.5226)	(1.3744)
Same Sector	(γ_1)	-2.1943***	-1.7963***	-1.9508***	-1.6942***	-1.5699**	-1.7417**
		(0.1141)	(0.2403)	(0.4861)	(0.3107)	(0.8304)	(0.7443)
Location	(γ_2)	-0.7501***	-0.3623**	-0.4870*	-0.5128	-0.8833	-0.7033
		(0.1056)	(0.1544)	(0.2801)	(0.3096)	(1.1022)	(0.9914)
Diff-in-Prod.	(γ_3)	-0.0102	-0.3438**	-0.4104	-0.3666**	0.1387	1.0021
		(0.0876)	(0.1433)	(0.2706)	(0.1627)	(0.5432)	(2.4465)
Patents	(γ_4)	-0.1432***	-0.0702***	-0.0710*	-0.1078***	-0.0831	-0.0944
		(0.0200)	(0.0228)	(0.0445)	(0.0400)	(0.0844)	(0.0895)
Sample size		1,014		347		165	

Notes: The dependent variable is log-R&D expenditure. A Firm's productivity is measured by its log-R&D capital stock. To compute the R&D capital stocks we use a perpetual inventory method based on the firms' R&D expenditures with a 15% depreciation rate [cf. Bloom et al., 2013; Hall et al., 2000]. Further, following Bloom et al. [2013], we use changes in the firm-specific tax of R&D to construct IVs for R&D stocks. Location is either the same country (full sample and SIC-28) or city (U.S. sample). The parameters $\boldsymbol{\theta} = (\rho, b, \boldsymbol{\delta}^\top, \boldsymbol{\gamma}^\top, \varkappa)$ correspond to Equation (24), where $\psi_{ij} = \boldsymbol{\gamma}^\top \mathbf{c}_{ij}$ and $\eta_i = \mathbf{X}_i\boldsymbol{\delta}$ (see Section 3.2). We make 50,000 MCMC draws where we drop the first 10,000 draws during a burn-in phase and keep every 10^{th} of the remaining draws to calculate the posterior mean (as point estimates) and posterior standard deviation (shown in parenthesis). All cases pass the convergence diagnostics provided by Geweke [1992] and Raftery et al. [1992]. The MCMC draws for ρ and b are shown in Figure G.1 in supplementary Appendix G. The asterisks $^{***}(^{**},^{*})$ indicate that its 99% (95%, 90%) highest posterior density range does not cover zero.

the linking cost function. This indicates that R&D collaborations between similar firms involve lower collaboration and coordination costs [see e.g., Hanaki et al., 2010; Nooteboom et al., 2007].

Columns 5 and 6 in Table 2 show the estimation results for a sample of U.S. manufacturing firms. In columns 1 to 4 productivity is measured by the log-R&D stock. A possible threat to our identification strategy might be that productivity could be correlated with unobserved firm characteristics and thus be endogenous in determining a firm's R&D investment. Due to this potential endogeneity of the R&D stocks, as a robustness check, we use R&D tax credits to instrument a firm's productivity in the U.S manufacturing sample (column 6 of Table 2) [cf. Bloom et al., 2013]. We regress the R&D stocks on R&D tax credits, and use the predicted R&D stock as an alternative measure for a firm's productivity. However, since the R&D tax credit data is only available for U.S. manufacturing sectors, we can do this only with a subset of the sample of matched U.S. manufacturing firms (see the summary statistics at the bottom of Table 1). We find that the estimated R&D spillover and substitutability effects are significant with the same sign and magnitude as in the other specifications. Moreover, the results are fairly similar with and without the instrumental variables in columns 5 and 6. This mitigates potential endogeneity concerns over our productivity measure. Thus, we are able to separately identify the technology spillover (ρ) and the product market rivalry effect (b) from the exogenous variation in the firms'

Table 3: Homogeneous versus heterogeneous technology spillovers.

		Homogeneous		Jaffe		Mahalanobis	
		DMH (1)	Logit (2)	DMH (3)	Logit (4)	DMH (5)	Logit (6)
R&D Spillover	(ρ)	0.0286***	0.0347***	0.0112**	0.0099**	0.0057**	0.0052***
		(0.0042)	(0.0032)	(0.0058)	(0.0043)	(0.0028)	(0.0019)
Substitutability	(b)	0.0002**	-	0.0002**	-	0.0002**	-
		(0.0001)	-	(0.0001)	-	(0.0001)	-
Productivity	(δ_1)	0.7305***	-	0.8665***	-	0.8702***	-
		(0.1041)		(0.1297)		(0.1308)	
Sector FE	(δ_2)	Yes	-	Yes	-	Yes	-
Linking Cost							
Constant	(γ_0)	12.38105***	12.6222***	11.1879***	11.2252***	11.2409***	11.2739***
		(0.9768)	(0.4959)	(0.7841)	(0.4822)	(0.8496)	(0.4936)
Same Sector	(γ_1)	-1.8362***	-1.5841***	-1.8549***	-1.8430***	-1.8693***	-1.8623***
		(0.6041)	(0.2745)	(0.4721)	(0.2797)	(0.5062)	(0.3000)
Location	(γ_2)	-0.3710	-0.4115**	-0.5325*	-0.5707***	-0.5553*	-0.5709***
		(0.4277)	(0.1842)	(0.3232)	(0.1812)	(0.3144)	(0.1816)
Diff-in-Prod.	(γ_3)	-0.4900	-0.3832**	-0.5018**	-0.4564***	-0.4701**	-0.4659***
		(0.3497)	(0.1540)	(0.2303)	(0.1470)	(0.2282)	(0.1428)
Patents	(γ_4)	-0.0491	-0.0398	-0.2030***	-0.2136***	-0.2032***	-0.2111***
		(0.0374)	(0.0273)	(0.0437)	(0.0269)	(0.0461)	(0.0279)
Cyclic Triangles	($\varkappa$)	-2.5025***	-1.6077***	-3.4586***	-2.2362***	-3.4415***	-2.2205***
		(0.4312)	(0.1801)	(0.2528)	(0.1573)	(0.2701)	(0.1630)

Notes: The dependent variable is log-R&D expenditure. A firm's productivity is measured by its log-R&D capital stock (lagged by one year). To compute the R&D capital stocks we use a perpetual inventory method based on the firms' R&D expenditures with a 15% depreciation rate [cf. Bloom et al., 2013; Hall et al., 2000]. The parameters $\boldsymbol{\theta} = (\rho, b, \boldsymbol{\delta}^\top, \boldsymbol{\gamma}^\top, \varkappa)$ correspond to Equation (24), where $\psi_{ij} = \boldsymbol{\gamma}^\top \mathbf{c}_{ij}$, $\varphi_{ij} = \varkappa t_{ij}$ and $\eta_i = \mathbf{X}_i\boldsymbol{\delta}$ (see Section 3.2). The estimation results are based on 347 firms from the SIC-28 sector. We make 50,000 MCMC draws where we drop the first 10,000 draws during a burn-in phase and keep every 10th of the remaining draws to calculate the posterior mean (as point estimates) and posterior standard deviation (shown in parenthesis). All cases pass the convergence diagnostics provided by Geweke [1992] and Raftery et al. [1992]. The asterisks ***(**,*) indicate that its 99% (95%, 90%) highest posterior density range does not cover zero. Heterogeneous spillovers are captured by the technological proximity matrix with elements f_{ij} using either the Jaffe or the Mahalanobis patent proximity metrics [Bloom et al., 2013; Jaffe, 1989].

productivities that affect both, their R&D investment levels as well as their propensities to form R&D collaborations.

In Table 3 we provide additional estimation results by taking into account heterogeneous technology spillover effects among collaborating firms. We also allow for a cyclic triangles effects in the linking cost function, where firms with common collaborators may experience lower collaboration costs [Hanaki et al., 2010]. In specifying heterogeneous technology spillovers, R&D collaborations are weighted by different technology proximity measures. More precisely, in columns 1 and 2 in Table 3 we consider as a benchmark a homogenous R&D collaboration matrix (i.e., assuming all weights are set to one), in columns 3 and 4 a matrix weighted by the technological proximity measure introduced by Jaffe [1989], and in columns 5 and 6 a matrix weighted by the Mahalanobis technological proximity (see Bloom et al. [2013] and supplementary Appendix F.4 for more details), respectively.[42] Notice that due to appearance of cyclic triangles effects, the link independence assumption can no longer be sustained and therefore we cannot use the LP algorithm for estimation. Each model specification is therefore estimated using the DMH algorithm outlined in Section 3.3.2 based on the subsample of firms in the SIC-28 sector. We are then able to determine potential variations of the estimated spillover effects due to alternative weights for

[42] We do not impose any row-normalization on these weighted R&D collaboration matrices.

the different technology proximity measures. Although the Jaffe and Mahalanobis measures are highly correlated (see the supplementary Appendix F.4), the estimated spillover coefficient based on the Jaffe measure (0.0112) is larger than the one based on the Mahalanobis measure (0.0057), and both are smaller than the homogeneous spillover coefficient (0.0286).

The results further show that the cyclic triangles effect is large and significantly negative for the linking cost, indicating that having mutual third-party collaborations effectively reduces the R&D collaboration cost. Although adding the cyclic triangles effect breaks the link independence condition (even conditional on R&D investment), the estimate of the spillover effect in the homogenous case (0.0286) remains similar to the baseline result (0.0312) in Table 2. In Table 3 we also compare the estimate from the DMH algorithm with the naive estimate of a logit model of R&D link formation conditional on output, i.e., the model in Equation (15), which entirely neglects the link dependence induced by the endogeneity of the output levels and the cyclic triangles effect. We find that omitting link dependence, the logit model generates downward biases on the estimates of the cyclic triangles effect in the linking cost function and the technology spillover effect in the heterogeneous spillovers cases.

3.5. Model Fit

In order to investigate whether the network formation model that we propose fits the observed network data, we adopt a model goodness-of-fit examination following Hunter et al. [2008]. We take the observed network data from the full sample of 1014 firms. Then we simulate one hundred artificial networks from our network formation model with parameters reported under the LP algorithm in Table 2, column 1. Model fitness is examined by comparing the similarity between simulated networks and the observed network in terms of distributions of four network statistics: degree, edge-wise shared partners, minimum geodesic distance and average nearest neighbor connectivity.[43] The examination results are illustrated in Figure 9 showing the mean and 95% confidence intervals from 100 simulated artificial networks. From the figure we find that the simulated networks and the observed network display similar distributions over these four statistics. This illustrates that our estimated model is able to capture the underlying network generating process.

4. Counterfactual Analyses

With our estimates from the previous section (taking column 3 in Table 2 as our baseline estimate), we are now able to perform various counterfactual studies restricted to firms in the SIC-28 sector. The first, discussed in Section 4.1, studies the impact on welfare of a firm exiting from the network. The second, discussed in Section 4.2, analyzes the welfare impact of a merger between firms in the same sector. The third policy intervention, discussed in Section 4.3, studies the welfare impact of a subsidy on the collaboration costs between pairs of firms, and aims at identifying the

[43] See supplementary Appendix B for the definitions of basic network terms such as neighborhood and degree. Moreover, the edge-wise shared partners contain information of a network related to the count of triangles in a network G. Its distribution consists of values $EP_G(0)/E_G, \cdots, EP_G(m-2)/E_G$, where $EP_G(k)$ denotes the number of edges whose endpoints both share edges with exactly k other nodes and E_G is the total number of edges in network G. Geodesic distance between any two nodes refers to the length of the shortest path joining these tow nodes. Its distribution consists of the proportions of the possible values of geodesic distances between two nodes [Hunter et al., 2008]. The average nearest neighbor connectivity is the average degree of the neighbors of a node.

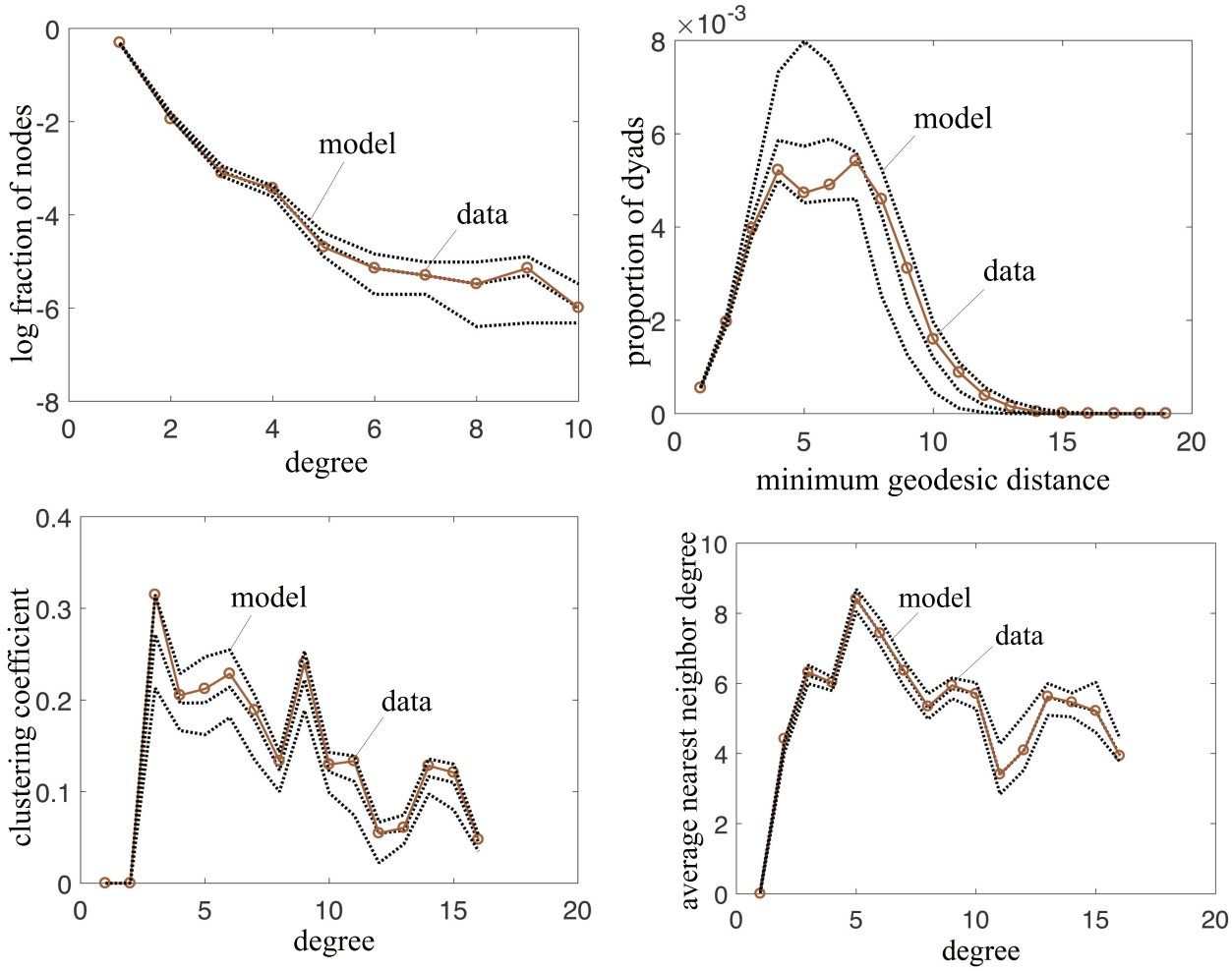

Figure 9: Goodness-of-fit statistics.

pair for which the subsidy yields the highest welfare gains. In all these counterfactual scenarios the output levels of the firms and the links between them are fully endogenous and respond to changes in the network or the parameters. Further, to evaluate the impact of any intervention under consideration we take a long run perspective and analyze welfare in the new stationary state, after the policy has been implemented.

4.1. Firm Exit and Key Players

In this section we evaluate the expected welfare loss from the exit of a firm from the network. The exit of a firm could either be due to financial reasons, such as the recession experienced by the American automobile manufacturing industry during the global financial downturn, or legal reasons, such as the recent emission-fraud scandal of Volkswagen. In the former case, policy makers want to know the overall welfare gain of "bailing out" a bankrupting firm, while, in the latter case, policy makers want to know the overall welfare cost they impose on the economy by inflicting high penalties that might threaten the continued existence of a firm.

The firm whose exit results in the highest expected welfare loss is termed the "key player" [Zenou, 2015]. This counterfactual analysis is related to Ballester et al. [2006], who perform a key player analysis where agents are ranked according to the reduction in aggregate output when they are removed from the network, and König et al. [2018] who do this for the reduction in welfare similar to our setup. However, while these authors have assumed that the network is exogenously given and does not adapt to the exit of a firm, here we can relax this assumption and allow the network to reconfigure endogenously after the removal of a firm. Formally, the *key firm* is defined

as

$$i^* = \underset{i \in \mathcal{N}}{\operatorname{argmin}} \left\{ \sum_{G \in \mathcal{G}^{n-1}} \int_{\mathcal{Q}^{n-1}} W_{-i}(\mathbf{q}, G) \mu^{\vartheta}(\mathbf{q}, G) d\mathbf{q} \right\}, \tag{32}$$

where the probability measure $\mu^{\vartheta}(\mathbf{q}, G)$ is given by Equation (7), the potential function from Equation (25), the welfare function $W(\mathbf{q}, G)$ is defined in Equation (19) and $W_{-i}(G, \mathbf{q})$ denotes the welfare function with firm i removed from the network.

We proceed by removing each firm from the network one at a time. Using the estimated model from Table 2, we then simulate the network evolution for the remaining $n-1$ firms. We use the same graph simulation algorithm that is part of the DMH estimation algorithm, which is explained in greater detail in supplementary Appendix G.1. We run the simulation for 10^4 iterations,[44] use the observation of the last iteration as the simulation outcome, and calculate the corresponding welfare value. We then repeat this procedure 100 times and report the average welfare value.

The results for the key player analysis focusing on the chemicals and allied products sector (SIC-28) can be seen in Table 4. In column six (ΔW_{F}) we consider the case of an exogenously fixed network, while in column five (ΔW) we allow the network to dynamically adjust to the exit of a firm. For the key firm, *Pfizer Inc.*, an American pharmaceutical company headquartered in New York City, and one of the world's largest pharmaceutical companies,[45] the reduction in welfare due to its exit amounts to 0.90% when we assume that the network is fixed, and 0.74% when we allow for an adaptive network. Comparing the cases with a fixed network versus an endogenous network, we observe that assuming a fixed network can both, over (e.g., for *Pfizer* ranked first, and *Novartis* ranked fourth) or underestimate (e.g., for *Johnson & Johnson* ranked second or *Abbott Laboratories* ranked sixth) the impact of firm exit. The difference between the two cases increases gradually towards the bottom of the list, showing that the assumption of an exogenous network typically underestimates the effect of the exit of a firm.

Table 4 also illustrates that the most important firms are not necessarily the ones with the highest market share, number of patents or degree, nor can they be identified with standard centrality measures in the literature (such as the betweenness or eigenvector centrality; see Wasserman and Faust [1994]). Rather, our results illustrate that in order to identify the key firms that are systemically relevant, we need to consider not only the market structure but also the spillovers generated though a network of R&D collaborations, and this network must be allowed to dynamically adjust upon the exit of a firm.

4.2. Mergers and Acquisitions

Our framework can be used to study mergers and acquisitions in innovative industries and their impact on welfare [Farrell and Shapiro, 1990; Salant et al., 1983]. Market concentration indices are not adequate to correctly account for the network effects of a merger on welfare [see e.g., Encaoua and Hollander, 2002]. This is because the effect of a merger on industry profits, consumer surplus, and welfare depends not only on the market structure (as for example in Bimpikis et al. [2014]) but

[44] We also tried 1.5×10^4 and 2×10^4 iterations and get similar results.
[45] *Pfizer Inc.* acquired *Wyeth* ranked number nine in Table 4 in 2009.

Table 4: Key player ranking for firms in the chemicals and allied products sector (SIC-28).

Firm	Mkt. Sh. [%][a]	Patents	Degree	ΔW [%][b]	ΔW_{F} [%][c]	SIC	Rank
Pfizer Inc.	2.7679	78061	15	-0.7353	-0.9031	283	1
Johnson & Johnson Inc.	3.0547	7460	7	-0.7109	-0.4996	283	2
Merck & Co. Inc.	1.2999	52847	10	-0.6982	-0.6291	283	3
Novartis	2.0691	18924	15	-0.6868	-0.9095	283	4
Amgen	0.8193	1885	13	-0.6773	-0.7291	283	5
Abbott Laboratories Inc.	1.2907	11160	3	-0.6458	-0.3148	283	6
Bristol-Myers Squibb Co.	1.0287	36114	6	-0.6313	-0.4279	283	7
Bayer	3.8340	133433	10	-0.6301	-0.6818	280	8
Wyeth	1.1686	7782	2	-0.6275	-0.2428	283	9
Unilever PLC	5.4914	14881	0	-0.5950	-0.2095	284	10
Schering-Plough Corp.	0.6057	52847	1	-0.5868	-0.1982	283	11
Takeda Pharmaceutical Co Ltd.	0.6445	19460	7	-0.5830	-0.3758	283	12
Akzo Nobel NV	11.7496	11366	2	-0.5769	-0.2408	285	13
Syngenta AG	4.1430	25796	0	-0.5577	-0.1458	287	14
Daiichi Sankyo Co. Ltd.	0.4590	5895	5	-0.5564	-0.3161	283	15
Monsanto Co.	3.7815	43441	0	-0.5518	-0.1816	287	16
L'Oreal SA	2.1873	46274	0	-0.5463	-0.1363	284	17
Eisai	0.3329	4541	1	-0.5380	-0.0607	283	18
Solvay SA	1.2445	22689	3	-0.5343	-0.2242	280	19
Allergan Inc.	0.1759	1900	3	-0.5274	-0.1485	283	20
Asahi Kasei Corp.	1.4715	9075	0	-0.5258	-0.0916	280	21
Genzyme Corp.	0.1830	1116	3	-0.5230	-0.1945	283	22
Kaocorp	1.1679	18213	0	-0.5166	-0.0989	284	23
Henkel AG	1.7648	58382	0	-0.5115	-0.1056	284	24
PPG Industries Inc.	7.5437	29784	0	-0.5111	-0.1607	285	25

[a] Market share in the primary 3-digit SIC sector in which the firm is operating.
[b] The relative welfare loss due to exit of a firm i is computed as $\Delta W = \left(\mathbb{E}_{\mu^\vartheta}[W_{-i}(\mathbf{q}, G)] - W(\mathbf{q}^{\mathrm{obs}}, G^{\mathrm{obs}})\right) / W(\mathbf{q}^{\mathrm{obs}}, G^{\mathrm{obs}})$, where $\mathbf{q}^{\mathrm{obs}}$ and G^{obs} denote the observed R&D expenditures and network, respectively.
[c] ΔW_{F} denotes the relative welfare loss due to exit of a firm assuming a fixed network of R&D collaborations.

also on potential R&D-efficiency gains from spillovers in the network. Due to these spillovers, mergers and the increased concentration they generate (both, in terms of the product market and the collaboration network) can be good or bad for welfare [Daughety, 1990], depending on the characteristics of the firms involved and their positions in the market as well as the network structure. Our framework allows us to determine which mergers lead to welfare losses due to market concentration, or to welfare gains through efficient R&D concentration. This counterfactual analysis is potentially important for antitrust policy makers. For example, in 2014, more than half of the merger proposals that were investigated by the U.S. Department of Justice involved R&D-efficiency claims [Marshall and Parra, 2015].

Based on our model we can assess the impact of a merger between two firms i and j which are competing in the same market. The merger that results (in expectation) in the greatest reduction in welfare is defined as

$$(i,j)^* = \underset{(i,j)\in\mathcal{N}\times\mathcal{N}}{\operatorname{argmin}} \left\{ \sum_{G\in\mathcal{G}^{n-1}} \int_{\mathcal{Q}^{n-1}} W_{i\cup j}(\mathbf{q}, G)\mu^\vartheta(\mathbf{q}, G)d\mathbf{q} \right\}, \tag{33}$$

where the probability measure $\mu^\vartheta(\mathbf{q}, G)$ is given by Equation (7), the potential function from Equation (25), the welfare function $W(\mathbf{q}, G)$ is defined in Equation (19) and $W_{i\cup j}(\mathbf{q}, G)$ denotes the welfare function with firms i and j being merged to a single firm k in the network G. That is, two incident nodes, i and j in G, are merged into a new node k, where each of the edges incident to k correspond to an edge incident to either i or j. In a similar way, the merger that results (in

expectation) in the greatest increase in welfare can be defined.[46]

Using the same simulation procedure as in Section 4.1, the merger rankings (for both, welfare gains and losses) can be found in Table 5. To prevent ambiguity on the sector identity of the merged firms, we restrict mergers to firms within the same 3-digit SIC sectors. Column ten (ΔW_{F}) in Table 5 shows the welfare change (ΔW_{F}) from a merger in fixed network. This is based on the assumption that the network does not adjust to the merger and can be interpreted as a short run analysis. In contrast, the ranking in column nine (ΔW) is based on an endogenous network, which adapts to a merger and can be interpreted as a long run analysis. The mergers resulting in the highest reduction or gain in welfare involve only firms in the drugs development sector (SIC 283), which is also the largest sector in our sample.

The highest loss in the endogenous network case is triggered by a merger between *Xoma* and *DOV Pharmaceutical Inc.*, two American biotech companies, yielding a reduction in welfare of 0.075%. In contrast, assuming a fixed network (ΔW_{F}) would predict a weak welfare gain from the merger, while ignoring the network structure altogether (ΔW_{N} in column eleven in Table 5) would predict a much larger welfare loss. This highlights the importance of taking into account network effects and their endogeneity. Further, the welfare loss due to a merger is typically lower than the welfare loss due to firm exit. In contrast, the highest welfare gain form a merger is obtained between *Novartis* and *Pfizer Inc.*, two large multinational pharmaceutical companies. In the endogenous case (ΔW) the welfare gain is 0.86%, while in the exogenous case (ΔW_{F}) it is only 0.05%. This indicates the importance of dynamic network effects in the industry.

Further, comparing the firms involved in mergers that lead to welfare gains in Table 5, as opposed to the ones that lead to a welfare loss, we see that mergers between firms with a larger number of patents and a larger number of collaborations (high degree) lead to welfare gains, while mergers between firms with few collaborations and fewer patents lead to a welfare loss. This indicates that welfare gains are largest when two well connected and R&D intensive firms merge, while welfare losses dominate when less connected and R&D intensive firms are involved in the merger. Moreover, from Table 5 we find that the highest welfare gains from a merger are larger than the highest welfare losses from a merger, indicating that the R&D spillover effects are larger than the market distortion effects. Finally, as expected, in the absence of the R&D collaboration network in column eleven in Table 5 (ΔW_{N}) a merger between two firms always leads to a reduction in welfare [Salant et al., 1983].

4.3. R&D Collaboration Subsidy

Many governments provide R&D subsidies to foster the R&D activities of private firms [see e.g., Cohen, 1994]. One example is the Advanced Technology Program (ATP) which was administered by the National Institute of Standards and Technology (NIST) in the U.S. [Feldman and Kelley, 2003]. In Europe, EUREKA is a Europe-wide network for industrial R&D. The main aim of this EU programme is to strengthen European competitiveness in the field of R&D by means of promoting market-driven collaborative research and technology development. EUREKA's total

[46] We note that we only consider mergers between firms in the same market. We also do not consider firms operating in multiple markets simultaneously, such as for example in Bimpikis et al. [2014]. However, we believe that our analysis of a very specific type of a merger can generate useful insights because it takes into account multiple sources of externalities that are typically ignored in other studies.

Table 5: Merger ranking for firms in the chemicals and allied products sector (SIC-28).

Firm i	Firm j	Mkt. Sh. i [%][a]	Mkt. Sh. j [%]	Pat. i	Pat. j	d_i	d_j	ΔW [%][b]	ΔW_{F} [%][c]	ΔW_{N} [%][d]	SIC	Rank
WELFARE LOSS												
Xoma	DOV Pharmaceutical Inc.	0.0017	0.0015	648	7	7	1	-0.0746	0.0492	-0.3016	283	1
Merck & Co Inc.	Daiichi Sankyo Co. Ltd.	0.4515	0.4590	52847	5895	3	5	-0.0703	-0.0581	-0.3867	283	2
Endo Pharmaceuticals Holdings	Medarex Inc.	0.0522	0.0028	554	168	0	9	-0.0688	-0.0232	-0.2644	283	3
Schering-Plough Corp.	Bristol-Myers Squibb Co.	0.6057	1.0287	52847	36114	1	6	-0.0658	-0.0795	-0.1398	283	4
Ariad Pharmaceuticals Inc.	Schering-Plough Corp.	0.0001	0.6057	31	52847	0	1	-0.0578	-0.0708	-0.2503	283	5
Merck & Co. Inc.	Novartis	0.4515	2.0691	52847	18924	3	15	-0.0575	-0.0787	-0.4363	283	6
Allergan Inc.	Bristol-Myers Squibb Co.	0.1759	1.0287	1900	36114	3	6	-0.0496	-0.0323	-0.4245	283	7
Merck & Co. Inc.	Abbott Laboratories Inc.	0.4515	1.2907	52847	11160	3	3	-0.0481	-0.0404	-0.5465	283	8
Gedeon Richter	Millennium Pharmaceuticals	0.0572	0.0280	32	1171	0	4	-0.0481	-0.0901	-0.3659	283	9
Theravance Inc.	Elan Corp.	0.0011	0.0322	382	462	0	3	-0.0472	0.0501	-0.3562	283	10
WELFARE GAIN												
Novartis	Pfizer Inc.	2.0691	2.7679	18924	78061	15	15	0.8554	0.0535	-0.3251	283	1
Amgen	Pfizer Inc.	0.8193	2.7679	1885	78061	13	15	0.8300	0.1995	-0.2587	283	2
Merck & Co Inc.	Pfizer Inc.	1.2999	2.7679	52847	78061	10	15	0.7520	0.0921	-0.1785	283	3
Medarex Inc.	Novartis	0.0028	2.0691	294	18924	9	15	0.7348	0.4663	-0.4912	283	4
Medarex Inc.	Wyeth	0.0028	1.1686	294	7782	9	2	0.7247	0.2122	-0.4367	283	5
Medarex Inc.	Amgen	0.0028	0.8193	294	1885	9	13	0.7083	0.3150	-0.1593	283	6
Medarex Inc.	Pfizer Inc.	0.0028	2.7679	294	78061	9	15	0.7020	0.3786	-0.3208	283	7
Exelixis	Pfizer Inc.	0.0057	2.7679	607	78061	7	15	0.6861	0.3199	-0.2785	283	8
Merck & Co. Inc.	Novartis	1.2999	2.0691	52847	18924	10	15	0.6707	-0.0458	-0.3573	283	9
Amgen	Novartis	0.8193	2.0691	1885	18924	13	15	0.6653	0.0169	-0.2565	283	10

[a] Market share in the primary 3-digit sector in which the firm is operating.
[b] The relative welfare change due to a merger of firms i and j is computed as $\Delta W = \left(\mathbb{E}_{\mu^\vartheta}[W_{i\cup j}(G,\mathbf{q})] - W(\mathbf{q}^{\mathrm{obs}}, G^{\mathrm{obs}})\right)/W(\mathbf{q}^{\mathrm{obs}}, G^{\mathrm{obs}})$, where $\mathbf{q}^{\mathrm{obs}}$ and G^{obs} denote the observed R&D expenditures and network, respectively.
[c] ΔW_{F} denotes the relative welfare change due to a merger of firms assuming a fixed network of R&D collaborations.
[d] ΔW_{N} denotes the relative welfare change due to a merger of firms in the absence of a network of R&D collaborations.

subsidies for cooperative R&D accumulated to more than €37 billion in 2015.[47] In this section we analyze the impact of R&D subsidies on aggregate welfare within a dynamic R&D network.

We analyze a counterfactual policy that selects a specific firm-pair, (i, j), and compensates their collaboration costs through a subsidy, i.e., setting $\psi_{ij} = 0$ (see Equation (23) and thereafter).[48] We then can evaluate the changes in welfare due to such a subsidy using our estimated model. The pair of firms for which the subsidy results in the largest gain in welfare is defined as

$$(i,j)^* = \underset{(i,j)\in\mathcal{E}}{\operatorname{argmax}} \left\{ \sum_{G\in\mathcal{G}^n} \int_{\mathcal{Q}^n} W(\mathbf{q}, G|\psi_{ij} = 0)\mu^{\vartheta}(\mathbf{q}, G)d\mathbf{q} \right\}, \tag{34}$$

where the probability measure $\mu^{\vartheta}(\mathbf{q}, G)$ is given by Equation (7), the welfare function $W(\mathbf{q}, G)$ is defined in Equation (19) and $W(\mathbf{q}, G|\psi_{ij} = 0)$ denotes the welfare function with firms i and j receiving a subsidy such that they do not incur a pair-specific collaboration cost (by setting $\psi_{ij} = 0$ permanently). The results can be seen in Table 6. In column nine (ΔW) we find that a subsidy between *Exelixis*, an American genomics-based drug discovery company, and *Colgate-Palmolive Co.*, an American worldwide consumer and pharmaceutical products company, would yield a welfare gain of 0.94 %. The welfare gain in column ten (ΔW_{F}) is much weaker when we impose a fixed network, highlighting the importance of dynamic network effects. The ranking illustrates that welfare gains from subsidizing R&D collaborations can be obtained for firms which otherwise would only be involved in few if any collaborations. Our framework could be used to guide governmental funding agencies that typically do not take into account the spillovers generated within a dynamic R&D network structure.

5. Conclusion

In this paper we have introduced a tractable model to analyze the coevolution of networks and behavior, and we have given an application to the formation of R&D collaboration networks in which firms are competitors on the product market. We provide a complete equilibrium characterization and show that our model can reproduce the observed patterns in real world networks. Moreover, the model can be conveniently estimated using state of the art Bayesian algorithms, and can be estimated even for large networks. Further, the model is amenable to policy analysis, and we illustrate this with examples for firm exit, M&As and subsidies in the context of R&D collaboration networks.

Due to the generality of the payoff function we consider (see Section 2.1), we believe that our model – both from a theoretical and empirical perspectives – can be applied to a variety of related contexts, where externalities can be modelled in the form of an adaptive network. Examples include peer effects in education, crime, risk sharing, scientific co-authorship, etc. [Jackson et al., 2015]. Our methodology can also be applied to study discrete choice models [Badev, 2013; König, 2016], and network games with local substitutes [Bramoullé and Kranton, 2007], when we assume

[47] For a theoretical and empirical analysis of R&D subsidies provided by the Finnish Funding Agency for Technology and Innovation see Takalo et al. [2013]. The effect of federal government R&D subsidies to stimulate collaboration activities between private firms in Germany is analyzed in Broekel and Graf [2012]. For a general discussion about the effectiveness of public R&D funding see Zúñiga-Vicente et al. [2014].

[48] Observe that in terms of the objective function of the planner the net effect of this policy intervention is zero. This is because the cost of the subsidy is exactly compensated for by the gain in firms' profits, which in turn, are part of the welfare function.

Table 6: Subsidy ranking for firms in the chemicals and allied products sector (SIC-28).

Firm i	Firm j	Mkt. Sh. i [%][a]	Mkt. Sh. j [%]	Pat. i	Pat. j	d_i	d_j	ΔW [%][b]	ΔW_{F} [%][c]	SIC i	SIC j	Rank
Exelixis	Colgate-Palmolive Co.	0.0057	1.3493	607	37685	7	0	0.9414	0.4166	283	284	1
Medicis Pharmaceutical Corp	Hospira Inc.	0.0226	0.1544	364	112	0	0	0.9139	0.3243	283	283	2
Dade Behring Inc.	Wyeth	0.0999	1.1686	152	7782	0	2	0.9066	0.4259	283	283	3
MannKind Corporation	Mitsui Chemicals Inc.	0.0000	2.5721	1876	16690	0	0	0.9038	0.4435	283	282	4
ZymoGenetics Inc.	Dade Behring Inc.	0.0015	0.0999	784	152	0	0	0.8890	0.4442	283	283	5
Human Genome Sciences Inc.	Solvay SA	0.0015	1.2445	898	22689	2	3	0.8851	0.2769	283	280	6
Mitsui Chemicals Inc.	Merck & Co. Inc.	2.5721	0.4515	16690	52847	0	3	0.8840	0.3256	282	283	7
Colgate-Palmolive Co	Millennium Pharmaceuticals	1.3493	0.0280	37685	1171	0	4	0.8815	0.5153	284	283	8
Elan Corp.	Genzyme Corp.	0.0322	0.1830	462	1116	3	3	0.8813	0.4486	283	283	9
Genzyme Corp	Bristol-Myers Squibb Co.	0.1830	1.0287	1116	36114	3	6	0.8804	0.2974	283	283	10
Dade Behring Inc.	Hospira Inc.	0.0999	0.1544	152	112	0	0	0.8785	0.3425	283	283	11
Solvay SA	Merck & Co. Inc.	1.2445	1.2999	22689	52847	3	10	0.8776	0.2966	280	283	12
ZymoGenetics Inc.	Rhodia	0.0015	0.6369	784	23705	0	0	0.8747	0.3416	283	280	13
Cephalon	Solvay SA	0.1005	1.2445	810	22689	1	3	0.8726	0.3796	283	280	14
Akzo Nobel NV	Takeda Pharmaceutical Co Ltd	11.7496	0.6445	11366	19460	2	7	0.8694	0.3993	285	283	15
Bayer	Bristol-Myers Squibb Co.	3.8340	1.0287	133433	36114	10	6	0.8651	0.3667	280	283	16
Human Genome Sciences Inc.	Elan Corp.	0.0015	0.0322	898	462	2	3	0.8632	0.2765	283	283	17
L'Oreal SA	Daiichi Sankyo Co. Ltd.	2.1873	0.4590	46274	5895	0	5	0.8566	0.3874	284	283	18
Clariant AG	Human Genome Sciences Inc.	1.5181	0.0015	21194	898	0	2	0.8554	0.3518	286	283	19
Shiseido Co. Ltd.	Johnson & Johnson Inc.	0.6585	3.0547	2922	7460	0	7	0.8551	0.4410	284	283	20
Shiseido Co. Ltd.	Celgene	0.6585	0.0516	2922	786	0	0	0.8551	0.3123	284	283	21
Colgate-Palmolive Co.	Abbott Laboratories Inc.	1.3493	1.2907	37685	11160	0	3	0.8514	0.4200	284	283	22
Showa Denko	Medarex Inc.	0.8288	0.0028	6692	168	0	9	0.8514	0.2575	280	283	23
Medarex Inc.	Human Genome Sciences Inc.	0.0028	0.0015	168	898	9	2	0.8508	0.4581	283	283	24
Sepracor	Mitsui Chemicals Inc.	0.0687	2.5721	1473	16690	1	0	0.8472	0.3379	283	282	25

[a] Market share in the primary 3-digit sector in which the firm is operating.

[b] The relative welfare gain due to subsidizing the R&D collaboration costs between firms i and j is computed as $\Delta W = \left(\mathbb{E}_{\mu^{\vartheta}}[W(\mathbf{q}, G|\psi_{ij}=0)] - W(\mathbf{q}^{\mathrm{obs}}, G^{\mathrm{obs}})\right)/W(\mathbf{q}^{\mathrm{obs}}, G^{\mathrm{obs}})$, where $\mathbf{q}^{\mathrm{obs}}$ and G^{obs} denote the observed R&D expenditures and network, respectively.

[c] ΔW_{F} denotes the relative welfare gain due to a subsidy assuming a fixed network of R&D collaborations.

a negative sign for the local externality parameter in our payoff function.

References

Airoldi, E., Goldenberg, A., Zheng, A., and Fienberg, S. (2009). A survey of statistical network models. *Machine Learning*, 2(2):129–233.

Anderson, S., Goeree, J., and Holt, C. (2004). Noisy directional learning and the logit equilibrium. *Scandinavian Journal of Economics*, 106(3):581–602.

Anderson, S. P., De Palma, A., and Thisse, J. F. (1992). *Discrete choice theory of product differentiation*. MIT Press.

Anderson, S. P., Goeree, J. K., and Holt, C. A. (2001). Minimum-effort coordination games: Stochastic potential and logit equilibrium. *Games and Economic Behavior*, 34(2):177–199.

Badev, A. (2013). Discrete games in endogenous networks: Theory and policy. *University of Pennsylvania Working Paper PSC 13–05*.

Ballester, C., Calvó-Armengol, A., and Zenou, Y. (2006). Who's who in networks. wanted: The key player. *Econometrica*, 74(5):1403–1417.

Belhaj, M., Bervoets, S., and Deroian, F. (2016). Optimal networks in games with local complementarities. *Theoretical Economics*, 11.

Ben-Akiva, M. and Watanatada, T. (1981). Application of a continuous spatial choice logit model. *Structural analysis of discrete data with econometric applications*, pages 320–343.

Bhamidi, S., Bresler, G., Sly, A., et al. (2011). Mixing time of exponential random graphs. *The Annals of Applied Probability*, 21(6):2146–2170.

Bimpikis, K., Ehsani, S., and Ilkilic, R. (2014). Cournot competition in networked markets. Forthcoming in *Management Science*.

Bisin, A., Horst, U., and Özgür, O. (2006). Rational expectations equilibria of economies with local interactions. *Journal of Economic Theory*, 127(1):74–116.

Bloom, N., Schankerman, M., and Van Reenen, J. (2013). Identifying technology spillovers and product market rivalry. *Econometrica*, 81(4):1347–1393.

Blume, L. (1993). The statistical mechanics of strategic interaction. *Games and Economic Behavior*, 5(3):387–424.

Blume, L. (2003). How noise matters. *Games and Economic Behavior*, 44(2):251–271.

Boguná, M. and Pastor-Satorras, R. (2003). Class of correlated random networks with hidden variables. *Physical Review E*, 68(3):036112.

Bramoullé, Y. and Kranton, R. (2007). Public goods in networks. *Journal of Economic Theory*, 135(1):478–494.

Brock, W. and Durlauf, S. (2001). Discrete choice with social interactions. *Review of Economic Studies*, 68(2):235–260.

Broekel, T. and Graf, H. (2012). Public research intensity and the structure of german R&D networks: a comparison of 10 technologies. *Economics of Innovation and New Technology*, 21(4):345–372.

Cabrales, A., Calvó-Armengol, A., and Zenou, Y. (2011). Social interactions and spillovers. *Games and Economic Behavior*, 72(2):339–360.

Calvo, G. A. (1983). Staggered prices in a utility-maximizing framework. *Journal of Monetary Economics*, 12(3):383–398.

Chandrasekhar, A. and Jackson, M. (2012). Tractable and consistent random graph models. *Available at SSRN 2150428*.

Cohen, L. (1994). When can government subsidize research joint ventures? politics, economics, and limits to technology policy. *The American Economic Review*, 84(2):159–163.

Cohen, W., Levin, R., and Mowery, D. (1987). Firm size and R&D intensity: a re-examination. *The Journal of Industrial Economics*, 35(4):543–565.

Copeland, A. and Fixler, D. (2012). Measuring the price of research and development output. *Review of Income and Wealth*, 58(1):166–182.

Cournot, A. (1838). *Researches into the Mathematical Principles of the Theory of Wealth*. Trans. N.T. Bacon, New York: Macmillan.

Czarnitzki, D., Hussinger, K., and Schneider, C. (2015). R&D collaboration with uncertain intellectual property rights. *Review of Industrial Organization*, 46(2):183–204.

D'Aspremont, C. and Jacquemin, A. (1988). Cooperative and noncooperative R&D in duopoly with spillovers. *The American Economic Review*, 78(5):1133–1137.

Daughety, A. F. (1990). Beneficial concentration. *The American Economic Review*, 80(5):1231–1237.

Daughety, A. F. (2005). *Cournot oligopoly: characterization and applications*. Cambridge University Press.

David, P. A. (1992). Heroes, herds and hysteresis in technological history: Thomas Edison and "The battle of the systems" reconsidered. *Industrial and Corporate Change*, 1(1):129–180.

Dawid, H. and Hellmann, T. (2014). The evolution of R&D networks. *Journal of Economic Behavior & Organization*, 105:158–172.

Deijfen, M. and Kets, W. (2009). Random intersection graphs with tunable degree distribution and clustering. *Probability in the Engineering and Informational Sciences*, 23(04):661–674.

Ehrhardt, G., Marsili, M., and Vega-Redondo, F. (2008). Networks emerging in a volatile world. Economics Working Papers.

Encaoua, D. and Hollander, A. (2002). Competition policy and innovation. *Oxford Review of Economic Policy*, 18(1):63–79.

Farrell, J. and Shapiro, C. (1990). Horizontal mergers: an equilibrium analysis. *The American Economic Review*, 80(1):107–126.

Feldman, M. P. and Kelley, M. R. (2003). Leveraging research and development: Assessing the impact of the U.S. advanced technology program. *Small Business Economics*, 20(2):153–165.

Feri, F. (2007). Stochastic stability in networks with decay. *Journal of Economic Theory*, 135(1):442–457.

Fosco, C., Vega-Redondo, F., and Marsili, M. (2010). Peer effects and peer avoidance: The diffusion of behavior in coevolving networks. *Journal of the European Economic Association*, 8(1):169–202.

Frank, O. and Strauss, D. (1986). Markov graphs. *Journal of the American Statistical Association*, 81(395):832–842.
Gabaix, X. (2014). A sparsity-based model of bounded rationality. *The Quarterly Journal of Economics*, 1661:1710.
Gabaix, X. (2016). Power laws in economics: An introduction. *The Journal of Economic Perspectives*, 30(1):185–205.
Geweke, J. (1992). Evaluating the accuracy of sampling-based approaches to the calculation of posterior moments. *Bayesian Statistics*, pages 169–193.
Geyer, C. J. (1991). *Markov chain Monte Carlo maximum likelihood*. Interface Foundation of North America.
Gibson, M. A. and Bruck, J. (2000). Efficient exact stochastic simulation of chemical systems with many species and many channels. *The Journal of Physical Chemistry A*, 104(9):1876–1889.
Goyal, S. and Moraga-Gonzalez, J. L. (2001). R&D networks. *RAND Journal of Economics*, 32(4):686–707.
Griffith, R., Redding, S., and Van Reenen, J. (2003). R&D and absorptive capacity: Theory and empirical evidence. *Scandinavian Journal of Economics*, 105(1):99–118.
Grimmett, G. (2010). *Probability on graphs*. Cambridge University Press.
Hall, B. H., Jaffe, A. B., Trajtenberg, M., 2000. Market value and patent citations: A first look. National Bureau of Economic Research, Working Paper No. 7741.
Hagedoorn, J. (2002). Inter-firm R&D partnerships: an overview of major trends and patterns since 1960. *Research Policy*, 31(4):477–492.
Hanaki, N., Nakajima, R., and Ogura, Y. (2010). The dynamics of R&D network in the IT industry. *Research Policy*, 39(3):386–399.
Hiller, T. (2013). Peer effects in endogenous networks. *Available at SSRN 2331810*.
Hojman, D. and Szeidl, A. (2008). Core and periphery in networks. *Journal of Economic Theory*, 139(1):295–309.
Hojman, D. A. and Szeidl, A. (2006). Endogenous networks, social games, and evolution. *Games and Economic Behavior*, 55(1):112–130.
Horn, R. A. and Johnson, C. R. (1990). *Matrix Analysis*. Cambridge University Press.
Hsieh, C.-s. and Lee, L.-f. (2013). Specification and estimation of network formation and network interaction models with the exponential probability distribution. *CUHK Working Paper*.
Hunter, D. R., Goodreau, S. M., and Handcock, M. S. (2008). Goodness of fit of social network models. *Journal of the American Statistical Association*, 103(481).
Jackson, M. (2008). *Social and Economic Networks*. Princeton University Press.
Jackson, M. O., Rogers, B., and Zenou, Y. (2017). The economic consequences of social network structure. *Journal of Economic Literature*, 55(1):49–95.
Jackson, M. O. and Rogers, B. W. (2007). Meeting strangers and friends of friends: How random are social networks? *American Economic Review*, 97(3):890–915.
Jackson, M. O. and Watts, A. (2002). The evolution of social and economic networks. *Journal of Economic Theory*, 106(2):265–295.
Jackson, M. O., Zenou, Y., et al. (2015). Games on networks. *Handbook of Game Theory with Economic Applications*, 4:95–163.
Jaffe, A. and Trajtenberg, M. (2002). *Patents, Citations, and Innovations: A Window on the Knowledge Economy*. MIT Press.
Jaffe, A. B. (1989). Characterizing the technological position of firms, with application to quantifying technological opportunity and research spillovers. *Research Policy*, 18(2):87 – 97.
Jin, I. H., Yuan, Y., and Liang, F. (2013). Bayesian analysis for exponential random graph models using the adaptive exchange sampler. *Statistics and its interface*, 6(4):559.
Kandori, M., Mailath, G., and Rob, R. (1993). Learning, mutation, and long run equilibria in games. *Econometrica*, 61(1):29–56.
Kelly, M. J., Schaan, J.-L., and Joncas, H. (2002). Managing alliance relationships: key challenges in the early stages of collaboration. *R&D Management*, 32(1):11–22.
Khalil, H. K. (2002). *Nonlinear Systems*. Prentice Hall.
Kitsak, M., Riccaboni, M., Havlin, S., Pammolli, F., and Stanley, H. (2010). Scale-free models for the structure of business firm networks. *Physical Review E*, 81:036117.
König, M., Tessone, C., and Zenou, Y. (2014a). Nestedness in networks: A theoretical model and some applications. *Theoretical Economics*, 9:695–752.
König, M. D. (2016). Diffusion of behavior in dynamic networks. *University of Zurich, Department of Economics Working Paper No. 222*.
König, M. D., Liu, X., and Zenou, Y. (2018). R&D networks: Theory, empirics and policy implications. Forthcoming in the *Review of Economics and Statistics*.
König, M. D., Lorenz, J., and Zilibotti, F. (2016). Innovation vs. imitation and the evolution of productivity distributions. *Theoretical Economics*, 11:1053–1102.
Lehmann, E. L. and Casella, G. (2006). *Theory of point estimation*. Springer Science & Business Media.
Liang, F. (2010). A double Metropolis–Hastings sampler for spatial models with intractable normalizing constants. *Journal of Statistical Computation and Simulation*, 80(9):1007–1022.
Liang, F., Jin, I. H., Song, Q., and Liu, J. S. (2015). An adaptive exchange algorithm for sampling from distributions with intractable normalizing constants. *Journal of the American Statistical Association*, 111(513):377–393.
Liang, F., Liu, C., and Carroll, R. (2011). *Advanced Markov chain Monte Carlo methods: learning from past samples*, volume 714. John Wiley & Sons.
Liang, F., Liu, C., and Carroll, R. J. (2007). Stochastic approximation in Monte Carlo computation. *Journal of the American Statistical Association*, 102(477):305–320.
Lychagin, S., Pinkse, J., Slade, M. E., and Van Reenen, J. (2016). Spillovers in space: does geography matter? *The Journal of Industrial Economics*, 64(2):295–335.
Mahadev, N. and Peled, U. (1995). *Threshold Graphs and Related Topics*. North Holland.
Marshall, G. and Parra, A. (2015). Mergers in innovative industries. *Mimeo, University of Illinois at Urbana-Champaign*.
Marsili, M., Vega-Redondo, F., and Slanina, F. (2004). The rise and fall of a networked society: a formal model. *Proceedings of the National Academy of Sciences*, 101(6):1439–1442.

McFadden, D. (1976). The mathematical theory of demand models. *Behavioral Travel Demand Models*, pages 305–314.
Mele, A. (2017). A structural model of dense network formation. *Econometrica*, 85(3):825–850.
Monderer, D. and Shapley, L. (1996). Potential Games. *Games and Economic Behavior*, 14(1):124–143.
Nooteboom, B., Van Haverbeke, W., Duysters, G., Gilsing, V., and Van Den Oord, A. (2007). Optimal cognitive distance and absorptive capacity. *Research Policy*, 36(7):1016–1034.
Norris, J. R. (1998). *Markov chains*. Cambridge University Press.
Park, J. and Newman, M. (2004). Statistical mechanics of networks. *Physical Review E*, 70(6):66117.
Powell, W. W., White, D. R., Koput, K. W., and Owen-Smith, J. (2005). Network dynamics and field evolution: The growth of interorganizational collaboration in the life sciences. *American Journal of Sociology*, 110(4):1132–1205.
Propp, J. G. and Wilson, D. B. (1996). Exact sampling with coupled markov chains and applications to statistical mechanics. *Random Structures & Algorithms*, 9(1-2):223–252.
Raftery, A. E., Lewis, S., Banfield, J. D., and Rafterv, A. E. (1992). How many iterations in the Gibbs sampler. *Bayesian Statistics*, page 4.
Rosenkopf, L. and Padula, G. (2008). Investigating the Microstructure of Network Evolution: Alliance Formation in the Mobile Communications Industry. *Organization Science*, 19(5):669–687.
Rosenkopf, L. and Schilling, M. (2007). Comparing alliance network structure across industries: Observations and explanations. *Strategic Entrepreneurship Journal*, 1:191–209.
Rudin, W. (1987). *Real and complex analysis*. Tata McGraw-Hill Education.
Salant, S. W., Switzer, S., and Reynolds, R. J. (1983). Losses from horizontal merger: the effects of an exogenous change in industry structure on Cournot-Nash equilibrium. *The Quarterly Journal of Economics*, 98(2):185–199.
Sandholm, W. (2010). *Population games and evolutionary dynamics*. MIT Press.
Schilling, M. (2009). Understanding the alliance data. *Strategic Management Journal*, 30(3):233–260.
Shalizi, C. R. and Rinaldo, A. (2013). Consistency under sampling of exponential random graph models. *The Annals of Statistics*, 41(2):508–535.
Smyth, G. K. (1996). Partitioned algorithms for maximum likelihood and other non-linear estimation. *Statistics and Computing*, 6(3):201–216.
Snijders, T. (2002). Markov chain Monte Carlo estimation of exponential random graph models. *Journal of Social Structure*, 3(2):1–40.
Snijders, T. A. (2001). The Statistical Evaluation of Social Network Dynamics. *Sociological Methodology*, 31(1):361–395.
Takalo, T., Tanayama, T., and Toivanen, O. (2013). Estimating the benefits of targeted R&D subsidies. *Review of Economics and Statistics*, 95(1):255–272.
Tomasello, M. V., Napoletano, M., Garas, A., and Schweitzer, F. (2016). The rise and fall of R&D networks. *Available at SSRN 2749230*.
Trajtenberg, M., Shiff, G., and Melamed, R. (2009). The "names game": Harnessing inventors, patent data for economic research. *Annals of Economics and Statistics*, (93/94):79–108.
Wainwright, M. J. and Jordan, M. I. (2008). Graphical models, exponential families, and variational inference. *Foundations and Trends in Machine Learning*, 1(1-2):1–305.
Wasserman, S. and Faust, K. (1994). *Social Network Analysis: Methods and Applications*. Cambridge University Press.
Watts, A. (2001). A dynamic model of network formation. *Games and Economic Behavior*, 34(2):331–341.
Westbrock, B. (2010). Natural concentration in industrial research collaboration. *The RAND Journal of Economics*, 41(2):351–371.
Wong, R. (2001). *Asymptotic approximations of integrals*, volume 34. Society for Industrial Mathematics.
Zenou, Y. (2015). Key players. *Oxford Handbook on the Economics of Networks, Y. Bramoulle, B. Rogers and A. Galeotti (Eds.), Oxford University Press*.
Zúñiga-Vicente, J. A. and Alonso-Borrego, C. and Forcadell, F. J. and Galán, J. I. (2014). Assessing the effect of public subsidies on firm R&D investment: a survey. *Journal of Economic Surveys*, 28(1):36–67.

Appendix

A. Proofs

We first prove that the potential function has the property that the marginal profit of a firm from adding or removing a link is exactly equivalent to the difference in the potential function from adding or removing a link. Similarly, the marginal profit of a firm from changing its output level is exactly equivalent to the change of the potential function.

Proof of Proposition 1. The potential $\Phi(\mathbf{q}, G)$ has the property that $\Phi(\mathbf{q}, G\oplus(i,j))-\Phi(\mathbf{q}, G) = \rho q_i q_j - \zeta = \pi_i(\mathbf{q}, G\oplus(i,j)) - \pi_i(\mathbf{q}, G)$, and similarly, $\Phi(\mathbf{q}, G\ominus(i,j)) - \Phi(\mathbf{q}, G) = \zeta - \rho q_i q_j = \pi_i(\mathbf{q}, G\ominus(i,j)) - \pi_i(\mathbf{q}, G)$ for any $\mathbf{q}\in\mathcal{Q}^n$ and $G\in\mathcal{G}^n$. From the properties of $\pi_i(\mathbf{q}, G)$ it also follows that $\Phi(q_i', \mathbf{q}_{-i}, G) - \Phi(q_i, \mathbf{q}_{-i}, G) = \pi_i(q_i', \mathbf{q}_{-i}, G) - \pi_i(q_i, \mathbf{q}_{-i}, G)$. □

We next show that the stationary distribution can be characterized by a Gibbs measure.

Proof of Theorem 1. First, note from Equation (6) that $q^\vartheta(\boldsymbol{\omega}, \boldsymbol{\omega}') > 0$ for any $\boldsymbol{\omega}\neq\boldsymbol{\omega}'$ and finite ϑ, so that there is a positive probability of a transition from any state $\boldsymbol{\omega}$ to any other state $\boldsymbol{\omega}'$, and there can be no absorbing state. The generator matrix $\mathbf{Q}^\vartheta = (q^\vartheta(\boldsymbol{\omega}, \boldsymbol{\omega}'))_{\boldsymbol{\omega},\boldsymbol{\omega}'\in\Omega}$ is therefore irreducible. Moreover, for an irreducible Markov chain on a finite state space Ω all states are positive recurrent. The Markov chain then is ergodic and has a unique stationary distribution [Norris, 1998].

The stationary distribution solves $\mu^\vartheta\mathbf{Q}^\vartheta = \mathbf{0}$ with the transition rates matrix $\mathbf{Q}^\vartheta$ of Equation (6). This equation is satisfied when the probability distribution μ^ϑ satisfies the following detailed balance condition [Norris, 1998]

$$\forall\boldsymbol{\omega},\boldsymbol{\omega}'\in\Omega: \quad \mu^\vartheta(\boldsymbol{\omega})q^\vartheta(\boldsymbol{\omega},\boldsymbol{\omega}') = \mu^\vartheta(\boldsymbol{\omega}')q^\vartheta(\boldsymbol{\omega}',\boldsymbol{\omega}). \tag{35}$$

Observe that the detailed balance condition is trivially satisfied if $\boldsymbol{\omega}'$ and $\boldsymbol{\omega}$ differ in more than one link or more than one quantity level. Hence, we consider only the case of link creation $G' = G\oplus(i,j)$ (and removal $G' = G\ominus(i,j)$) or an adjustment in quantity $q_i'\neq q_i$ for some $i\in\mathcal{N}$. For the case of link creation with a transition from $\boldsymbol{\omega} = (\mathbf{q}, G)$ to $\boldsymbol{\omega}' = (\mathbf{q}, G\oplus(i,j))$ we can write the detailed balance condition as follows

$$\frac{1}{\mathscr{Z}_\theta}e^{\vartheta(\Phi(\mathbf{q},G)-m\ln\left(\frac{\xi}{\tau}\right))}\frac{e^{\vartheta\Phi(\mathbf{q},G\oplus(i,j))}}{e^{\vartheta\Phi(\mathbf{q},G\oplus(i,j))}+e^{\vartheta\Phi(\mathbf{q},G)}}\tau = \frac{1}{\mathscr{Z}_\theta}e^{\vartheta(\Phi(\mathbf{q},G\oplus(i,j))-(m+1)\ln\left(\frac{\xi}{\tau}\right))}\frac{e^{\vartheta\Phi(\mathbf{q},G)}}{e^{\vartheta\Phi(\mathbf{q},G)}+e^{\vartheta\Phi(\mathbf{q},G\oplus(i,j))}}\xi.$$

This equality is trivially satisfied. A similar argument holds for the removal of a link with a transition from $\boldsymbol{\omega} = (\mathbf{q}, G)$ to $\boldsymbol{\omega}' = (\mathbf{q}, G\ominus(i,j))$ where the detailed balance condition reads

$$\frac{1}{\mathscr{Z}_\theta}e^{\vartheta(\Phi(\mathbf{q},G)-m\ln\left(\frac{\xi}{\tau}\right))}\frac{e^{\vartheta\Phi(\mathbf{q},G\ominus(i,j))}}{e^{\vartheta\Phi(\mathbf{q},G\ominus(i,j))}+e^{\vartheta\Phi(\mathbf{q},G)}}\xi = \frac{1}{\mathscr{Z}_\theta}e^{\vartheta(\Phi(\mathbf{q},G\ominus(i,j))-(m-1)\ln\left(\frac{\xi}{\tau}\right))}\frac{e^{\vartheta\Phi(\mathbf{q},G)}}{e^{\vartheta\Phi(\mathbf{q},G)}+e^{\vartheta\Phi(\mathbf{q},G\ominus(i,j))}}\tau.$$

For a change in the output level with a transition from $\boldsymbol{\omega} = (q_i, \mathbf{q}_{-i}, G)$ to $\boldsymbol{\omega}' = (q_i', \mathbf{q}_{-i}, G)$ we get for the following detailed balance condition

$$\frac{1}{\mathscr{Z}_\theta}e^{\vartheta(\Phi(q_i,\mathbf{q}_{-i},G)-m\ln\left(\frac{\xi}{\tau}\right))}\frac{e^{\vartheta\pi_i(q_i',\mathbf{q}_{-i},G)}}{\int_{\mathcal{Q}}e^{\vartheta\pi_i(q',\mathbf{q}_{-i},G)}dq'}\chi = \frac{1}{\mathscr{Z}_\theta}e^{\vartheta(\Phi(q_i',\mathbf{q}_{-i},G)-m\ln\left(\frac{\xi}{\tau}\right))}\frac{e^{\vartheta\pi_i(q_i,\mathbf{q}_{-i},G)}}{\int_{\mathcal{Q}}e^{\vartheta\pi_i(q',\mathbf{q}_{-i},G)}dq'}\chi.$$

This can be written as $e^{\vartheta(\Phi(q_i,\mathbf{q}_{-i},G)-\Phi(q_i',\mathbf{q}_{-i},G))} = e^{\vartheta(\pi_i(q_i,\mathbf{q}_{-i},G)-\pi_i(q_i',\mathbf{q}_{-i},G))}$, which is satisfied since we have for the potential $\Phi(q_i, \mathbf{q}_{-i}, G)-\Phi(q_i', \mathbf{q}_{-i}, G) = \pi_i(q_i, \mathbf{q}_{-i}, G)-\pi_i(q_i', \mathbf{q}_{-i}, G)$. Hence, the probability measure μ^ϑ satisfies a detailed balance condition of Equation (35) and therefore is the stationary distribution of the Markov chain with transition rate matrix $\mathbf{Q}^\vartheta$. □

We next state a useful lemma that will be needed in the proofs that follow.

Lemma 1. *Consider a binary sequence $h_1, h_2, \ldots, h_n$ with elements $h_i \in \{0,1\}$ and a real sequence $c_1, c_2, \ldots, c_n$ with elements $c_i \in \mathbb{R}$ for $i = 1, \ldots, n$ and $n \geq 1$. Let $\mathcal{H}^n$ be the set of all binary sequences $\mathbf{h} = (h_1, \ldots, h_n)$ with n elements. Then we have that*

$$\sum_{\mathbf{h} \in \mathcal{H}^n} e^{\sum_{i=1}^n h_i c_i} = \prod_{i=1}^n \sum_{h_i \in \{0,1\}} e^{h_i c_i}. \tag{36}$$

Proof of Lemma 1. We give a proof by induction. For the induction basis consider $n = 2$ (the case of $n = 1$ is trivially true). Then $\mathcal{H}^2 = \{(0,0), (1,0), (0,1), (1,1)\}$, and we have that

$$\sum_{\mathbf{h} \in \mathcal{H}^2} e^{\sum_{i=1}^2 h_i c_i} = 1 + e^{c_1} + e^{c_2} + e^{c_1 + c_2}.$$

On the other hand, we have that

$$\prod_{i=1}^2 \sum_{h_i \in \{0,1\}} e^{h_i c_i} = \prod_{i=1}^2 (1 + e^{c_i}) = 1 + e^{c_1} + e^{c_2} + e^{c_1 + c_2}.$$

Next, for the induction step, assume that Equation (36) holds for some $n \geq 2$. Note that all binary sequences $\mathbf{h} \in \mathcal{H}^{n+1}$ can be constructed from a binary sequence $\mathbf{h} \in \mathcal{H}^n$ with one additional element, h_{n+1}, added to the sequence $h_1, \ldots, h_n$ where h_{n+1} takes on the two possible values 0 or 1. Hence, we can write

$$\begin{aligned}
\sum_{\mathbf{h} \in \mathcal{H}^{n+1}} e^{\sum_{i=1}^{n+1} h_i c_i} &= \sum_{\mathbf{h} \in \mathcal{H}^{n+1}} \prod_{i=1}^{n+1} e^{h_i c_i} \\
&= \sum_{\mathbf{h} \in \mathcal{H}^n} \prod_{i=1}^{n} e^{h_i c_i} + \sum_{\mathbf{h} \in \mathcal{H}^n} \prod_{i=1}^{n} e^{h_i c_i} e^{c_{n+1}} \\
&= \sum_{\mathbf{h} \in \mathcal{H}^n} \prod_{i=1}^{n} e^{h_i c_i} \left(1 + e^{c_{n+1}}\right) \\
&= \prod_{i=1}^{n} \sum_{h_i \in \{0,1\}} e^{h_i c_i} \left(1 + e^{c_{n+1}}\right) \\
&= \prod_{i=1}^{n+1} \sum_{h_i \in \{0,1\}} e^{h_i c_i},
\end{aligned}$$

where we have used the induction hypothesis that Equation (36) holds for n. This concludes the proof. □

Proof of Proposition 2. We start with the proof of the first part of the proposition. Observe that the potential of Equation (2) can be written as

$$\Phi(\mathbf{q}, G) = \underbrace{\sum_{i=1}^n \left(\eta - \nu q_i - \frac{b}{2} \sum_{j \neq i}^n q_j \right) q_i}_{\psi(\mathbf{q})} + \sum_{i=1}^n \sum_{j=i+1}^n a_{ij} \underbrace{(\rho q_i q_j - \zeta)}_{\sigma_{ij}} = \psi(\mathbf{q}) + \sum_{i=1}^n \sum_{j=i+1}^n a_{ij} \sigma_{ij}. \tag{37}$$

We then have that $e^{\vartheta \Phi(\mathbf{q}, G)} = e^{\vartheta \psi(\mathbf{q})} e^{\vartheta \sum_{i<j}^n a_{ij} \sigma_{ij}}$, where only the second factor is network dependent. Observing that the sequence $(a_{ij})_{1 \leq i < j \leq n} = (a_{12}, a_{13}, \ldots, a_{n-1,n})$ is a binary sequence as in Lemma 1, we then can use the fact that for any constant, symmetric $\sigma_{ij} = \sigma_{ji}$, $1 \leq i, j \leq n$, we

can write[49]

$$\sum_{G\in\mathcal{G}^n} e^{\vartheta\sum_{i<j}^n a_{ij}\sigma_{ij}} = \prod_{i=1}^n \prod_{j=i+1}^n \left(1+e^{\vartheta\sigma_{ij}}\right). \tag{38}$$

From Equation (38) we then obtain

$$\sum_{G\in\mathcal{G}^n} e^{\vartheta\Phi(\mathbf{q},G)} = e^{\vartheta\psi(\mathbf{q})}\prod_{i<j}^n \left(1+e^{\vartheta\sigma_{ij}}\right) = \prod_{i=1}^n e^{\vartheta\left(\eta_i-\nu q_i-\frac{b}{2}\sum_{j\neq i}^n q_j\right)q_i}\prod_{i<j}^n \left(1+e^{\vartheta(\rho q_i q_j-\zeta)}\right). \tag{39}$$

We can use Equation (39) to compute the marginal distribution

$$\begin{aligned}
\mu^\vartheta(\mathbf{q}) &= \frac{1}{\mathscr{Z}_\vartheta}\sum_{G\in\mathcal{G}^n} e^{\vartheta\Phi(\mathbf{q},G)} \\
&= \frac{1}{\mathscr{Z}_\vartheta}\prod_{i=1}^n e^{\vartheta\left(\eta_i-\nu q_i-\frac{b}{2}\sum_{j\neq i} q_j\right)q_i}\prod_{i<j}^n \left(1+e^{\vartheta(\rho q_i q_j-\zeta)}\right) \\
&= \frac{1}{\mathscr{Z}_\vartheta}e^{\vartheta\sum_{i=1}^n\left(\eta_i-\nu q_i-\frac{b}{2}\sum_{j\neq i} q_j\right)q_i}e^{\sum_{i<j}^n \ln\left(1+e^{\vartheta(\rho q_i q_j-\zeta)}\right)} \\
&= \frac{1}{\mathscr{Z}_\vartheta}e^{\vartheta\mathscr{H}_\vartheta(\mathbf{q})},
\end{aligned} \tag{40}$$

where we have introduced the Hamiltonian

$$\mathscr{H}_\vartheta(\mathbf{q}) \equiv \sum_{i=1}^n \left(\eta q_i - \nu q_i^2 + \sum_{j>i}^n \left(\frac{1}{\vartheta}\ln\left(1+e^{\vartheta(\rho q_i q_j-\zeta)}\right) - b q_i q_j\right)\right). \tag{41}$$

Using the fact that $\int_{\mathcal{Q}^n}\mu^\vartheta(\mathbf{q})d\mathbf{q}=1$, it follows from Equation (40) that we can write the partition function as

$$\mathscr{Z}_\vartheta = \int_{\mathcal{Q}^n} e^{\vartheta\mathscr{H}_\vartheta(\mathbf{q})}d\mathbf{q}.$$

We next make the Laplace approximation [Wong, 2001, Theorem 3, p. 495]

$$\mathscr{Z}_\vartheta \sim \left(\frac{2\pi}{\vartheta}\right)^{\frac{n}{2}}\left|\left(\frac{\partial^2\mathscr{H}_\vartheta}{\partial q_i\partial q_j}\right)_{q_i=q^*}\right|^{-\frac{1}{2}} e^{\vartheta\mathscr{H}_\vartheta(\mathbf{q}^*)}, \tag{42}$$

for large ϑ, where $\mathbf{q}^* = \text{argmax}_{\mathbf{q}\in[0,\bar{q}]^n}\mathscr{H}_\vartheta(\mathbf{q})$, and the Hessian is given by $\frac{\partial^2\mathscr{H}_\vartheta}{\partial q_i\partial q_j}$ for $1\leq i,j\leq n$. From Equation (41) we find that

$$\frac{\partial\mathscr{H}_\vartheta}{\partial q_i} = \eta - 2\nu q_i + \sum_{j\neq i}^n\left(\frac{\rho}{2}\left(1+\tanh\left(\frac{\vartheta}{2}\left(\rho q_i q_j-\zeta\right)\right)\right)-b\right)q_j. \tag{43}$$

The first order conditions $\frac{\partial\mathscr{H}_\vartheta}{\partial q_i}=0$ in Equation (43) imply that

$$\eta - 2\nu q_i = \sum_{j\neq i}^n\left(b-\frac{\rho}{2}\left(1+\tanh\left(\frac{\vartheta}{2}\left(\rho q_i q_j-\zeta\right)\right)\right)\right)q_j.$$

[49]Note that Equation (38) requires the σ_{ij} to be constant, and in particular, to be independent. In this case the summation over all networks only needs to count the number of possible networks in which the link ij is present. In contrast, when σ_{ij} depends on the other links in the network, then this simple summation formula would no longer hold.

This system of equations has a symmetric solution, $q_i = q$ for all $i = 1, \ldots, n$, where

$$(b(n-1) + 2\nu)q - \eta = \frac{(n-1)\rho}{2}\left(1 + \tanh\left(\frac{\vartheta}{2}\left(\rho q^2 - \zeta\right)\right)\right) q.$$

Introducing the variables $\eta^* \equiv \eta/(n-1)$ and $\nu^* \equiv \nu/(n-1)$, this can be written as

$$(b + 2\nu^*)q - \eta^* = \frac{\rho}{2}\left(1 + \tanh\left(\frac{\vartheta}{2}\left(\rho q^2 - \zeta\right)\right)\right) q. \tag{44}$$

Let the RHS of Equation (44) be denoted by $F(q)$ so that we can write it as $(b + 2\nu^*)q - \eta^* = F(q)$. Then we have that $F(0) = 0$, $F'(q) \geq 0$ and $F(q) \sim \rho q$ for $q \to \infty$. It follows that $(b + 2\nu^*)q - \eta^* = F(q)$ has at least one solution when $b + 2\nu^* > \rho$.[50] Moreover, any iteration $(b + 2\nu^*)q_{t+1} - \eta^* = F(q_t)$ starting at $q_0 = 0$ converges to the smallest fixed point q^* such that $(b + 2\nu^*)q^* - \eta^* = F(q^*)$.

We next compute the average output level $\bar{q} = \frac{1}{n}\sum_{i=1}^n q_i$. We have that

$$\begin{aligned}
\mathbb{E}_{\mu^\vartheta}\left(\sum_{i=1}^n q_i\right) &= \sum_{G\in\mathcal{G}^n}\int_{\mathcal{Q}^n} d\mathbf{q}\left(\sum_{i=1}^n q_i\right)\mu^\vartheta(\mathbf{q}, G) = \frac{1}{\mathscr{Z}_\vartheta}\sum_{G\in\mathcal{G}^n}\int_{\mathcal{Q}^n} d\mathbf{q}\left(\sum_{i=1}^n q_i\right)e^{\vartheta\Phi(\mathbf{q},G)} \\
&= \frac{1}{\mathscr{Z}_\vartheta}\sum_{G\in\mathcal{G}^n}\int_{\mathcal{Q}^n} d\mathbf{q}\frac{1}{\vartheta}\frac{\partial}{\partial\eta}e^{\vartheta\Phi(\mathbf{q},G)} = \frac{1}{\vartheta}\frac{1}{\mathscr{Z}_\vartheta}\frac{\partial\mathscr{Z}_\vartheta}{\partial\eta} = \frac{1}{\vartheta}\frac{\partial\ln\mathscr{Z}_\vartheta}{\partial\eta} = -\frac{1}{\vartheta}\frac{\partial\mathscr{F}_\vartheta}{\partial\eta},
\end{aligned}$$

where we have denoted $\mathscr{F}_\vartheta \equiv -\ln\mathscr{Z}_\vartheta$. The average output is then given by

$$\mathbb{E}_{\mu^\vartheta}\left(\frac{1}{n}\sum_{i=1}^n q_i\right) = -\frac{1}{n\vartheta}\frac{\partial\mathscr{F}_\vartheta}{\partial\eta}.$$

With Equation (42) we get

$$\mathscr{F}_\vartheta \sim -\frac{n}{2}\ln\left(\frac{2\pi}{\vartheta}\right) + \frac{1}{2}\ln\left|\left(\frac{\partial^2\mathscr{H}_\vartheta}{\partial q_i\partial q_j}\right)_{q_i=q^*}\right| - \vartheta\mathscr{H}_\vartheta(\mathbf{q}^*).$$

We then find that

$$\begin{aligned}
\frac{\partial\mathscr{F}_\vartheta}{\partial\eta} &= -\vartheta\frac{\partial\mathscr{H}_\vartheta(\mathbf{q}^*)}{\partial\eta} + \frac{1}{2}\frac{\partial}{\partial\eta}\ln\left|\left(\frac{\partial^2\mathscr{H}_\vartheta}{\partial q_i\partial q_j}\right)_{q_i=q^*}\right| \\
&= -\vartheta\frac{\partial\mathscr{H}_\vartheta(\mathbf{q}^*)}{\partial\eta} + \frac{1}{2}\mathrm{tr}\left(\left(\frac{\partial^2\mathscr{H}_\vartheta}{\partial q_i\partial q_j}\right)^{-1}\frac{\partial}{\partial\eta}\left(\frac{\partial^2\mathscr{H}_\vartheta}{\partial q_i\partial q_j}\right)\right)_{q_i=q^*},
\end{aligned}$$

where we have used Jacobi's formula [Horn and Johnson, 1990].[51] From Equation (43) we further have that

$$\frac{\partial^2\mathscr{H}_\vartheta}{\partial q_i^2} = -2\nu + \frac{\vartheta\rho^2}{4}\sum_{j\neq i}^n q_j^2\left(1 - \tanh\left(\frac{\vartheta}{2}\left(\rho q_i q_j - \zeta\right)\right)^2\right), \tag{45}$$

[50] Since the RHS, $F(q)$, of Equation (44) is increasing (one can see this from taking the derivative), is zero at $q = 0$, i.e. $F(0) = 0$, and asymptotically grows linearly as ρq, it follows that when $b + 2\nu^* > \rho$ there must exist at least one fixed point. This is because the LHS, $(b + 2\nu^*)q - \eta^*$, of Equation (44) starts below zero at $q = 0$ (where it is $-\eta^*$), both LHS and RHS are increasing, and the RHS approaches asymptotically a line with a slope smaller than the slope $b + 2\nu^*$ of the LHS. Hence they must intersect at some $q \geq 0$.

[51] For any invertible matrix $\mathbf{M}(x)$ for all x, Jacobi's formula states that $\frac{d}{dx}|\mathbf{M}(x)| = |\mathbf{M}(x)|\ \mathrm{tr}\left(\mathbf{M}(x)^{-1}\frac{d}{dx}\mathbf{M}(x)\right)$, which can be written more compactly as $\frac{d}{dx}\ln|\mathbf{M}(x)| = \mathrm{tr}\left(\mathbf{M}(x)^{-1}\frac{d}{dx}\mathbf{M}(x)\right)$.

and for $j \neq i$ we have that

$$\frac{\partial^2 \mathscr{H}_\vartheta}{\partial q_i \partial q_j} = -b + \frac{\rho}{2}\left(1 + \tanh\left(\frac{\vartheta}{2}\left(\rho q_i q_j - \zeta\right)\right)\right)\left(1 + \frac{\vartheta\rho}{2} q_i q_j \left(1 - \tanh\left(\frac{\vartheta}{2}\left(\rho q_i q_j - \zeta\right)\right)\right)\right). \tag{46}$$

This shows that $\frac{\partial}{\partial \eta}\left(\frac{\partial^2 \mathscr{H}_\vartheta}{\partial q_i \partial q_j}\right) = 0$, so that $\frac{\partial \mathscr{F}_\vartheta}{\partial \eta} = -\vartheta \frac{\partial \mathscr{H}_\vartheta(\mathbf{q}^*)}{\partial \eta}$, and the expected average output level is then given by

$$\mathbb{E}_{\mu^\vartheta}\left(\frac{1}{n}\sum_{i=1}^n q_i\right) = \frac{1}{n}\frac{\partial \mathscr{H}_\vartheta(\mathbf{q}^*)}{\partial \eta}.$$

Using the fact that $\frac{\partial \mathscr{H}_\vartheta(\mathbf{q}^*)}{\partial \eta} = \sum_{i=1}^n q_i = n q^*$, we then get in leading order terms for large ϑ that

$$\mathbb{E}_{\mu^*}\left(\frac{1}{n}\sum_{i=1}^n q_i\right) = \lim_{\vartheta\to\infty} \mathbb{E}_{\mu^\vartheta}\left(\frac{1}{n}\sum_{i=1}^n q_i\right) = q^*.$$

Next, we compute the output distribution. It can be written as follows

$$\mu^\vartheta(\mathbf{q}) = \frac{1}{\mathscr{Z}_\vartheta}\sum_{G\in\mathcal{G}^n} e^{\vartheta\Phi(\mathbf{q},G)} = \frac{1}{\mathscr{Z}_n^\vartheta} e^{\vartheta \mathscr{H}_\vartheta(\mathbf{q})},$$

where the Hamiltonian is implicitly defined by $e^{\vartheta \mathscr{H}_\vartheta(\mathbf{q})} = \sum_{G\in\mathcal{G}^n} e^{\vartheta\Phi(\mathbf{q},G)}$. From a Taylor expansion around $\mathbf{q}^*$ we have that

$$\mathscr{H}_\vartheta(\mathbf{q}) = \mathscr{H}_\vartheta(\mathbf{q}^*) + (\mathbf{q}-\mathbf{q}^*)\nabla\mathscr{H}_\vartheta(\mathbf{q}^*) + \frac{1}{2}(\mathbf{q}-\mathbf{q}^*)^\top \Delta\mathscr{H}_\vartheta(\mathbf{q}^*)(\mathbf{q}-\mathbf{q}^*) + o\left(\|\mathbf{q}-\mathbf{q}^*\|^2\right),$$

as $\vartheta\to\infty$, where $\mathbf{q}^* = \mathrm{argmax}_{\mathbf{q}\in[0,\bar{q}]^n} \mathscr{H}_\vartheta(\mathbf{q})$, the gradient is $\nabla\mathscr{H}_\vartheta(\mathbf{q}) = \left(\frac{\partial \mathscr{H}_\vartheta}{\partial q_i}\right)_{i=1,\dots,n}$, and the Hessian is $\Delta\mathscr{H}_\vartheta(\mathbf{q}) = \left(\frac{\partial^2 \mathscr{H}_\vartheta}{\partial q_i \partial q_j}\right)_{i,j=1,\dots,n}$. As the gradient $\nabla\mathscr{H}_\vartheta(\mathbf{q})$ vanishes at $\mathbf{q}^*$, we have that

$$\mathscr{H}_\vartheta(\mathbf{q}) = \mathscr{H}_\vartheta(\mathbf{q}^*) + \frac{1}{2}(\mathbf{q}-\mathbf{q}^*)^\top \Delta\mathscr{H}_\vartheta(\mathbf{q}^*)(\mathbf{q}-\mathbf{q}^*) + o\left(\|\mathbf{q}-\mathbf{q}^*\|^2\right).$$

We then can write

$$\mu^\vartheta(\mathbf{q}) = \frac{1}{\mathscr{Z}_n^\vartheta} e^{\vartheta\mathscr{H}_\vartheta(\mathbf{q}^*)} \exp\left\{-\frac{1}{2}\vartheta(\mathbf{q}-\mathbf{q}^*)^\top(-\nabla\mathscr{H}_\vartheta(\mathbf{q}^*))(\mathbf{q}-\mathbf{q}^*)\right\} + o\left(\|\mathbf{q}-\mathbf{q}^*\|^2\right).$$

Normalization implies that

$$\begin{aligned}\mathscr{Z}_n^\vartheta = \int_{\mathcal{Q}^n} d\mathbf{q} e^{\mathscr{H}_\vartheta(\mathbf{q})} &= e^{\vartheta\mathscr{H}_\vartheta(\mathbf{q}^*)}\int_{\mathcal{Q}^n} d\mathbf{q} \exp\left\{-\frac{1}{2}\vartheta(\mathbf{q}-\mathbf{q}^*)^\top(-\Delta\mathscr{H}_\vartheta(\mathbf{q}^*))(\mathbf{q}-\mathbf{q}^*)\right\} + o\left(\|\mathbf{q}-\mathbf{q}^*\|^2\right)\\ &= e^{\vartheta\mathscr{H}_\vartheta(\mathbf{q}^*)}(2\pi)^{\frac{n}{2}}\left|-\Delta\mathscr{H}_\vartheta(\mathbf{q}^*)\right|^{-\frac{1}{2}} + o\left(\|\mathbf{q}-\mathbf{q}^*\|^2\right).\end{aligned}$$

The Laplace approximation of $\mu^\vartheta(\mathbf{q})$ is then given by

$$\mu^\vartheta(\mathbf{q}) = \left(\frac{2\pi}{\vartheta}\right)^{-\frac{n}{2}}\left|-\Delta\mathscr{H}_\vartheta(\mathbf{q}^*)\right|^{\frac{1}{2}} \exp\left\{-\frac{1}{2}\vartheta(\mathbf{q}-\mathbf{q}^*)^\top(-\Delta\mathscr{H}_\vartheta(\mathbf{q}^*))(\mathbf{q}-\mathbf{q}^*)\right\} + o\left(\|\mathbf{q}-\mathbf{q}^*\|^2\right). \tag{47}$$

That is, in the limit of large ϑ, $\mathbf{q}$ is asymptotically normally distributed with mean $\mathbf{q}^*$ and variance $-\frac{1}{\vartheta}\nabla\mathscr{H}_\vartheta(\mathbf{q}^*)^{-1}$.

Imposing symmetry, $q_i = q$ for all $i = 1, \ldots, n$, in Equation (45) we can write

$$\left.\frac{\partial^2 \mathscr{H}_\vartheta}{\partial q_i^2}\right|_{q_i=q} = -2\nu + (n-1)\frac{\vartheta\rho^2}{4}q^2\left(1-\tanh\left(\frac{\vartheta}{2}\left(\rho q^2-\zeta\right)\right)\right)\left(1+\tanh\left(\frac{\vartheta}{2}\left(\rho q^2-\zeta\right)\right)\right),$$

and for $j \neq i$ we have from Equation (45) that

$$\left.\frac{\partial^2 \mathscr{H}_\vartheta}{\partial q_i \partial q_j}\right|_{q_i=q_j=q} = -b + \frac{\rho}{2}\left(1+\tanh\left(\frac{\vartheta}{2}\left(\rho q^2-\zeta\right)\right)\right)\left(1+\frac{\vartheta\rho}{2}q^2\left(1-\tanh\left(\frac{\vartheta}{2}\left(\rho q^2-\zeta\right)\right)\right)\right).$$

Using Equation (44), from which we get

$$\frac{\rho}{2}\left(1+\tanh\left(\frac{\vartheta}{2}\left(\rho q^2-\zeta\right)\right)\right) = \frac{((n-1)b+2\nu)q-\eta}{(n-1)q},$$

and

$$\frac{\rho}{2}\left(1-\tanh\left(\frac{\vartheta}{2}\left(\rho q_i q_j-\zeta\right)\right)\right) = \frac{((n-1)(\rho-b)-2\nu)q+\eta}{(n-1)q},$$

we then can write

$$\left.\frac{\partial^2 \mathscr{H}_\vartheta}{\partial q_i^2}\right|_{q_i=q} = -2\nu + \frac{\vartheta(((n-1)(\rho-b)-2\nu)q+\eta)(((n-1)b+2\nu)q-\eta)}{n-1},$$

and

$$\left.\frac{\partial^2 \mathscr{H}_\vartheta}{\partial q_i \partial q_j}\right|_{q_i=q_j=q} = -b + \frac{((n-1)b+2\nu)q-\eta}{(n-1)q}\left(1+\frac{\vartheta q(((n-1)(\rho-b)-2\nu)q+\eta)}{n-1}\right).$$

Denoting by $\nu^* \equiv \nu/(n-1)$ and $\eta^* \equiv \eta/(n-1)$ we can further write

$$\left.\frac{\partial^2 \mathscr{H}_\vartheta}{\partial q_i^2}\right|_{q_i=q} = (n-1)\left(-2\nu^* + \vartheta q^2\left(\rho - b - 2\nu^* + \frac{\eta^*}{q}\right)\left(b+2\nu^*-\frac{\eta^*}{q}\right)\right), \tag{48}$$

and

$$\left.\frac{\partial^2 \mathscr{H}_\vartheta}{\partial q_i \partial q_j}\right|_{q_i=q_j=q} = -b + \left(b+2\nu^*-\frac{\eta^*}{q}\right)\left(1+\vartheta q^2\left(\rho-b-2\nu^*+\frac{\eta^*}{q}\right)\right). \tag{49}$$

Note that due to symmetry, the Hessian $\Delta\mathscr{H}_\vartheta(\mathbf{q}^*)$ with components in Equations (48) and (49) is a special case of a circulant matrix. Denoting by a the diagonal elements of $\Delta\mathscr{H}_\vartheta(\mathbf{q}^*)$ and by b the off-diagonal elements, the determinant in Equation (47) follows from the general formula [Horn and Johnson, 1990]:

$$|-\Delta\mathscr{H}_\vartheta(\mathbf{q}^*)| = \begin{vmatrix} a & b & b & \ldots \\ b & a & b & \ldots \\ b & b & a & \\ \vdots & \vdots & & \ddots \end{vmatrix} = (a-b)^{n-1}(a+(n-1)b).$$

Similarly, for a circulant matrix (by applying the Sherman-Morrison formula (Horn and Johnson

[1990]) we get for the inverse in Equation (47) that

$$-\Delta\mathscr{H}_\vartheta(\mathbf{q}^*)^{-1} = \begin{pmatrix} a & b & b & \dots \\ b & a & b & \dots \\ b & b & a & \\ \vdots & \vdots & & \ddots \end{pmatrix}^{-1}$$
$$= \frac{1}{a^2+(n-2)ab-(n-1)b^2}\begin{pmatrix} a+(n-2)b & -b & -b & \dots \\ -b & a+(n-2)b & -b & \dots \\ -b & -b & a+(n-2)b & \\ \vdots & \vdots & & \ddots \end{pmatrix},$$

For large n we see from Equations (48) and (49) that the off-diagonal elements vanish relative to the diagonal elements. As $\mathbf{q}$ is asymptotically normally distributed with mean $\mathbf{q}^*$ and variance $-\frac{1}{\vartheta}\Delta\mathscr{H}_\vartheta(\mathbf{q}^*)^{-1}$, this implies that, in the limit of $n \to \infty$, the individual firms' output levels become independent. The diagonal entries are given by

$$-\frac{1}{\vartheta}\left(\Delta\mathscr{H}_\vartheta(\mathbf{q}^*)\right)^{-1}_{ii} \sim \frac{1}{\vartheta}\frac{n}{2\nu^* + \vartheta(bq-\eta^*+2\nu^* q)(q(b+2\nu^*-\rho)-\eta^*)} \equiv \sigma^2.$$

Next, we compute the expected average degree $\bar{d}$. The expected number of links can be obtained as follows

$$\mathbb{E}_{\mu^\vartheta}(m) = \sum_{G\in\mathcal{G}^n}\int_{\mathcal{Q}^n} m\mu^\vartheta(\mathbf{q},G)d\mathbf{q} = \frac{1}{\mathscr{Z}_\vartheta}\sum_{G\in\mathcal{G}^n}\int_{\mathcal{Q}^n}\underbrace{me^{\vartheta\Phi(\mathbf{q},G)}}_{-\frac{1}{\vartheta}\frac{\partial}{\partial\zeta}e^{\vartheta\Phi(\mathbf{q},G)}} d\mathbf{q} = -\frac{1}{\vartheta}\frac{1}{\mathscr{Z}_\vartheta}\frac{\partial\mathscr{Z}_\vartheta}{\partial\zeta} = \frac{1}{\vartheta}\frac{\partial\mathscr{F}_\vartheta}{\partial\zeta},$$

where we have denoted $\mathscr{F}_\vartheta \equiv -\ln\mathscr{Z}_\vartheta$. From the Laplace approximation in Equation (42) we find that

$$\frac{\partial\mathscr{F}_\vartheta}{\partial\zeta} = -\vartheta\frac{\partial\mathscr{H}_\vartheta(\mathbf{q}^*)}{\partial\zeta} + \frac{1}{2}\frac{\partial}{\partial\zeta}\ln\left|\left(\frac{\partial^2\mathscr{H}_\vartheta}{\partial q_i\partial q_j}\right)_{q_i=q^*}\right|$$
$$= -\vartheta\frac{\partial\mathscr{H}_\vartheta(\mathbf{q}^*)}{\partial\zeta} + \frac{1}{2}\mathrm{tr}\left(\left(\frac{\partial^2\mathscr{H}_\vartheta}{\partial q_i\partial q_j}\right)^{-1}\frac{\partial}{\partial\zeta}\left(\frac{\partial^2\mathscr{H}_\vartheta}{\partial q_i\partial q_j}\right)\right)_{q_i=q^*},$$

where we have used Jacobi's formula [see e.g. Horn and Johnson, 1990]. Consequently, the expected number of links is

$$\mathbb{E}_{\mu^\vartheta}(m) = -\frac{\partial\mathscr{H}_\vartheta(\mathbf{q}^*)}{\partial\zeta} + \frac{1}{2\vartheta}\mathrm{tr}\left(\left(\frac{\partial^2\mathscr{H}_\vartheta}{\partial q_i\partial q_j}\right)^{-1}\frac{\partial}{\partial\zeta}\left(\frac{\partial^2\mathscr{H}_\vartheta}{\partial q_i\partial q_j}\right)\right)_{q_i=q^*}.$$

Further, we have that

$$\frac{\partial\mathscr{H}_\vartheta}{\partial\zeta} = -\frac{1}{2}\sum_{i=1}^n\sum_{j>i}^n\left(1+\tanh\left(\frac{\vartheta}{2}\left(\rho q_i q_j-\zeta\right)\right)\right),$$

and in the symmetric equilibrium this is

$$\left.\frac{\partial\mathscr{H}_\vartheta}{\partial\zeta}\right|_{q_i=q} = -\frac{n(n-1)}{4}\left(1+\tanh\left(\frac{\vartheta}{2}\left(\rho q^2-\zeta\right)\right)\right).$$

The expected number of links can then be written as

$$\mathbb{E}_{\mu^\vartheta}(m) = \frac{n(n-1)}{2}\left(1+\tanh\left(\frac{\vartheta}{2}\left(\rho q^2-\zeta\right)\right)\right) + \frac{1}{2\vartheta}\mathrm{tr}\left(\left(\frac{\partial^2\mathscr{H}_\vartheta}{\partial q_i\partial q_j}\right)^{-1}\frac{\partial}{\partial\zeta}\left(\frac{\partial^2\mathscr{H}_\vartheta}{\partial q_i\partial q_j}\right)\right)_{q_i=q^*}.$$

Using the fact that

$$\frac{\rho}{2}\left(1+\tanh\left(\frac{\vartheta}{2}\left(\rho q^2-\zeta\right)\right)^2\right)=b+2\nu^*-\frac{\eta^*}{q},$$

where $\nu^*=\frac{\nu}{n-1}$ and $\eta^*=\frac{\eta}{n-1}$, we can write

$$\left.\frac{\partial\mathscr{H}_\vartheta}{\partial\zeta}\right|_{q_i=q}=-\frac{n(n-1)}{2\rho}\left(b+2\nu^*-\frac{\eta^*}{q}\right).$$

In the limit of $\vartheta\to\infty$ in the low equilibrium, where $q=\frac{\eta^*}{b+2\nu^*}$ and therefore $\frac{\eta^*}{q}=b+2\nu^*$, we then get

$$\left.\frac{\partial\mathscr{H}_\vartheta}{\partial\zeta}\right|_{q_i=q}=0.$$

In contrast, in the limit of $\vartheta\to\infty$ in the high equilibrium, where $q=\frac{\eta^*}{b+2\nu^*-\rho}$, and $\frac{\eta^*}{q}=b+2\nu^*-\rho$ we find that

$$\left.\frac{\partial\mathscr{H}_\vartheta}{\partial\zeta}\right|_{q_i=q}=-\frac{n(n-1)}{2}.$$

Further, the derivatives with respect to ζ in Equation (45) are given by

$$\frac{\partial}{\partial\zeta}\frac{\partial^2\mathscr{H}_\vartheta}{\partial q_i^2}=\frac{\vartheta^2\rho^2}{4}\sum_{j\neq i}^{n}\tanh\left(\frac{\vartheta}{2}\left(\rho q_iq_j-\zeta\right)\right)\left(1-\tanh\left(\frac{\vartheta}{2}\left(\rho q_iq_j-\zeta\right)\right)^2\right),$$

and for $j\neq i$ from Equation (46) we get that

$$\frac{\partial}{\partial\zeta}\frac{\partial^2\mathscr{H}_\vartheta}{\partial q_i\partial q_j}=-\frac{\vartheta\rho}{4}\left(1-\tanh\left(\frac{\vartheta}{2}\left(\rho q_iq_j-\zeta\right)\right)^2\right)\left(1-\vartheta\rho q_iq_j\tanh\left(\frac{\vartheta}{2}\left(\rho q_iq_j-\zeta\right)\right)\right).$$

Imposing symmetry, $q_i=q$ for all $i=1,\dots,n$, we then can write

$$\left.\frac{\partial}{\partial\zeta}\frac{\partial^2\mathscr{H}_\vartheta}{\partial q_i^2}\right|_{q_i=q}=\frac{(n-1)\vartheta^2\rho^2}{4}\tanh\left(\frac{\vartheta}{2}\left(\rho q^2-\zeta\right)\right)\left(1-\tanh\left(\frac{\vartheta}{2}\left(\rho q^2-\zeta\right)\right)^2\right),\tag{50}$$

and

$$\left.\frac{\partial}{\partial\zeta}\frac{\partial^2\mathscr{H}_\vartheta}{\partial q_i\partial q_j}\right|_{q_i=q_j=q}=-\frac{\vartheta\rho}{4}\left(1-\tanh\left(\frac{\vartheta}{2}\left(\rho q^2-\zeta\right)\right)^2\right)\left(1-\vartheta\rho q^2\tanh\left(\frac{\vartheta}{2}\left(\rho q^2-\zeta\right)\right)\right).\tag{51}$$

For a circulant matrix (by applying the Sherman-Morrison formula [Horn and Johnson, 1990] we have that

$$\begin{pmatrix}a&b&b&\dots\\b&a&b&\dots\\b&b&a&\\\vdots&\vdots&&\ddots\end{pmatrix}^{-1}=\frac{1}{a^2+(n-2)ab-(n-1)b^2}\begin{pmatrix}a+(n-2)b&-b&-b&\dots\\-b&a+(n-2)b&-b&\dots\\-b&-b&a+(n-2)b&\\\vdots&\vdots&&\ddots\end{pmatrix},$$

and

$$\operatorname{tr}\begin{pmatrix}c&d&d&\dots\\d&c&d&\dots\\d&d&c&\\\vdots&\vdots&&\ddots\end{pmatrix}\begin{pmatrix}e&f&f&\dots\\f&e&f&\dots\\f&f&e&\\\vdots&\vdots&&\ddots\end{pmatrix}=n(ce+(n-1)df),$$

so that

$$\operatorname{tr}\begin{pmatrix} a & b & b & \dots \\ b & a & b & \dots \\ b & b & a & \\ \vdots & \vdots & & \ddots \end{pmatrix}^{-1}\begin{pmatrix} e & f & f & \dots \\ f & e & f & \dots \\ f & f & e & \\ \vdots & \vdots & & \ddots \end{pmatrix} = \frac{n((a+(n-2)b)e-(n-1)bf)}{a^2+(n-2)ab-(n-1)b^2}.$$

The expected number of links can then be written as follows

$$\mathbb{E}_{\mu^\vartheta}(m) = \frac{n(n-1)}{2}\left(1+\tanh\left(\frac{\vartheta}{2}\left(\rho q^2-\zeta\right)\right)\right)+\frac{1}{2\vartheta}\mathscr{R}_\vartheta,$$

where

$$\mathscr{R}_\vartheta \equiv \frac{n((c_1+(n-2)c_2)c_3-(n-1)c_2c_4)}{c_1^2+(n-2)c_1c_2-(n-1)c_2^2},$$

with

$$\begin{aligned}
c_1 &\equiv -2\nu+(n-1)\frac{\vartheta\rho^2q^2}{4}\left(1-\tanh\left(\frac{\vartheta}{2}\left(\rho q^2-\zeta\right)\right)^2\right),\\
c_2 &\equiv -b+\frac{\rho}{2}\left(1+\tanh\left(\frac{\vartheta}{2}\left(\rho q^2-\zeta\right)\right)\right)\left(1+\frac{\vartheta\rho q^2}{2}\left(1-\tanh\left(\frac{\vartheta}{2}\left(\rho q^2-\zeta\right)\right)\right)\right),\\
c_3 &\equiv \frac{(n-1)\vartheta^2\rho^2}{4}\tanh\left(1-\tanh\left(\frac{\vartheta}{2}\left(\rho q^2-\zeta\right)\right)^2\right),\\
c_4 &\equiv -\frac{\rho\vartheta}{4}\left(1-\tanh\left(\frac{\vartheta}{2}\left(\rho q^2-\zeta\right)\right)^2\right)\left(1-\vartheta\rho q^2\tanh\left(\frac{\vartheta}{2}\left(\rho q^2-\zeta\right)\right)\right).
\end{aligned}$$

In the following we compute the degree distribution. From our previous discussion we know that each firm i has an output level q distributed identically and independently with density $\mu^\vartheta(q)$ given by $\mathcal{N}(q^*,\sigma^2)$ and converging to $\delta(q-q^*)$ in the limit $\vartheta\to\infty$. With the marginal distribution from Equation (40) and the potential in Equation (37) we then can write the conditional distribution as

$$\begin{aligned}
\mu^\vartheta(G|\mathbf{q}) = \frac{\mu^\vartheta(\mathbf{q},G)}{\mu^\vartheta(\mathbf{q})} = \frac{e^{\vartheta\Phi(\mathbf{q},G)}}{\sum_{G'\in\mathcal{G}^n}e^{\vartheta\Phi(\mathbf{q},G')}} &= \frac{e^{\psi(\mathbf{q})}e^{\vartheta\sum_{i<j}^n a_{ij}(\rho q_iq_j-\zeta)}}{e^{\psi(\mathbf{q})}\prod_{i<j}\left(1+e^{\vartheta(\rho q_iq_j-\zeta)}\right)}\\
&= \frac{e^{\vartheta\sum_{i<j}^n a_{ij}(\rho q_iq_j-\zeta)}}{\prod_{i<j}\left(1+e^{\vartheta(\rho q_iq_j-\zeta)}\right)}\\
&= \prod_{i<j}\frac{e^{\vartheta a_{ij}(\rho q_iq_j-\zeta)}}{1+e^{\vartheta(\rho q_iq_j-\zeta)}}\\
&= \prod_{i<j}\left(\frac{e^{\vartheta(\rho q_iq_j-\zeta)}}{1+e^{\vartheta(\rho q_iq_j-\zeta)}}\right)^{a_{ij}}\left(1-\frac{e^{\vartheta(\rho q_iq_j-\zeta)}}{1+e^{\vartheta(\rho q_iq_j-\zeta)}}\right)^{1-a_{ij}}\\
&= \prod_{i<j}p^\vartheta(q_i,q_j)^{a_{ij}}\left(1-p^\vartheta(q_i,q_j)\right)^{1-a_{ij}}. \qquad (52)
\end{aligned}$$

Hence, we obtain the likelihood of an inhomogeneous random graph with link probability[52]

$$p^\vartheta(q_i,q_j) = \frac{e^{\vartheta(\rho q_iq_j-\zeta)}}{1+e^{\vartheta(\rho q_iq_j-\zeta)}} = \frac{g^\vartheta(q_i,q_j)}{1+g^\vartheta(q_i,q_j)}, \qquad (53)$$

where we have denoted $g^\vartheta(q,q')\equiv e^{\vartheta(\rho qq'-\zeta)}$. The probability of observing the network G, given

[52] See also supplementary Appendix B, Boguná and Pastor-Satorras [2003] and and Söderberg [2002].

the output levels $\mathbf{q}$ can then be written as follows

$$\mu^{\vartheta}(G|\mathbf{q}) = \prod_{i=1}^{n}\prod_{j=i+1}^{n}\left(\frac{g^{\vartheta}(q_i,q_j)}{1+g^{\vartheta}(q_i,q_j)}\right)^{a_{ij}}\left(\frac{1}{1+g^{\vartheta}(q_i,q_j)}\right)^{1-a_{ij}} = \prod_{i=1}^{n}\prod_{j=i+1}^{n}\frac{1}{1+g^{\vartheta}(q_i,q_j)}\prod_{i=1}^{n}\prod_{j=i+1}^{n}g^{\vartheta}(q_i,q_j)^{a_{ij}},$$

which can be written as

$$\mu^{\vartheta}(G|\mathbf{q}) = \mathscr{C}_{\vartheta}(\mathbf{q})\prod_{i=1}^{n}\prod_{j=i+1}^{n}g^{\vartheta}(q_i,q_j)^{a_{ij}},$$

with the normalizing constant

$$\mathscr{C}_{\vartheta}(\mathbf{q}) \equiv \prod_{i=1}^{n}\prod_{j=i+1}^{n}\left(1+g^{\vartheta}(q_i,q_j)\right).$$

Since $\sum_{G\in\mathcal{G}^n}\mathbb{P}\left(G|\,\mathbf{q}\right)=1$, $\mathscr{C}_{\vartheta}(\mathbf{q})$ can also be written as

$$\mathscr{C}_{\vartheta}(\mathbf{q}) = \sum_{G\in\mathcal{G}^n}\prod_{i=1}^{n}\prod_{j=i+1}^{n}g^{\vartheta}(q_i,q_j)^{a_{ij}}.$$

Next, we consider the probability generating function of the vector of degrees, $(d_i(G))_{i=1}^n$, given by

$$\begin{aligned}
\mathbb{E}_{\mu^{\vartheta}}\left(\prod_{i=1}^{n}x_i^{d_i(G)}\middle|\,\mathbf{q}\right) &= \mathbb{E}\left(\prod_{i=1}^{n}\prod_{j=i+1}^{n}(x_ix_j)^{a_{ij}}\middle|\,\mathbf{q}\right) \qquad (54)\\
&= \sum_{G\in\mathcal{G}^n}\mathbb{P}\left(G|\,\mathbf{q}\right)\prod_{i=1}^{n}\prod_{j=i+1}^{n}(x_ix_j)^{a_{ij}}\\
&= \frac{1}{\mathscr{C}_{\vartheta}(\mathbf{q})}\sum_{G\in\mathcal{G}^n}\prod_{i=1}^{n}\prod_{j=i+1}^{n}g^{\vartheta}(q_i,q_j)^{a_{ij}}\prod_{i=1}^{n}\prod_{j=i+1}^{n}(x_ix_j)^{a_{ij}}\\
&= \frac{1}{\mathscr{C}_{\vartheta}(\mathbf{q})}\sum_{G\in\mathcal{G}^n}\prod_{i=1}^{n}\prod_{j=i+1}^{n}\left(g^{\vartheta}(q_i,q_j)x_ix_j\right)^{a_{ij}}\\
&= \frac{\sum_{G\in\mathcal{G}^n}\prod_{i=1}^{n}\prod_{j=i+1}^{n}\left(g^{\vartheta}(q_i,q_j)x_ix_j\right)^{a_{ij}}}{\prod_{i=1}^{n}\prod_{j=i+1}^{n}(1+g^{\vartheta}(q_i,q_j))}\\
&= \prod_{i=1}^{n}\prod_{j=i+1}^{n}\frac{1+g^{\vartheta}(q_i,q_j)x_ix_j}{1+g^{\vartheta}(q_i,q_j)}, \qquad (55)
\end{aligned}$$

where we have used the fact that $\sum_{G\in\mathcal{G}^n}\prod_{i=1}^{n}\prod_{j=i+1}^{n}\left(g^{\vartheta}(q_i,q_j)x_ix_j\right)^{a_{ij}} = \prod_{i=1}^{n}\prod_{j=i+1}^{n}\left(1+g^{\vartheta}(q_i,q_j)x_ix_j\right)$. To compute the generating function of $d_1(G)$, we simply set $x_i=1$ for all $i>1$. Then

$$\begin{aligned}
\mathbb{E}_{\mu^{\vartheta}}\left(x_1^{d_1(G)}\right) &= \mathbb{E}_{\mu^{\vartheta}}\left(\mathbb{E}_{\mu^{\vartheta}}\left(x_1^{d_1(G)}\middle|\,q_1\right)\right)\\
&= \mathbb{E}_{\mu^{\vartheta}}\left(\mathbb{E}_{\mu^{\vartheta}}\left(\prod_{j=2}^{n}\frac{1+g^{\vartheta}(q_1,q_j)x_1}{1+g^{\vartheta}(q_1,q_j)}\middle|\,q_1\right)\right)\\
&= \mathbb{E}_{\mu^{\vartheta}}\left(\left(\mathbb{E}_{\mu^{\vartheta}}\left(\frac{1+g^{\vartheta}(q_1,q_2)x_1}{1+g^{\vartheta}(q_1,q_2)}\middle|\,q_1\right)\right)^{n-1}\right),
\end{aligned}$$

where we have used symmetry and the independence of $q_1,\ldots,q_n$. Further, note that

$$\frac{1+xy}{1+x} = 1+(y-1)x+O\left(x^2\right).$$

Hence, for $g^\vartheta(q_1,q_2)$ small in the sparse graph limit, we can write

$$\begin{aligned}\mathbb{E}_{\mu^\vartheta}\left(\frac{1+g^\vartheta(q_1,q_2)x_1}{1+g^\vartheta(q_1,q_2)}\middle|\, q_1\right) &= \int_{\mathcal{Q}}\frac{1+g^\vartheta(q_1,q_2)x_1}{1+g^\vartheta(q_1,q_j)}\mu^\vartheta(dq_2)\\ &= 1+(x_1-1)\int_{\mathcal{Q}} g^\vartheta(q_1,q_2)\mu^\vartheta(dq_2)+o(1)\\ &= 1+(x_1-1)\nu^\vartheta(q_1)+o(1),\end{aligned}$$

where we have denoted $\nu^\vartheta(q)\equiv\int_{\mathcal{Q}} g^\vartheta(q,q')\mu^\vartheta(dq')$. It then follows that

$$\mathbb{E}_{\mu^\vartheta}\left(x_1^{d_1(G)}\right)=\mathbb{E}_{\mu^\vartheta}\left(\left(1+(x_1-1)\nu^\vartheta(q_1)\right)^{n-1}\right)(1+o(1))=\mathbb{E}_{\mu^\vartheta}\left(e^{(x_1-1)(n-1)\nu^\vartheta(q_1)}\right)(1+o(1)),$$

where we have used the fact that $e^{(x_1-1)\nu^\vartheta(q)}=1+(x_1-1)\nu^\vartheta(q)+o(1)$. This is the probability generating function of a mixed Poisson random variable with mixing parameter $\nu^\vartheta(q)$. In particular, since $p^\vartheta(q,q')=g^\vartheta(q,q')+o(1)$, we can write $n\nu^\vartheta(q)=n\int_{\mathcal{Q}}p(q,q')\mu^\vartheta(dq')=\sum_{j=1}^n\int_{\mathcal{Q}}p^\vartheta(q,q_j)\mu^\vartheta(dq_j)=\sum_{j=1}^n\mathbb{P}\left(a_{1j}=1|\, q_1=q\right)=\mathbb{E}_{\mu^\vartheta}\left(d_1(G)|\, q_1=q\right)$, which is the expected degree of a firm with output q, and we denote it by $\bar{d}(q)$. Further, it then follows that

$$\begin{aligned}\mathbb{E}_{\mu^\vartheta}\left(x_1^{d_1(G)}\right) &= \sum_{k=0}^n x_1^k\mathbb{P}\left(d_1(G)=k\right)\\ &= \mathbb{E}_{\mu^\vartheta}\left(e^{(x_1-1)\bar{d}(q_1)}\right)(1+o(1))\\ &= \mathbb{E}_{\mu^\vartheta}\left(e^{-\bar{d}(q_1)}\sum_{k=0}^n\frac{(x_1\bar{d}(q_1))^k}{k!}\right)(1+o(1))\\ &\sum_{k=0}^n x_1^k\mathbb{E}_{\mu^\vartheta}\left(\frac{e^{-\bar{d}(q_1)}\bar{d}(q_1)^k}{k!}\right)(1+o(1)).\end{aligned}$$

Let the empirical degree distribution be given by $\bar{P}^\vartheta(k)=\frac{1}{n}\sum_{i=1}^n\mathbb{1}_{\{d_i(G)=k\}}$, and denoted by $P^\vartheta(k)\equiv\mathbb{E}_{\mu^\vartheta}\left(\bar{P}^\vartheta(k)\right)$. Then we have that

$$P^\vartheta(k)=\mathbb{P}\left(d_1(G)=k\right)=\mathbb{E}_{\mu^\vartheta}\left(\frac{e^{-\bar{d}(q_1)}\bar{d}(q_1)^k}{k!}\right)(1+o(1)).$$

We now give a proof of part (ii) of the proposition. In the limit of $\vartheta\to\infty$ we obtain from the FOC in Equation (44) that

$$(b+2\nu^*)q-\eta^*=\begin{cases}\rho q, & \text{if } \zeta<\rho q^2,\\ 0, & \text{if } \rho q^2<\zeta.\end{cases}$$

This shows that the right hand side of Equation (10) has a point of discontinuity at $\sqrt{\frac{\zeta}{\rho}}$ (see Figure 1). It then follows that, in the limit of $\vartheta\to\infty$ (for the stochastically stable equilibrium), we have

$$q^*=\begin{cases}\frac{\eta}{b+2\nu^*-\rho}, & \text{if } \zeta<\frac{\rho(\eta^*)^2}{(b+2\nu^*)^2},\\ \left\{\frac{\eta^*}{b+2\nu^*-\rho},\frac{\eta^*}{b+2\nu^*}\right\}, & \text{if } \frac{\rho(\eta^*)^2}{(b+2\nu^*)^2}<\zeta<\frac{\rho\eta^2}{(b+2\nu^*-\rho)^2},\\ \frac{\eta^*}{b+2\nu^*}, & \text{if } \frac{\rho(\eta^*)^2}{(b+2\nu^*-\rho)^2}<\zeta,\end{cases}\tag{56}$$

which is increasing in ρ and η^*, and decreasing in ζ and b (see Figure 1). Next, note that

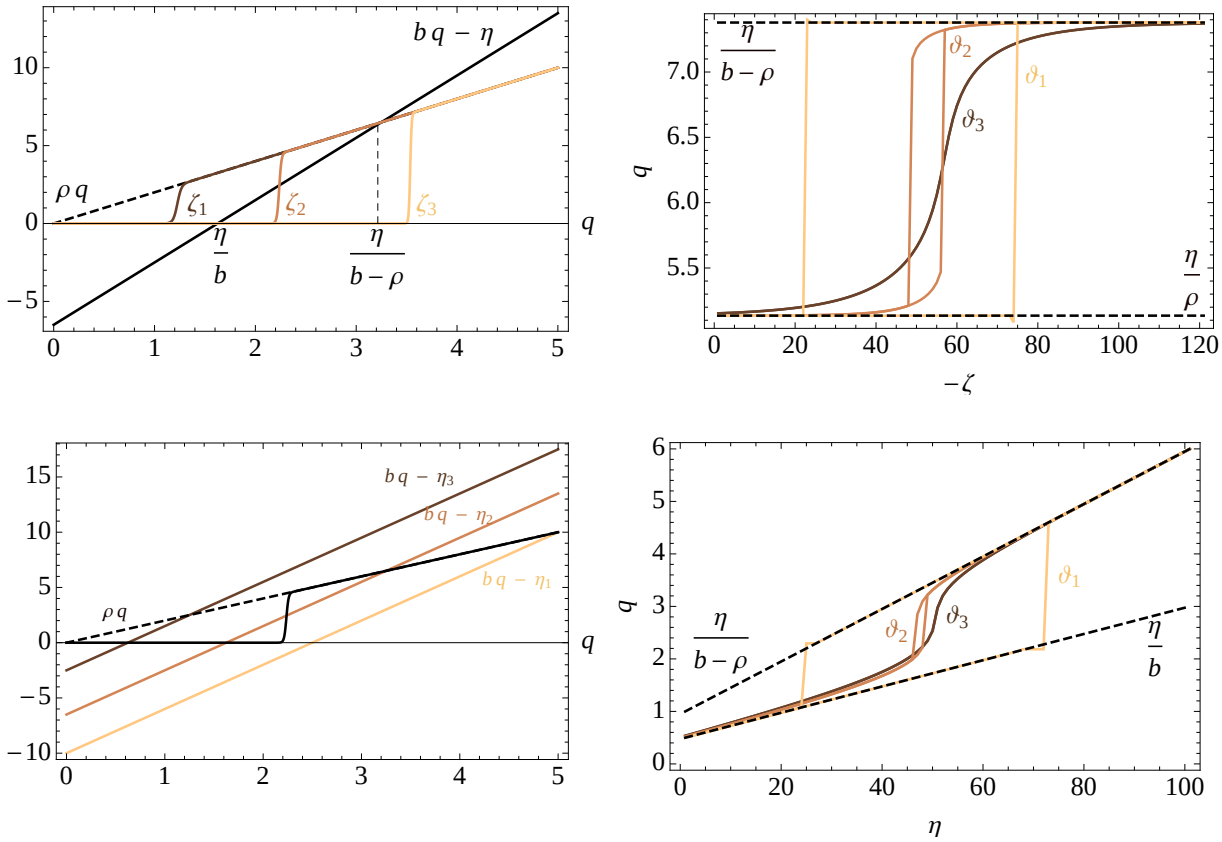

Figure 1: (Top left panel) The right hand side of Equation (10) for different values of $\zeta_1 = 25$, $\zeta_2 = 10$, $\zeta_3 = 3$ and $b = 4$, $\rho = 2$, $\eta = 6.5$, $\nu = 0$ and $\vartheta = 10$. (Top right panel) The values of q solving Equation (10) for different values of ζ with $b = 1.48$, $\rho = 0.45$ and $\vartheta_1 = 49.5$, $\vartheta_2 = 0.495$, $\vartheta_3 = 0.2475$. (Bottom left panel) The right hand side of Equation (10) for different values of $\eta_1 = 2.5$, $\eta_2 = 6.5$, $\eta_3 = 10$ and $b = 4$, $\rho = 2$, $\zeta = 10$ and $\vartheta = 10$. (Bottom right panel) The values of q solving Equation (10) for different values of η with $b = 4$, $\rho = 2$ and $\vartheta_1 = 10$, $\vartheta_2 = 0.26$, $\vartheta_3 = 0.2$.

$$\mathbb{E}_{\mu^\vartheta}\left(\sum_{i=1}^n q_i^2\right) = \sum_{G\in\mathcal{G}^n}\int_{\mathcal{Q}^n} d\mathbf{q}\left(\sum_{i=1}^n q_i^2\right)\mu^\vartheta(\mathbf{q},G) = \frac{1}{\mathscr{Z}_\vartheta}\sum_{G\in\mathcal{G}^n}\int_{\mathcal{Q}^n} d\mathbf{q}\left(\sum_{i=1}^n q_i^2\right)e^{\vartheta\Phi(\mathbf{q},G)}$$
$$= \frac{1}{\mathscr{Z}_\vartheta}\sum_{G\in\mathcal{G}^n}\int_{\mathcal{Q}^n} d\mathbf{q}\frac{1}{\vartheta^2}\frac{\partial^2}{\partial\eta^2}e^{\vartheta\Phi(\mathbf{q},G)} = \frac{1}{\mathscr{Z}_\vartheta}\frac{1}{\vartheta^2}\frac{\partial^2\mathscr{Z}_\vartheta}{\partial\eta^2},$$

where we have denoted $\mathscr{F}_\vartheta \equiv -\ln\mathscr{Z}_\vartheta$. We further have that

$$\frac{\partial^2\ln\mathscr{Z}_\vartheta}{\partial\eta^2} = \frac{1}{\mathscr{Z}_\vartheta}\frac{\partial^2\mathscr{Z}_\vartheta}{\partial\eta^2} - \frac{1}{\mathscr{Z}_\vartheta^2}\left(\frac{\partial\mathscr{Z}_\vartheta}{\partial\eta}\right)^2 = \frac{1}{\mathscr{Z}_\vartheta}\frac{\partial^2\mathscr{Z}_\vartheta}{\partial\eta^2} - \left(\frac{\partial\ln\mathscr{Z}_\vartheta}{\partial\eta}\right)^2 = \vartheta^2\mathbb{E}_{\mu^\vartheta}\left(\sum_{i=1}^n q_i^2\right) - \vartheta^2\mathbb{E}_{\mu^\vartheta}\left(\sum_{i=1}^n q_i\right)^2.$$

We then get

$$\mathrm{Var}_{\mu^\vartheta}\left(\sum_{i=1}^n q_i\right) = \mathbb{E}_{\mu^\vartheta}\left(\sum_{i=1}^n q_i^2\right) - \mathbb{E}_{\mu^\vartheta}\left(\sum_{i=1}^n q_i\right)^2 = \frac{1}{\vartheta^2}\frac{\partial^2\ln\mathscr{Z}_\vartheta}{\partial\eta^2} = -\frac{1}{\vartheta^2}\frac{\partial^2\mathscr{F}_\vartheta}{\partial\eta^2}.$$

The variance of the mean is then given by

$$\mathrm{Var}_{\mu^\vartheta}\left(\frac{1}{n}\sum_{i=1}^n q_i\right) = -\frac{1}{n^2\vartheta^2}\frac{\partial^2\mathscr{F}_\vartheta}{\partial\eta^2}.$$

We have that

$$\frac{\partial^2\mathscr{F}_\vartheta}{\partial\eta^2} = -\vartheta\frac{\partial^2\mathscr{H}_\vartheta(\mathbf{q}^*)}{\partial\eta^2} = 0,$$

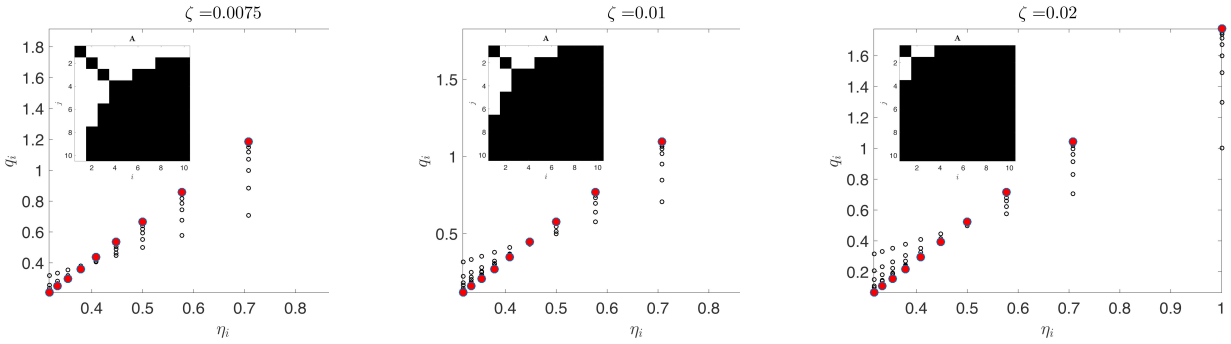

Figure 2: The output iteration of Equation (59) over the firm fixed effects η_i. Filled circles indicate the fixed points. The insets show the adjacency matrix $\mathbf{A} = (a_{ij})_{1\leq i,j,n}$ with elements are given by $a_{ij} = \mathbb{1}_{\left\{q_i q_j > \frac{\zeta}{\rho}\right\}}$ (see also Figure 4), where the vector $\mathbf{q}$ is the fixed point of Equation (59). The panels from the left to the right correspond to increasing linking costs $\zeta \in \{0.0075, 0.01, 0.02\}$. The parameters used are $n = 10$, $\nu = 0.5$, $b = 0.06$, $\rho = 0.02$ and $\boldsymbol{\eta} = (1.00, 0.71, 0.58, 0.50, 0.45, 0.41, 0.38, 0.35, 0.33, 0.32)^\top$.

and we get

$$\mathrm{Var}_{\mu^*}\left(\frac{1}{n}\sum_{i=1}^{n} q_i\right) = \lim_{\vartheta\to\infty} \mathrm{Var}_{\mu^\vartheta}\left(\frac{1}{n}\sum_{i=1}^{n} q_i\right) = 0.$$

Note that the variance of the average output can be equal to zero only if it is equal to its expectation in all of its support. This can only happen if the average output is equal to q^* with probability one in the large ϑ limit.

Further, in the limit of $\vartheta \to \infty$, for both, the low equilibrium, where $q = \frac{\eta^*}{b+2\nu^*}$ and therefore $\frac{\eta^*}{q} = b + 2\nu^*$, as well as the high equilibrium, where $q = \frac{\eta^*}{b+2\nu^*-\rho}$, and $\frac{\eta^*}{q} = b + 2\nu^* - \rho$ we find from Equation (50) that

$$\frac{\partial}{\partial\zeta}\left.\frac{\partial^2 \mathscr{H}_\vartheta}{\partial q_i^2}\right|_{q_i=q} = 0,$$

and from Equation (51) we get

$$\frac{\partial}{\partial\zeta}\left.\frac{\partial^2 \mathscr{H}_\vartheta}{\partial q_i \partial q_j}\right|_{q_i=q_j=q} = 0.$$

Hence, we find that in the high equilibrium $\mathbb{E}_{\mu^*}(m) = \lim_{\vartheta\to\infty}\mathbb{E}_{\mu^\vartheta}(m) = \frac{n(n-1)}{2}$, while in the low equilibrium $\mathbb{E}_{\mu^*}(m) = \lim_{\vartheta\to\infty}\mathbb{E}_{\mu^\vartheta}(m) = 0$. Consequently, the expected average degree in the high equilibrium is $\mathbb{E}_{\mu^*}\left(\frac{1}{n}\sum_{i=1}^{n} d_i\right) = \lim_{\vartheta\to\infty}\mathbb{E}_{\mu^\vartheta}\left(\frac{1}{n}\sum_{i=1}^{n} d_i\right) = n - 1$, where we have a complete graph, K_n, and zero in the low equilibrium where we obtain an empty graph, $\overline{K}_n$. □

We next give the proof of Proposition 3, which generalizes Proposition 2 by allowing for firm heterogeneity.

Proof of Proposition 3. We first give a proof of part (i) of the proposition. We have that $\mu^\vartheta(\mathbf{q}, G) = \mu^\vartheta(G|\mathbf{q})\mu^\vartheta(\mathbf{q})$. Analogous to the proof of Proposition 2 one can show that $\mu^\vartheta(G|\mathbf{q}) = \prod_{i<j} p^\vartheta(q_i, q_j)^{a_{ij}} \left(1 - p^\vartheta(q_i, q_j)\right)^{1-a_{ij}}$ where $p^\vartheta(q_i, q_j)$ is given by Equation (53), which corresponds to an inhomogeneous random graph with linking probability $p^\vartheta : \mathcal{Q}\times\mathcal{Q} \to [0, 1]$. The output distribution is given by

$$\mu^\vartheta(\mathbf{q}) = \frac{1}{\mathscr{Z}_\vartheta}\sum_{G\in\mathcal{G}^n} e^{\vartheta\Phi(\mathbf{q},G)} = \frac{1}{\mathscr{Z}_n^\vartheta} e^{\vartheta\mathscr{H}_\vartheta(\mathbf{q})},$$

where the Hamiltonian is implicitly defined by $e^{\vartheta\mathscr{H}_\vartheta(\mathbf{q})} = \sum_{G\in\mathcal{G}^n} e^{\vartheta\Phi(\mathbf{q},G)}$. From a Taylor expan-

sion around $\mathbf{q}^*$ (for large ϑ) we have that

$$\mathscr{H}_\vartheta(\mathbf{q}) = \mathscr{H}_\vartheta(\mathbf{q}^*) + (\mathbf{q}-\mathbf{q}^*)\nabla\mathscr{H}_\vartheta(\mathbf{q}^*) + \frac{1}{2}(\mathbf{q}-\mathbf{q}^*)^\top \Delta\mathscr{H}_\vartheta(\mathbf{q}^*)(\mathbf{q}-\mathbf{q}^*) + o\left(\|\mathbf{q}-\mathbf{q}^*\|^2\right),$$

as $\vartheta \to \infty$, where $\mathbf{q}^* = \operatorname{argmax}_{\mathbf{q}\in[0,\bar{q}]^n} \mathscr{H}_\vartheta(\mathbf{q})$, the gradient is $\nabla\mathscr{H}_\vartheta(\mathbf{q}) = \left(\frac{\partial\mathscr{H}_\vartheta}{\partial q_i}\right)_{i=1,\dots,n}$, and the Hessian is $\Delta\mathscr{H}_\vartheta(\mathbf{q}) = \left(\frac{\partial^2\mathscr{H}_\vartheta}{\partial q_i \partial q_j}\right)_{i,j=1,\dots,n}$. As the gradient $\nabla\mathscr{H}_\vartheta(\mathbf{q})$ vanishes at $\mathbf{q}^*$, we have that

$$\mathscr{H}_\vartheta(\mathbf{q}) = \mathscr{H}_\vartheta(\mathbf{q}^*) + \frac{1}{2}(\mathbf{q}-\mathbf{q}^*)^\top \Delta\mathscr{H}_\vartheta(\mathbf{q}^*)(\mathbf{q}-\mathbf{q}^*) + o\left(\|\mathbf{q}-\mathbf{q}^*\|^2\right).$$

We then can write

$$\mu^\vartheta(\mathbf{q}) = \frac{1}{\mathscr{Z}_n^\vartheta} e^{\vartheta\mathscr{H}_\vartheta(\mathbf{q}^*)} \exp\left\{-\frac{1}{2}\vartheta(\mathbf{q}-\mathbf{q}^*)^\top(-\nabla\mathscr{H}_\vartheta(\mathbf{q}^*))(\mathbf{q}-\mathbf{q}^*)\right\} + o\left(\|\mathbf{q}-\mathbf{q}^*\|^2\right).$$

Normalization, $\int_{\mathcal{Q}^n} \mu^\vartheta(\mathbf{q})d\mathbf{q} = 1$, implies that

$$\begin{aligned}\mathscr{Z}_n^\vartheta &= \int_{\mathcal{Q}^n} e^{\mathscr{H}_\vartheta(\mathbf{q})}d\mathbf{q} = e^{\vartheta\mathscr{H}_\vartheta(\mathbf{q}^*)} \int_{\mathcal{Q}^n} \exp\left\{-\frac{1}{2}\vartheta(\mathbf{q}-\mathbf{q}^*)^\top(-\Delta\mathscr{H}_\vartheta(\mathbf{q}^*))(\mathbf{q}-\mathbf{q}^*)\right\} d\mathbf{q} + o\left(\|\mathbf{q}-\mathbf{q}^*\|^2\right) \\ &= e^{\vartheta\mathscr{H}_\vartheta(\mathbf{q}^*)}(2\pi)^{\frac{n}{2}} |-\Delta\mathscr{H}_\vartheta(\mathbf{q}^*)|^{-\frac{1}{2}} + o\left(\|\mathbf{q}-\mathbf{q}^*\|^2\right).\end{aligned}$$

The Laplace approximation of $\mu^\vartheta(\mathbf{q})$ is then given by [Wong, 2001, Theorem 3, p. 495]

$$\mu^\vartheta(\mathbf{q}) = \left(\frac{2\pi}{\vartheta}\right)^{-\frac{n}{2}} |-\Delta\mathscr{H}_\vartheta(\mathbf{q}^*)|^{\frac{1}{2}} \exp\left\{-\frac{1}{2}\vartheta(\mathbf{q}-\mathbf{q}^*)^\top(-\Delta\mathscr{H}_\vartheta(\mathbf{q}^*))(\mathbf{q}-\mathbf{q}^*)\right\} + o\left(\|\mathbf{q}-\mathbf{q}^*\|^2\right).$$

That is, in the limit of large ϑ, $\mathbf{q}$ is asymptotically normally distributed with mean $\mathbf{q}^*$ and variance $-\frac{1}{\vartheta}\delta\mathscr{H}_\vartheta(\mathbf{q}^*)^{-1}$, where $\Delta\mathscr{H}_\vartheta(\mathbf{q}) = \left(\frac{\partial^2\mathscr{H}_\vartheta}{\partial q_i\partial q_j}\right)_{i,j=1,\dots,n}$ with $\frac{\partial^2\mathscr{H}_\vartheta}{\partial q_i^2}$ given by Equation (45) while, for any $i \neq j$, $\frac{\partial^2\mathscr{H}_\vartheta}{\partial q_i\partial q_j}$ is given by Equation (46).

We next turn to part (ii) of the proposition. We show that the networks G in the support of the stationary distribution $\mu^\vartheta(\mathbf{q}, G)$ in the limit of vanishing noise $\vartheta \to \infty$ is a nested split graph. A graph G is a nested split graph if for every node $i \in \mathcal{N}$ there exist a weight x_i and a threshold T such that vertices i and j are linked if and only if $x_i + x_j \geq T$ [Mahadev and Peled, 1995].

In the limit $\vartheta \to \infty$ the conditional probability of the network G can be written as $\mu^*(G|\mathbf{q}) = \lim_{\vartheta\to\infty}\mu^\vartheta(G|\mathbf{q}) = \prod_{i<j}^n \mathbb{1}_{\{\rho q_i q_j > \zeta\}}^{a_{ij}} \mathbb{1}_{\{\rho q_i q_j < \zeta\}}^{1-a_{ij}}$. Assume that G is a stochastically stable network, that is for $G \in \Omega^*$, we must have that $\mu^*(\mathbf{q}, G) = \lim_{\vartheta\to\infty}\mu^\vartheta(\mathbf{q}, G) > 0$. Since, $\mu^*(\mathbf{q}, G) = \mu^*(G|\mathbf{q})\mu^*(\mathbf{q})$ this implies that $\mu^*(G|\mathbf{q}) > 0$. It follows that $\rho q_i q_j > \zeta$ for all $a_{ij} = 1$ and $\rho q_i q_j < \zeta$ for all $a_{ij} = 0$. We then define the weights $x_i \equiv \log q_i$, $x_j \equiv \log q_j$ and a threshold $T \equiv \log\zeta - \log\rho$, and conclude that G is a nested split graph (or threshold graph, see also supplementary Appendix B).

Moreover, the output distribution is given by $\mu^\vartheta(\mathbf{q}) = \frac{1}{\mathscr{Z}_\vartheta}\sum_{G\in\mathcal{G}^n} e^{\vartheta\Phi(\mathbf{q},G)} = \frac{1}{\mathscr{Z}_n^\vartheta} e^{\vartheta\mathscr{H}_\vartheta(\mathbf{q})}$, where the Hamiltonian is given by Equation (41). The output profile that maximizes the Hamiltonian can be found from the FOC , $\frac{\partial\mathscr{H}_\vartheta}{\partial q_i} = 0$, from which we get

$$q_i = \frac{\eta_i}{2\nu} + \frac{1}{2\nu}\sum_{j\neq i}^n \left(\frac{\rho}{2}\left(1 + \tanh\left(\frac{\vartheta}{2}(\rho q_i q_j - \zeta)\right)\right) - b\right) q_j.$$

Taking the limit $\vartheta \to \infty$ and noting that

$$\lim_{\vartheta\to\infty}\frac{1}{2}\left(1 + \tanh\left(\frac{\vartheta}{2}(\rho q_i q_j - \zeta)\right)\right) = \begin{cases}1, & \text{if } \rho q_i q_j > \zeta, \\ 0, & \text{if } \rho q_i q_j < \zeta,\end{cases}$$

we thus obtain[53]

$$q_i = \frac{\eta_i}{2\nu} + \frac{1}{2\nu}\sum_{j\neq i}^{n} q_j \left(\rho \mathbb{1}_{\left\{q_i q_j > \frac{\zeta}{\rho}\right\}} - b\right). \tag{57}$$

Note that for any profile of output levels $\mathbf{q}$ there exists a unique nested split graph with adjacency matrix $\mathbf{A} = (a_{ij})_{1\leq i,j,n}$ whose elements are given by $a_{ij} = \mathbb{1}_{\left\{q_i q_j > \frac{\zeta}{\rho}\right\}}$. Then we can write Equation (57) as follows

$$q_i = \frac{\eta_i}{2\nu} + \frac{\rho}{2\nu}\sum_{j\neq i}^{n} a_{ij} q_j - \frac{b}{2\nu}\sum_{j\neq i}^{n} q_j. \tag{58}$$

Moreover, assume that $\eta_i > \eta_j$, then we want to show that $q_j > q_i$ for the output profile $\mathbf{q}$ solving Equation (57). For this purpose we consider the iteration

$$q_{i,t+1} = f_i(\mathbf{q}_t) \equiv \max\left\{0, \frac{\eta_i}{2\nu} + \frac{\rho}{2\nu}\sum_{j\neq i}^{n} q_{j,t}\mathbb{1}_{\left\{q_{i,t}q_{j,t} > \frac{\zeta}{\rho}\right\}} - \frac{b}{2\nu}\sum_{j\neq i}^{n} q_j\right\}, \tag{59}$$

starting from the initial vector $\mathbf{q}_0 = (0,\ldots,0)^\top$. We then observe that the map $f_i : \mathbb{R}_+ \to \mathbb{R}_+$ is η-order preserving. That is, if $\eta_i > \eta_j$ and $q_{i,t} > q_{j,t}$, then also $q_{i,t+1} > q_{j,t+1}$. To show this we proceed by induction. For the induction basis consider $t = 0$. Then $q_{i,1} = \eta_i$ for all $i = 1,\ldots,n$, and the claim follows. Next, consider the induction step, assuming that the claim holds for some $t > 0$. Then

$$q_{i,t+1} - q_{j,t+1} = f_i(\mathbf{q}_t) - f_j(\mathbf{q}_t) = \frac{b}{2\nu}(\eta_i - \eta_j) + \frac{\rho}{2\nu}\sum_{k\in\mathcal{N}_{i,t}\setminus\mathcal{N}_{j,t}} q_{k,t} + \frac{b}{2\nu}(q_{i,t} - q_{j,t}) > 0,$$

where we have used the fact that the condition $q_{i,t}q_{j,t} > \frac{\zeta}{\rho}$ for i and j being linked represents a nested split graph, and for such a graph if $q_{i,t} > q_{j,t}$ (so that $d_{i,t} > d_{j,t}$) then $\mathcal{N}_{j,t} \subset \mathcal{N}_{i,t}$. Hence, for all t, the claim holds, and in particular, taking the limit as $t \to \infty$ it holds for the fixed point $\mathbf{q}$ solving Equation (57).

We now give a proof of part (iii) of the proposition. From Equation (17) we know that in the stochastically stable state the output levels satisfy the following equation

$$\mathbf{g}(\mathbf{q}) \equiv (\mathbf{I}_n + b\mathbf{B} - \rho\mathbf{A})\,\mathbf{q} = \boldsymbol{\eta}, \tag{60}$$

where $\mathbf{B}$ is a matrix of ones with zero diagonal and $\mathbf{A}$ has elements $a_{ij} = \mathbb{1}_{\{\rho q_i q_j > \zeta\}}$. When the $(\eta_i)_{i=1}^n$ are real valued random variables with probability density function f, then the probability density function μ of $\mathbf{q}$ is given by

$$\mu(\mathbf{q}) = \left|\det\left(\frac{d\mathbf{g}(\mathbf{q}))}{d\mathbf{q}}\right)\right| f(\eta),$$

where $\left(\frac{d\mathbf{g}(\mathbf{q})}{d\mathbf{q}}\right)_{ij} = \frac{\partial \mathbf{g}_i(\mathbf{q})}{\partial q_i}$. From Equation (60) we get $\frac{d\mathbf{g}(\mathbf{q})}{d\mathbf{q}} = \mathbf{I}_n + b\mathbf{B} - \rho\mathbf{A}$, and we denote this by $\mathbf{M}$. It then follows that $\mu(\mathbf{q}) = |\det(\mathbf{M})| f(\mathbf{M}\mathbf{q})$. In particular, if the $(\eta_i)_{i=1}^n$ are identically and independently Pareto distributed with density function $f(\eta) = (\gamma-1)\eta^{-\gamma}$ for $\eta \geq 1$ then

$$\mu(\mathbf{q}) = (\gamma-1)^n |\det(\mathbf{M})| \prod_{i=1}^{n} (\mathbf{M}\mathbf{q})_i^{-\gamma}.$$

Next, consider $\mathbf{q} = c\mathbf{u}$, $c > 0$, with $\mathbf{u}$ being a vector of all ones. Then $\mathbf{M} = \mathbf{I}_n + (b-\rho)\mathbf{B}$ for c large enough (because $\rho q_i q_j = c^2\rho > \zeta$ for c large enough), and $\det(\mathbf{M}) = (1 + (n-1)(b-\rho))\,(1+$

[53] Note that $\mathscr{H}_\vartheta(\mathbf{q})$ is a real valued function that converges pointwise and whose derivatives converge uniformly on a closed interval $[0,\bar{q}]$ so that we can exchange the derivative with the limit [Rudin, 1987].

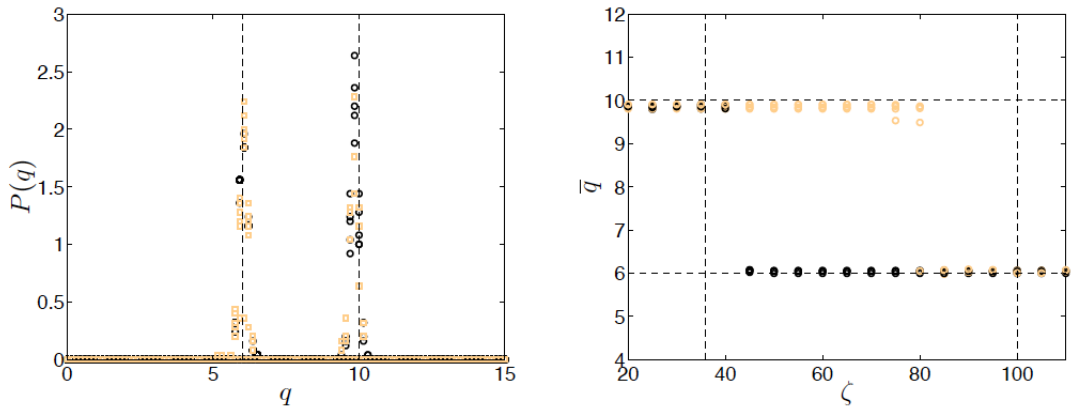

Figure 3: (Left panel) The stationary output distribution. The vertical dashed lines indicate the theoretical predictions from Equation (56). (Right panel) The average output level from numerical simulations with $\vartheta = 1$ starting with different initial conditions (indicated with different colors). The horizontal dashed lines indicate the equilibrium quantities and the vertical dashed lines the threshold cost levels from Equation (13). In the region of the cost ζ between the lower and upper thresholds two equilibria exist.

$b+\rho)^{n-1}$. Further, $(\mathbf{Mq})_i = 1+(n-1)(b-\rho)$, so that we can write

$$\mu(c\mathbf{u}) = (1+(n-1)(b-\rho))\,(1+b+\rho)^{n-1}(\gamma-1)^n\,(1+(n-1)(b-\rho))^{-n\gamma}\,c^{-n\gamma},$$

and we conclude that $\mu(c\mathbf{u}) \sim \prod_{i=1}^n O\left(c^{-\gamma}\right)$ as $c \to \infty$. □

Figure 2 shows the output iteration of Eq. (59) over the firm fixed effects η_i together with the adjacency matrix $\mathbf{A} = (a_{ij})_{1\leq i,j,n}$ (see also Figure 4) whose elements are given by $a_{ij} = \mathbb{1}_{\left\{q_i q_j > \frac{\zeta}{\rho}\right\}}$ and the vector $\mathbf{q}$ is the fixed point of Equation (59). We observe that firms with higher η_i also have higher output levels. Moreover, the corresponding adjacency matrix is stepwise, characterizing a nested split graph (see also supplementary Appendix B), and becomes increasingly sparse with increasing linking costs ζ.

An illustration with the average output level from numerical simulations starting with different initial conditions and a comparison with the predictions of Equation (56) can be seen in Figure 3.

Proof of Proposition 4. We first give a proof of part (i) of the proposition. Welfare can be written as follows

$$\begin{aligned}
W(\mathbf{q}) &= U(\mathbf{q}) + \Pi(\mathbf{q}, G) \\
&= \frac{1}{2}\sum_{i=1}^n q_i^2 + \frac{b}{2}\sum_{i=1}^n\sum_{j\neq i}^n q_i q_j + \sum_{i=1}^n\left(\eta q_i - \nu q_i^2 - b\sum_{j\neq i}^n q_i q_j + \rho\sum_{j=1}^n a_{ij}(q_i q_j - \zeta)\right) \\
&= \eta\sum_{i=1}^n q_i - \frac{2\nu-1}{2}\sum_{i=1}^n q_i^2 - \frac{b}{2}\sum_{i=1}^n\sum_{j\neq i}^n q_i q_j + \sum_{i=1}^n\sum_{j\neq i}^n a_{ij}(\rho q_i q_j - \zeta).
\end{aligned}$$

The only network dependent part in $W(\mathbf{q}, G)$ is the last term $\sum_{i=1}^n\sum_{j\neq i}^n a_{ij}(\rho q_i q_j - \zeta)$. For a given output vector $\mathbf{q}$ the network that maximizes this term is a nested split graph G (see also supplementary Appendix B) where each link $ij \in G$ if and only if $\rho q_i q_j > \zeta$.[54] Hence, we can

[54] A graph G is a nested split graph if for every node $i \in \mathcal{N}$ there exist a weight x_i and a threshold T such that vertices i and j are linked if and only if $x_i + x_j \geq T$ [Mahadev and Peled, 1995]. Then by letting $\ln q_i = x_i$ and $\ln(\zeta/\rho) = T$ yields $\rho q_i q_j > \zeta$ iff $x_i + x_j \geq T$ the conclusion follows.

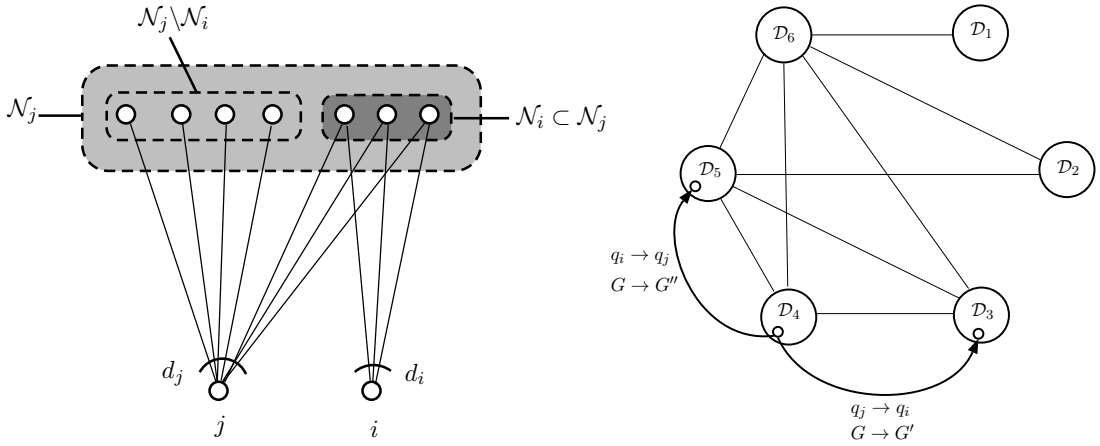

Figure 4: (Left panel) An illustration of the neighborhoods of i, j such that $\mathcal{N}_i \subset \mathcal{N}_j$. (Right panel) A schematic representation of a nested split graph G (see supplementary Appendix B).

write welfare reduced to this class of networks as follows

$$W(\mathbf{q}) = \eta \sum_{i=1}^{n} q_i - \frac{2\nu - 1}{2} \sum_{i=1}^{n} q_i^2 - \frac{b}{2} \sum_{i=1}^{n} \sum_{j \neq i}^{n} q_i q_j + \sum_{i=1}^{n} \sum_{j \neq i} (\rho q_i q_j - \zeta) \mathbb{1}_{\{\rho q_i q_j > \zeta\}}.$$

The necessary first order condition (FOC) can be written as follows

$$\frac{\partial W}{\partial q_i} = \eta - (2\nu - 1) q_i - b \sum_{j \neq i}^{n} q_j + \rho \sum_{j \neq i}^{n} q_j \mathbb{1}_{\{\rho q_i q_j > \zeta\}} = 0. \tag{61}$$

We next consider a symmetric solution $q_i = q$ for all $i = 1, \ldots, n$ with the property that $\rho q^2 > \zeta$. Then Equation (61) implies that

$$\eta - (2\nu - 1) q + (2\rho - b)(n - 1) q = 0,$$

from which we deduce that

$$q = \frac{\eta^*}{b + 2\nu^* - 2\rho - \frac{1}{n-1}},$$

where we have denoted $\eta^* = \eta/(n-1)$ and $\nu^* = \nu/(n-1)$. The corresponding network is a complete graph, K_n. Further, for a symmetric solution with $\rho q^2 < \zeta$ from Equation (61) we must have that

$$\eta + (1 - 2\nu) q - b(n - 1) q = 0,$$

from which we deduce that

$$q = \frac{\eta^*}{b + 2\nu^* - \frac{1}{n-1}}.$$

The corresponding network is an empty graph, $\overline{K}_n$. Note that welfare in the complete network K_n and the empty network $\overline{K}_n$ is the same if $\zeta = \zeta^*$ where ζ^* is given in Equation (21).

Consider a degree partition $\mathcal{D}_1, \mathcal{D}_2, \ldots, \mathcal{D}_m$ (see also supplementary Appendix B) in a nested split graph G such that $d_i < d_j$ if $i \in \mathcal{D}_k$, $j \in \mathcal{D}_{k'}$ with $k' > k$. From the symmetry of the FOC in Equation (61) it follows that for any $i, j \in \mathcal{D}_k$ it must hold that $q_i = q_j$. Moreover, from the FOC we also observe that when $d_i < d_j$ then $q_i < q_j$.

Further, we show that either the complete network K_n or the empty network $\overline{K}_n$ are efficient. To do so, assume that G is efficient, and it is neither empty nor complete. Let the output profile in G be $\mathbf{q}$. We know that the efficient network is a nested split graph. Consider i, j such that $q_j > q_i$ and $\mathcal{N}_i \subset \mathcal{N}_j$. Let G' be the graph obtained from G with the links of j in $\mathcal{N}_j \backslash \mathcal{N}_i$ removed. Further, let $\mathbf{q}' = (q_i, \ldots, q_{j-1}, q_i, q_{j+1}, \ldots, q_n)$, that is, $\mathbf{q}'$ is obtained from $\mathbf{q}$ be replacing q_j with

q_i. An illustration can be seen in the left panel of Figure 4. We then have that

$$W(\mathbf{q}', G') - W(\mathbf{q}, G) = (q_i - q_j)\left[\eta + \frac{1-2\nu}{2}(q_i + q_j) - b\sum_{k\neq j} q_k + 2\rho\sum_{k\in\mathcal{N}_i} q_k\right] - 2\sum_{k\in\mathcal{N}_j\setminus\mathcal{N}_i}(\rho q_j q_k - \zeta).$$

Similarly, consider the graph G'' obtained from G with the links in $\mathcal{N}_j\setminus\mathcal{N}_i$ added to i. Further, let $\mathbf{q}'' = (q_i, \ldots, q_{i-1}, q_j, q_{i+1}, \ldots, q_n)$, that is, $\mathbf{q}''$ is obtained from $\mathbf{q}$ be replacing q_i with q_j. Then we have that

$$W(\mathbf{q}'', G'') - W(\mathbf{q}, G) = (q_j - q_i)\left[\eta + \frac{1-2\nu}{2}(q_i + q_j) - b\sum_{k\neq j} q_k + 2\rho\sum_{k\in\mathcal{N}_i} q_k\right] + 2\sum_{k\in\mathcal{N}_j\setminus\mathcal{N}_i}(\rho q_j q_k - \zeta).$$

It follows that $W(\mathbf{q}'', G'') - W(\mathbf{q}, G) + W(\mathbf{q}', G') - W(\mathbf{q}, G) = 0$. There are three possible cases to consider such that this equality holds. First, if $W(\mathbf{q}'', G'') - W(\mathbf{q}, G) < 0$ then we must have that $W(\mathbf{q}', G') - W(\mathbf{q}, G) > 0$. This means that $W(\mathbf{q}', G') > W(\mathbf{q}, G)$ and $(\mathbf{q}, G)$ is not efficient. Second, if $W(\mathbf{q}', G') - W(\mathbf{q}, G) < 0$ then we must have that $W(\mathbf{q}'', G'') - W(\mathbf{q}, G) > 0$. This means that $W(\mathbf{q}'', G'') > W(\mathbf{q}, G)$ and $(\mathbf{q}, G)$ is not efficient. The third case to consider is $W(\mathbf{q}'', G'') - W(\mathbf{q}, G) = 0$. Then we must have that $W(\mathbf{q}'', G'') = W(\mathbf{q}', G') = W(\mathbf{q}, G)$.

From the definition of $\mathbf{q}''$ and G'' we see that the transition from G to G'' corresponds to moving a node from a degree partition $\mathcal{D}_k$ to a partition $\mathcal{D}_l$ with $l > k$, while leaving welfare unchanged. An illustration can be seen in the right panel in Figure 4. In particular, $(\mathbf{q}'', G'')$ must be efficient. We then can repeat this procedure to move up the node to the next higher partition while leaving welfare unchanged. Doing this across all partitions and for all nodes shows that we end up with the complete graph, K_n, with the same welfare as the original graph G. However, this is a contradiction to our initial assumption that the complete graph is not efficient. This shows that either the empty, $\overline{K}_n$, or the complete graph, K_n, must be efficient.

We next consider part (ii) of the proposition. In the case of heterogeneous firms, welfare can be written as

$$W(\mathbf{q}) = \sum_{i=1}^n \eta_i q_i - \frac{2\nu-1}{2}\sum_{i=1}^n q_i^2 - \frac{b}{2}\sum_{i=1}^n\sum_{j\neq i}^n q_i q_j + \sum_{i=1}^n\sum_{j\neq i}^n a_{ij}(\rho q_i q_j - \zeta).$$

The only network dependent part in $W(\mathbf{q}, G)$ is the last term $\sum_{i=1}^n\sum_{j\neq i}^n a_{ij}(\rho q_i q_j - \zeta)$, and, as in part (i), for a given output vector $\mathbf{q}$ the network that maximizes this term is a nested split graph G where each link $ij \in G$ if and only if $\rho q_i q_j > \zeta$. Moreover, from the necessary FOC we obtain

$$q_i = f_i(\mathbf{q}) \equiv \max\left\{0, \frac{\eta_i}{2\nu-1} - \frac{b}{2\nu-1}\sum_{j\neq i}^n q_j + \frac{\rho}{2\nu-1}\sum_{j\neq i}^n q_j \mathbb{1}_{\{\rho q_i q_j > \zeta\}}\right\}. \tag{62}$$

We can compare this to the equilibrium output levels of Equation (57), which were given by

$$q_i = g_i(\mathbf{q}) \equiv \max\left\{0, \frac{\eta_i}{2\nu} - \frac{b}{2\nu}\sum_{j\neq i}^n q_j + \frac{\rho}{2\nu}\sum_{j\neq i}^n q_j \mathbb{1}_{\{\rho q_i q_j > \zeta\}}\right\}. \tag{63}$$

We have for any $\mathbf{q} \in \mathcal{Q}^n$ that $f_i(\mathbf{q}) > g_i(\mathbf{q})$. This is because

$$f_i(\mathbf{q}) - g_i(\mathbf{q}) = \left(\frac{1}{2\nu-1} - \frac{1}{2\nu}\right)\left(\eta_i - b\sum_{j\neq i}^n q_j + \rho\sum_{j\neq i}^n q_j \mathbb{1}_{\{\rho q_i q_j > \zeta\}}\right) \geq 0.$$

Next, consider the differential equations $\frac{d\mathbf{x}}{dt} = \mathbf{f}(\mathbf{x}) - \mathbf{x}$ and $\frac{d\mathbf{y}}{dt} = \mathbf{g}(\mathbf{y}) - \mathbf{y}$, both with initial condition $\mathbf{x}_0 = \mathbf{y}_0 = (0, \ldots, 0)^\top$. Because $\mathbf{f}(\mathbf{x}) > \mathbf{g}(\mathbf{x})$, the comparison lemma implies that $\mathbf{x}(t) > \mathbf{y}(t)$ for all $t \geq 0$ (see Khalil [2002], Lemma 3.4). In particular, we can conclude that the

fixed point $\mathbf{f}(\mathbf{q}) = \mathbf{q}$ must be higher than the fixed point $\mathbf{g}(\mathbf{q}) = \mathbf{q}$. That is, in the stochastically stable equilibrium output levels are too low compared to the social optimum. Moreover, because a link is only present if $\rho q_i q_j > \zeta$ there are fewer links in the stochastically stable network than in the efficient network. □